π-Conjugated Macrocycles Bearing Angle-Strained Alkynes

Koji Miki*[a] and Kouichi Ohe*[a]

Dedication ((optional))

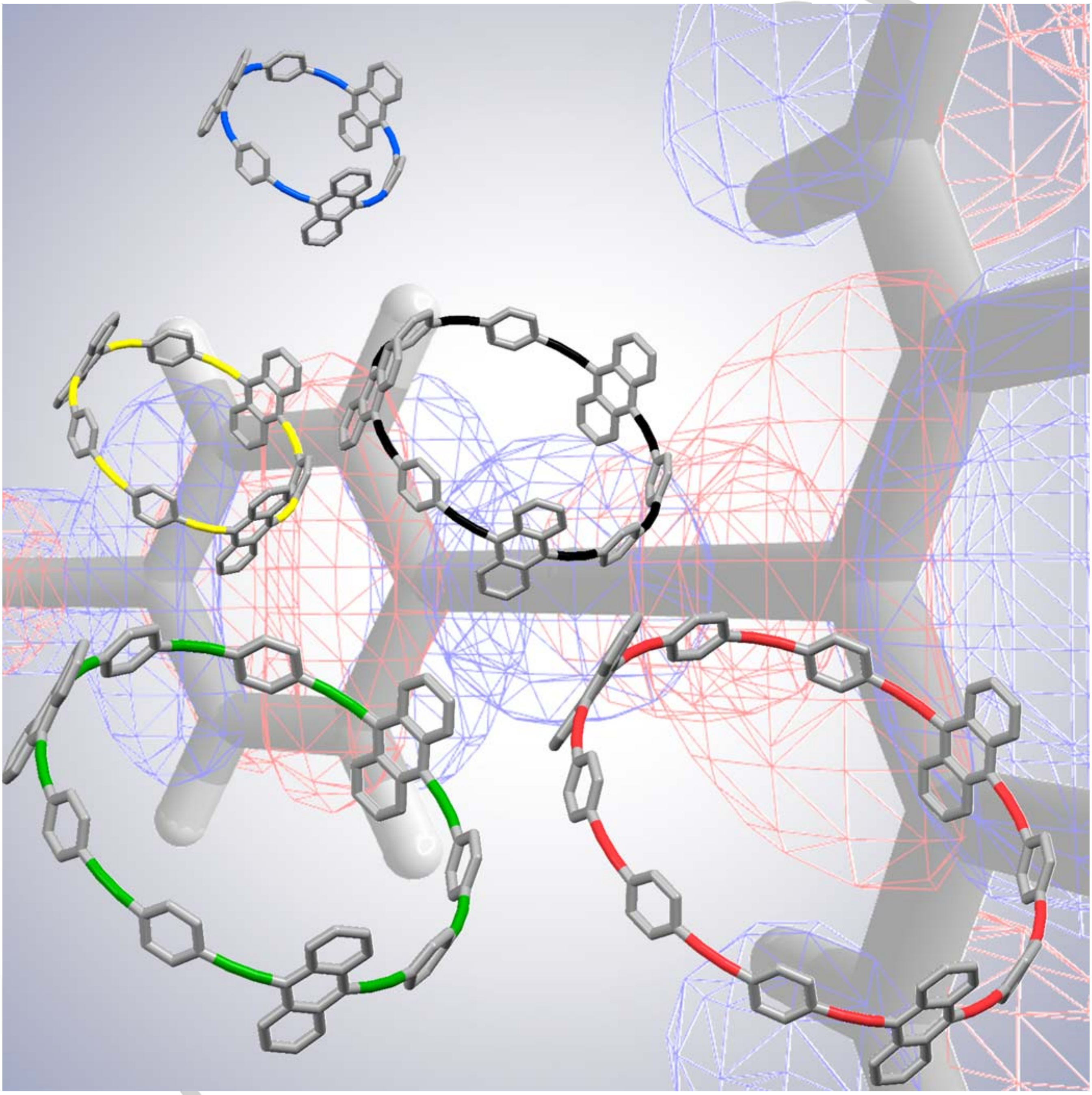

Abstract: Angle-strained alkyne-containing π-conjugated macrocycles are attractive compounds both in functional materials chemistry and biochemistry. Their interesting reactivity as well as photophysical and supramolecular properties have been revealed in the past three decades. This review highlights the recent advances in angle-strained alkyne-containing π-conjugated macrocycles, especially their synthetic methods, the bond angles of alkynes ($\angle_{sp}$ at $C\equiv C$–C), and their functions. The theoretical and experimental researches on cyclo[n]carbons and *para*-cyclophynes consisting of ethynylenes and *para*-phenylenes are mainly summarized. Related macrocycles bearing other linkers, such as *ortho*-phenylenes, *meta*-phenylenes, heteroaromatics, biphenyls, extended aromatics, are also overviewed. Bond angles of strained alkynes in π-conjugated macrocycles, which are generable, detectable, and isolable, are summarized at the end of this review.

1. Introduction

Curved π-conjugated systems, including angle-strained alkynes, are one of the most attractive molecular architectures because the distortion of π-conjugation leads to their specific structural and electronic features.[1] Because of the low overlap of outer p-orbitals, highly angle-strained alkynes are more reactive than unstrained alkynes, thereby being widely applied in organic transformations, such as bioorthogonal labeling and natural product synthesis.[2–6] In general, the straightforward approach to construct angle-strained alkynes is the conjugation of both acetylene carbons with a short linker. The simplest examples are arynes and cycloalkynes (Figure 1a). *ortho*-Arynes, such as benzyne, are well studied and widely utilized as a reactive intermediate in organic synthesis.[5–7] Because of their instability, their application in materials chemistry is avoided. The small-ring-sized cycloalkynes, such as cyclopentyne, cyclohexyne, and cycloheptyne, have been experimentally validated as reaction intermediates despite their very short lifetime.[8–12] In contrast, a series of isolable cyclooctynes is widely applied as promising reagents for strain-promoted azide–alkyne cycloaddition in bioorthogonal chemistry.[2–4,13,14]

Cyclocarbon, also called cyclyne, is one of the simplest curved π-conjugated macrocycles composed of only sp carbons (Figure 1b).[15] Cyclocarbons have not so far been isolated because of their extremely high reactivity, although their generation was confirmed by spectrometry and microscopy.[15–20] Compared with cyclocarbons, cycloparaphenylenes (CPPs, Figure 1b) are stable enough to be handled under ambient conditions.[21–23] To date, several elegant synthetic approaches have been developed by Jasti and Bertozzi,[24] Itami,[25] and Yamago.[26] Because of their fascinating and challenging architectures, studies on cyclocarbon derivatives consisting of angle-strained oligoynes and *para*-phenylene moieties (ethynylene units > phenylene units) have been intensively pursued since the early 1990s. Owing to the tolerance of benzene ring against the structural distortion, π-conjugated macrocycles bearing angle-strained monoynes and *para*-phenylene or oligo(*para*-phenylene) moieties (ethynylene units ≤ phenylene units), such as cycloparaphenyleneacetylenes (CPPAs),[27] have been developed. Since the fullerene inclusion complexes of CPPA were prepared in 2003,[28] several inclusion complexes of π-conjugated macrocycles have been reported. Stimulated by these significant milestones, a variety of macrocycles containing angle-strained alkynes have been synthesized and characterized in the past three decades. This review mainly summarizes the synthesis of π-conjugated macrocycles (*para*-cyclophynes) consisting of angle-strained alkynes and *para*-phenylenes, especially focusing on their synthetic methods, the bond angles of alkynes ($\angle_{sp}$ at $C\equiv C$–C, Figure 2a), and their functions. Besides *para*-phenylene spacers, angle-strained alkyne-containing macrocycles bearing other π-systems, such as *ortho*- and *meta*-phenylene, heteroaromatics, and extended aromatics, are also described in this review. Most recently, Stępień and a co-worker published an excellent review summarizing curved aromatic molecules and synthetic approaches to curved *para*-phenylene and ethynylene in macrocycles.[29]

In this review, “angle-strained” is defined as a bond angle of the alkyne ($\angle_{sp} < 170°$) according to a profound notion urged by Krebs and Wilke.[30] Because of classification based on this definition, alkyne-containing π-conjugated macrocycles without strain ($\angle_{sp} > 170°$) are not included. The development of angle-strained alkyne-containing macrocycles has been described in several excellent reviews.[31–40] For alkyne-containing shape-persistent macrocycles without strain[41–47] and macrocyclic metal complexes,[48–50] refer to other reviews.

In this review, the bond angles ($\angle_{sp}$) of compounds are calculated by Mercury software (The Cambridge Crystallographic Data Centre (CCDC)) using X-ray crystallographic data (cif) deposited in the CCDC. The detailed data, including the standard deviations of bond angles, are omitted. For accessibility to deposited data, all published CCDC numbers are included. The bond angles of optimized structures are also evaluated by the same software when the coordinates are available.

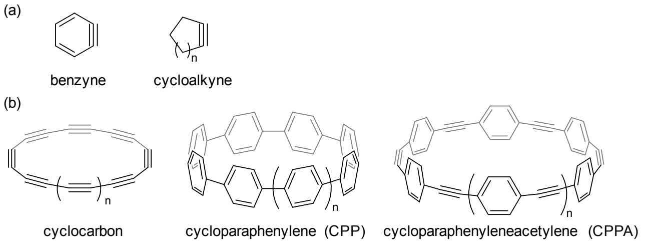

Figure 1. (a) Benzyne and cycloalkynes. (b) π-Conjugated macrocycles consisting of sp-carbons (cyclocarbon), sp^2-carbons (cycloparaphenylene), and both sp- and sp^2-carbons (cycloparaphenyleneacetylene).

---

[a] Prof. Dr. K. Miki, Prof. Dr. K. Ohe
Department of Energy and Hydrocarbon Chemistry
Graduate School of Engineering, Kyoto University
Katsura, Nishikyo-ku, Kyoto 615-8510 (Japan)
E-mail: kojimiki@scl.kyoto-u.ac.jp; ohe@scl.kyoto-u.ac.jp

ORCID identification numbers for the authors of this article can be found under: https://doi.org/10.1002/chem.000000000.

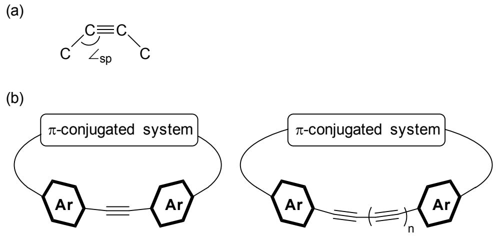

Figure 2. (a) Bond angle of alkyne (∠$_{sp}$). (b) π-Conjugated macrocycles bearing angle-strained alkynes.

2. Synthetic methods of π-conjugated macrocycles containing angle-strained alkynes

In this section, we summarize the preparation of angle-strained alkyne-containing π-conjugated macrocycles. As to synthesis, it is surprising that limited numbers of synthetic methods are available for the preparation of angle-strained alkyne-containing macrocycles. Those methods are briefly summarized (Figure 3).

2.1. Direct method: single-step macrocyclization approach to angle-strained alkyne-containing macrocycles

Angle-strained oligoyne-containing macrocycles cannot be obtained through single-step macrocyclization due to the instability of the oligoyne under macrocyclization conditions. A milder transformation without transition metal reagents is awaited. A less-strained tetrayne-containing macrocycle could be obtained by Glaser coupling (Figure 4a). This implies that other Glaser-type methods, such as Eglinton, Hay, and Cadiot–Chodkiewicz couplings,[51–54] will be applicable to angle-strained oligoyne-containing macrocycles.

Because of the stability of diynes under the conditions, copper-mediated Glaser coupling reaction, as well as modified methods, directly affords macrocycles containing angle-strained diynes. By considering that these methods efficiently provide strained macrocyclic structures, two alkyne moieties require nonlinear conformation in the intermediate for a reductive elimination step (Figure 4b). The mechanistic study of Glaser coupling is still ongoing experimentally[55] and theoretically.[56–60] These studies suggest that the proposed intermediates **I**–**IV** depend on the valence at the copper metals. The researchers have to pay attention to the copper precatalyst used, which may affect the efficiency of macrocyclization.

Palladium-catalyzed coupling reactions are also useful methods to construct angle-strained diynes. Haley and co-workers employed palladium-catalyzed and copper-mediated alkyne homocoupling in macrocyclization (Figure 5).[61–63] The homocoupling using a palladium catalyst, especially including *cis*-bidentate bisphosphine ligand, afforded dehydrobenzo[14]annulene-containing macrocycle **V-b** selectively, whereas the Eglinton coupling with copper(II) acetate gave dehydrobenzo[15]annulene-containing macrocycle **V-a** as the major product. These results imply that desired macrocyclization is finely tunable by palladium catalysts having a variety of ligands.

Template-assisted macrocyclization is one of the most powerful and efficient methods to create strained macrocycles. As to porphyrin nanorings developed by Anderson and co-workers,[64] the template-assisted macrocyclization utilizing Glaser coupling as well as Sonogashira–Hagihara coupling effectively afforded the corresponding nanorings bearing angle-strained diynes and monoynes. In the case of Sonogashira–Hagihara coupling, the square planar alkynyl(aryl)palladium(II) complex is formed prior to reductive elimination. This indicates that transition metal-catalyzed macrocyclization, such as Sonogashira–Hagihara coupling, would be applied to the direct synthesis of macrocycles bearing angle-strained diynes and monoynes.

2.2. Stepwise method: macrocyclization and aromatization or alkyne formation

Although many approaches to macrocycles were examined, photoinduced retro-[2+2]cyclization (Tobe's method) and photoinduced decarbonylation (Rubin's method) are the ways to obtain macrocycles bearing angle-strained oligoyne-containing *para*-cyclophynes (Figure 3a). This indicates that these methods might be applicable to the synthesis of less-strained oligoyne-containing isolable macrocycles. Since Diederich's cyclocarbon synthesis was reported,[15] the laser irradiation-induced elimination of anthracene,[15] carbon monoxide,[17,20] and indane[18,19,65,66] has been applied to the synthesis of cyclocarbons (Figure 6). These methods are considered to be candidates for the preparation of angle-strained oligoyne-containing macrocycles.

Koji Miki received his Ph.D. in chemistry from Kyoto University with Prof. Sakae Uemura in 2003. After studying as a postdoctoral fellow with Prof. K. C. Nicolaou (The Scripps Research Institute), with Prof. Yoshito Tobe (Osaka University), and with Prof. Timothy M. Swager (Massachusetts Institute of Technology), he was appointed as a program-specific Assistant Professor at Kyoto University in 2005. He became an Assistant Professor in 2008, a Lecturer in 2009, and an Associate Professor in 2014.

Kouichi Ohe was born in Kyoto, Japan in 1960. Kyoto Univ. (BS 1984, MS 1986, Ph.D. 1989, Profs. Masaya Okano, Nobuyuki Sugita, and Sakae Uemura). Assistant Professor (Prof. Shinji Murai, Osaka Univ. 1989-1994), Associate Professor (Uemura's group, Kyoto Univ. 1994-2003), Professor (2003-present). Visiting Researcher (1992-1993, Prof. K. C. Nicolaou, TSRI).

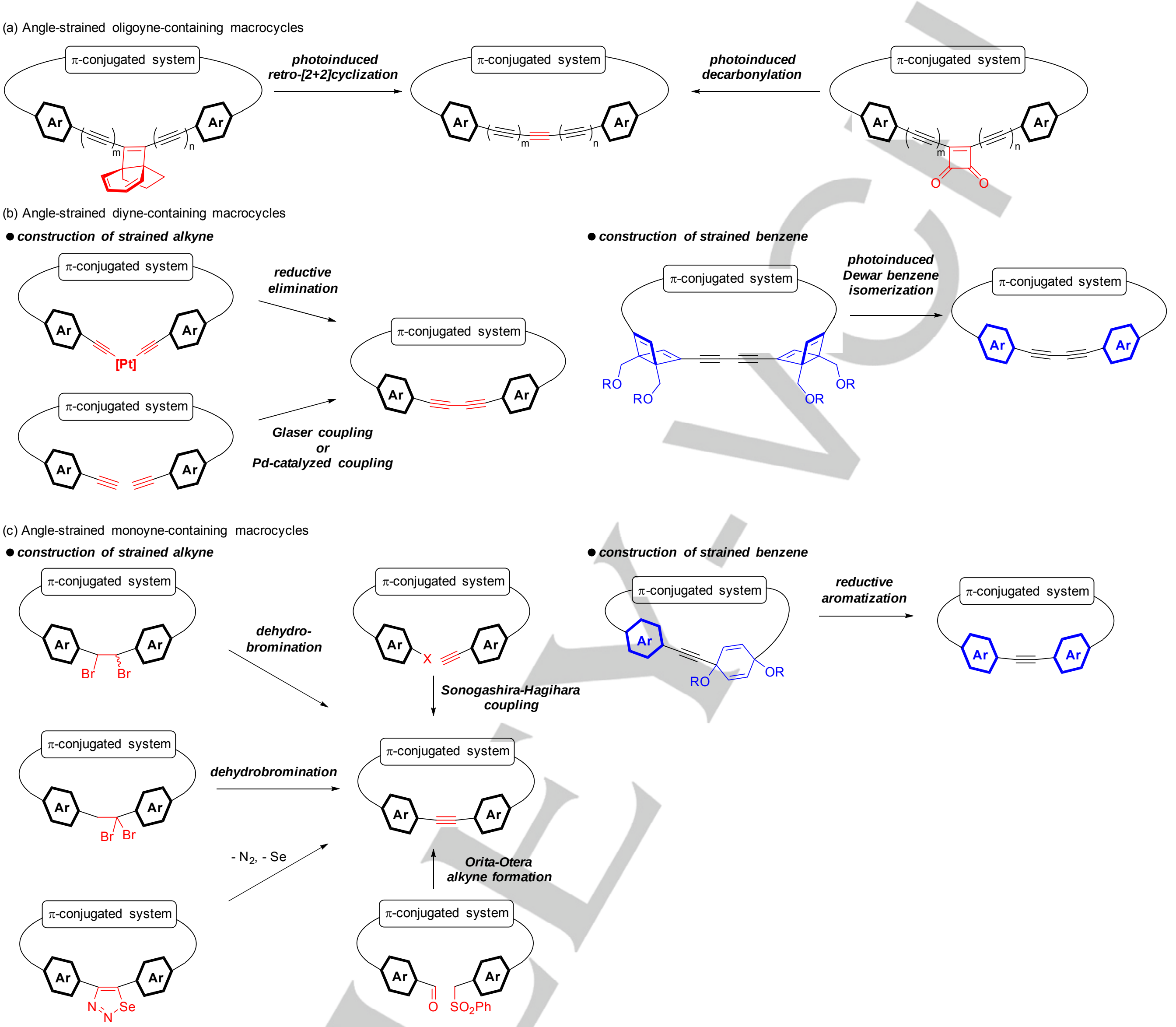

Figure 3. Synthetic methods to construct angle-strained (a) oligoyne-, (b) diyne-, and (c) monoyne-containing macrocycles.

Compared with oligoyne-containing macrocycles, angle-strained butadiyne in a macrocyclic system could be more easily constructed. Photoinduced transformation of Dewar-benzene-containing macrocycles is one of the best approaches to angle-strained diyne-containing macrocycles (Figure 3b). Because of the photostability of angle-strained diynes, Tobe's and Rubin's photoinduced transformations shown above might be applicable to the preparation of the related compounds. The reductive elimination from platinum complexes generates angle-strained diyne-containing macrocycles. This transformation is much better when the target molecule is photosensitive.

The reductive aromatization using sodium naphthalenide or tin(II) reagents is not successfully applied to the preparation of macrocycles, including angle-strained diynes or oligoynes, probably due to their instability under the reaction conditions. On the other hand, the tin(II)-mediated reductive aromatization could be applied to the synthesis of angle-strained monoyne-containing macrocycles (Figure 3c). When compounds are sensitive to acids, the use of preformed tetrachlorostannate(II) (H_2SnCl_4) might be better in the synthesis.

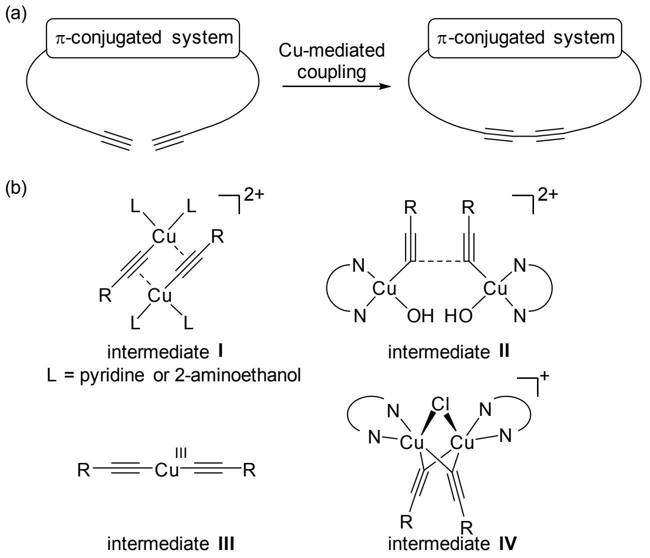

Figure 4. Mechanisms of Glaser coupling proposed.

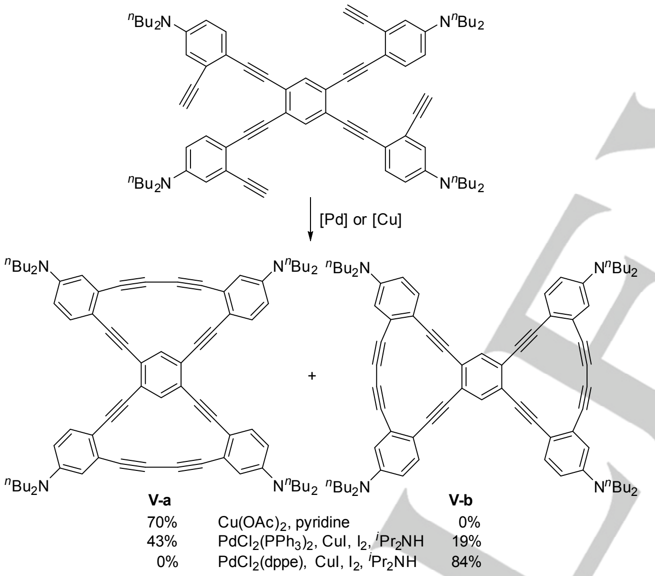

Figure 5. Selective macrocyclization through palladium-catalyzed or copper-mediated alkyne homo-coupling.

For angle-strained monoyne-containing macrocycle synthesis, bromination of alkenes followed by dehydrobromination is one of the most reliable methods. This method was applied to the synthesis of a series of CPPAs and thiophene-containing strained macrocycles. Macrocycles containing an angle-strained alkyne and an alkyl tether were also prepared by this method.[67–70] Orita–Otera alkyne formation is one of the best methods to construct angle-strained alkyne-containing macrocycles because the reaction proceeds under mild basic conditions at low temperature. The dehydrobromination of a *gem*-dibromo compound, as well as the elimination of a nitrogen molecule, could afford a highly strained macrocycle.

The formation of a dicobalt–alkyne complex followed by macrocyclization and demetalation was considered to be another method to create angle-strained alkyne-containing macrocycles; however, the demetalation conditions are so harsh that strained alkynes cannot survive under the conditions (Figure 11a).

Regarding strained CPP synthesis, a variety of synthetic approaches to construct angle-strained *para*-phenylenes were reported (Figure 7).[21–23,29] These methods are potentially applicable but have not yet been applied to the synthesis of angle-strained alkyne-containing macrocycles, except the reductive aromatization using sodium naphthalenide.

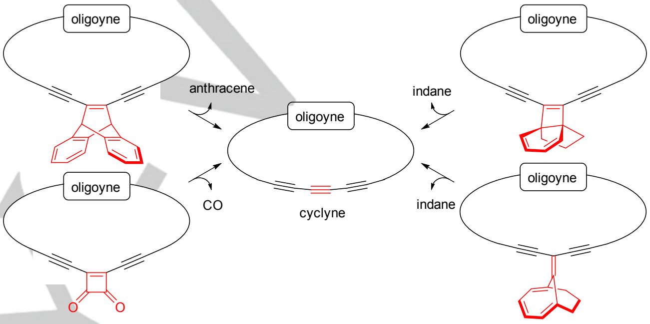

Figure 6. Synthetic methods of cyclocarbons.

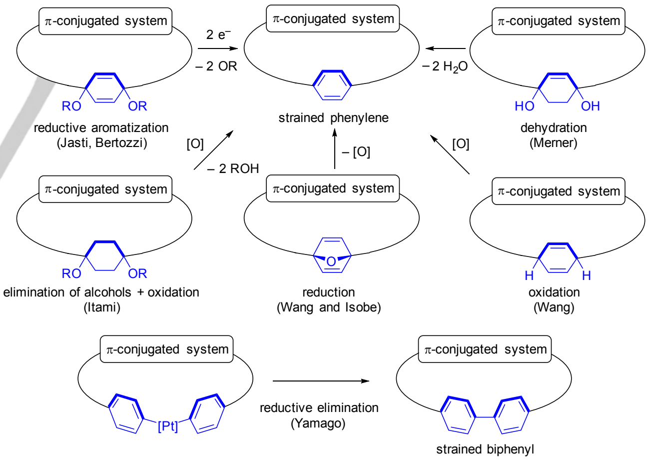

Figure 7. Synthetic methods for construction of angle-strained phenylene moieties in macrocycles.

3. Angle-strained alkyne-containing π-conjugated macrocycles.

3.1. Cyclocarbon

The simplest angle-strained alkyne-containing π-conjugated macrocycle is cyclocarbon (Figure 8), but until now cyclocarbons have not be isolated. The generation of cyclocarbons was confirmed by spectroscopic measurements. These results are summarized in preceding reviews.[1,48,71,72] In this section, studies on cyclocarbons are briefly summarized.

The structure of cyclo[n]carbon can be classified into four isomers. For example, logical structures of cyclo[10]carbon include polyyne D_{5h}, polyyne C_{5h}, cumulene D_{10h}, and cumulene D_{5h} (Figure 9a). In the case of a smaller ring size, a cumulene structure seems to be more stable than a polyyne structure.[73] The most stable structure of each cyclo[n]carbon is dependent on the calculation functional and basis sets.[74–76] A density functional theory (DFT) calculation suggests that larger cyclocarbons are less stable than "fullerene"-like carbon clusters.[77] In the case of C_{24}, the "fullerene"-like structure is thermodynamically favored by ≈335 kJ mol^{-1} over the ring structure.[78] Most recently, the microscopic observation revealed the polyynic structure of cyclo[18]carbon (Figure 9b).[20]

Diederich and co-workers reported the first synthesis of cyclo[18]carbon by the photoirradiation of **1** (Figure 10a).[15] Other precursors of cyclocarbons are summarized in Figure 10c. The generation of cyclocarbons from the precursors **2**,[17,79] **5**,[18,19] **6**,[19,65] and **7**[66] was confirmed by mass spectrometry and ultraviolet photoelectron spectroscopy.[80] Although the demetalation of cobalt complexes successfully proceeded to form linear oligoynes,[81] the synthesis of strained cyclo[n]carbons from precursors **3** has not succeeded so far.[16,82] The acid-mediated hydrolysis of benzylidene groups in **4** was unsuccessful.[83] The computational modeling of cyclocarbons pointed out the possibility of their deposition on graphene.[84] Anderson and co-workers most recently succeeded in the generation of cyclo[18]carbon and its observation using a microscope (Figures 9b and 10b).[20] The elimination of carbon monoxide from the precursor **2a** successfully proceeded to afford cyclo[18]carbon on bilayer NaCl on Cu(111) at low temperature (5 K). The observation by high-resolution atomic force microscopy (AFM) revealed its polyyne structure with bond length alternation. The AFM observation captured the reaction intermediates, indicating that the on-surface formation of cyclo[18]carbon is stepwise.[72] The method is capable of providing direct experimental insights into the structure of other unstable molecules.

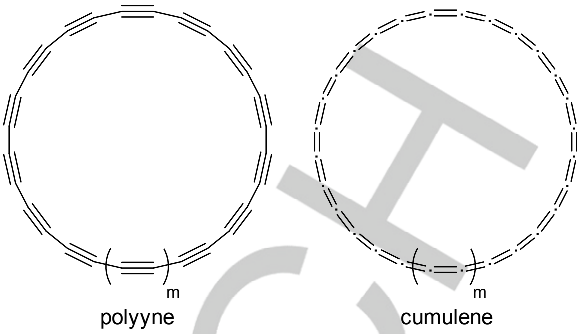

Figure 8. Cyclo[n]carbon: cyclic polyyne and cumulene structures.

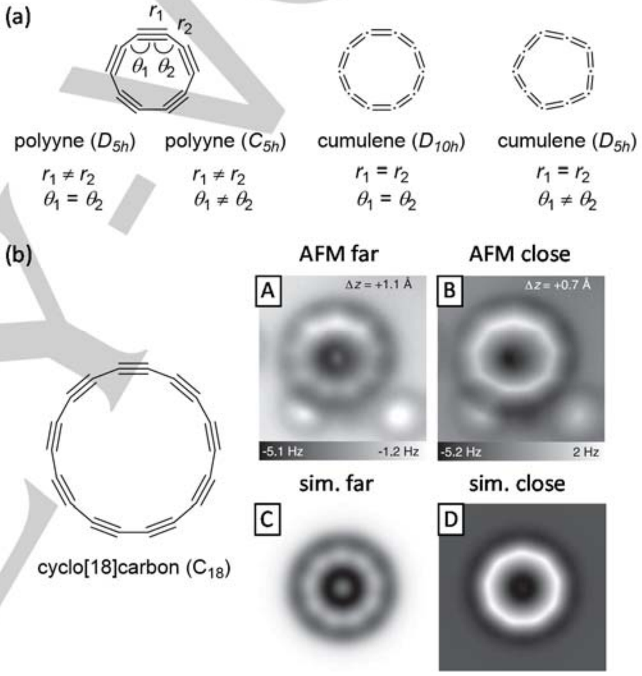

Figure 9. (a) Logical structures of cyclo[10]carbon. (b) AFM images (A and B) of cyclo[18]carbon and their simulated images (C and D). Reproduced with permission from ref. 20. Copyright 2019 The American Association for the Advancement of Science (AAAS), Washington, D.C.

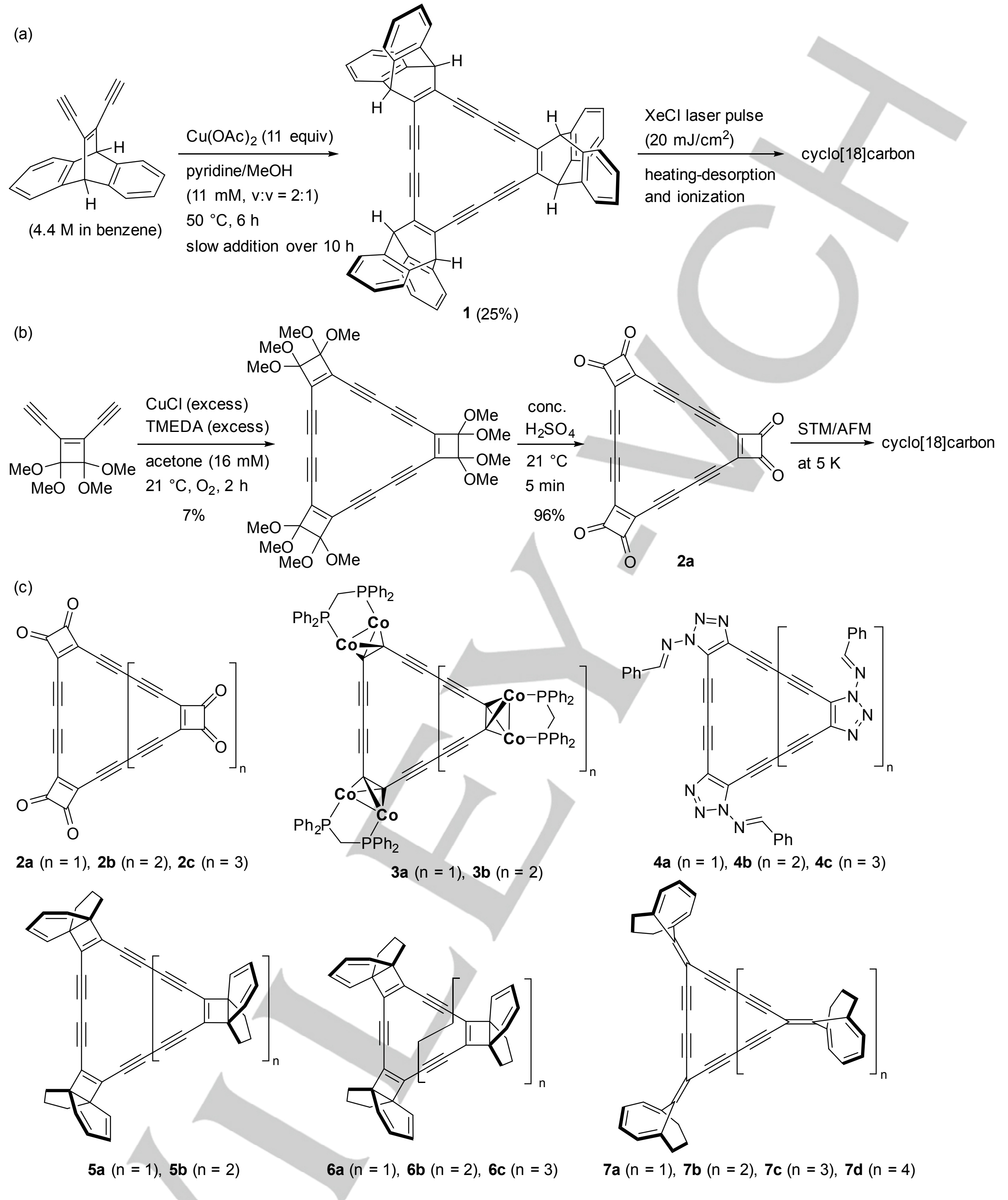

Figure 10. (a),(b) Synthesis of cyclo[18]carbon. (c) Precursors of cyclo[n]carbons. TMEDA: *N*,*N*,*N'*,*N'*-tetramethylethylenediamine, **Co**: $Co(CO)_2$, STM: scanning tunneling microscopy, AFM: atomic force microscopy.

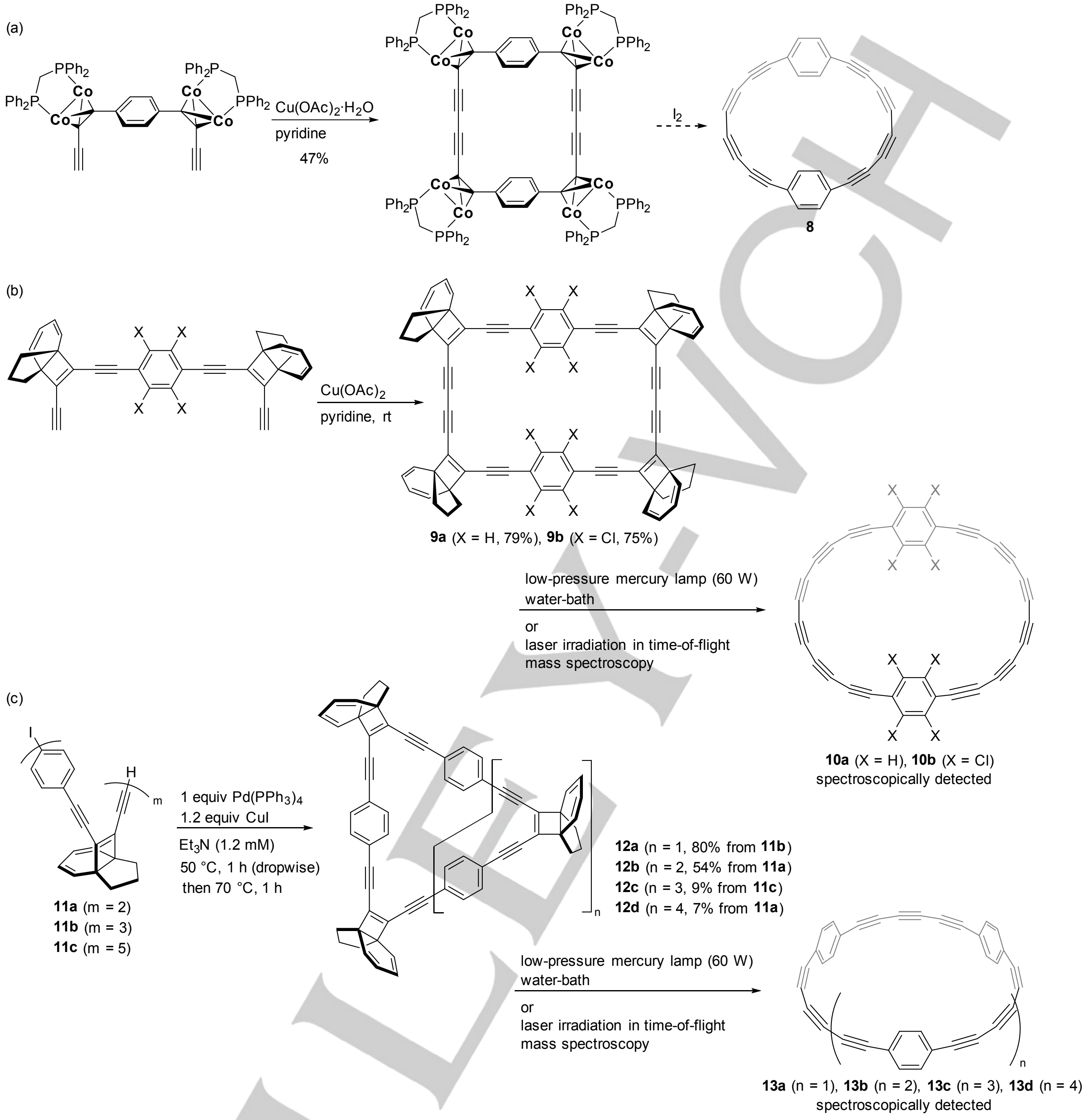

Figure 11. Preparation of (a) [8$_2$]paracyclophyne **8**, (b) [12$_2$]paracyclophynes **10**, and (c) [6$_n$]cyclophynes **13**. **Co** = Co(CO)$_2$.

3.2. *para*-Cyclophynes: ethynylene units > phenylene units

Cyclocarbons have not been isolated so far due to their high reactivity. Because linear polyynes are highly reactive, thermally cross-linkable, and explosive,[85] the protection by cyclic molecules, such as cyclodextrins,[86] and the capping by transition metal complexes[81,87–89] is basically essential. In contrast, both cyclic and linear oligo- and polyphenylenes are stable under ambient conditions. Despite its highly strained structure, [5]cycloparaphenylene (average diameter: 0.669 nm) was isolated.[90,91] By inserting *para*-phenylene units into a cyclocarbon structure, the isolation of hybrid macrocycles, so-called *para*-cyclophynes, has been attempted. The pioneering works on cyclophynes consisting of *para*-phenylene and ethynylene units were reported in the 1990s.

Diederich and co-workers synthesized a cyclocarbon–cobalt complex as a potent precursor of cyclocarbon because cobalt carbonyls can be removed to restore an alkyne moiety.[16] This approach was applied to the preparation of strained macrocycles bearing curved *para*-phenylene and ethynylene units. Haley and co-workers attempted to prepare [8_2]cyclophynes **8** through demetalation of cobalt complexes (Figure 11a).[92] The precursor of cyclophyne **8** was synthesized by copper-mediated Eglinton homocoupling reaction of biscobalt–diyne; however, the isolation of **8** failed, probably due to its instability under oxidative demetalation conditions.

Tobe and co-workers reported the propellanediyne-containing π-conjugated macrocycles **9** and their transformation to [12_2]*para*-cyclophynes **10** under light or laser irradiation (Figure 11b).[93] The precursors **9** were prepared by Cu-mediated Eglinton homocoupling reaction. The generation of **10a** involving the elimination of indanes under irradiation by a low-pressure mercury lamp at 77 K was confirmed by UV–vis absorption spectroscopy; however, the isolation was unsuccessful due to their high reactivity.

Tobe and co-workers then applied this synthetic method to the preparation of [6_n]cyclophynes **13** (Figure 11c).[94] The precursors **12** having propellane moieties were synthesized by Sonogashira–Hagihara coupling reaction of **11**. While cyclotrimer **12a** and cyclotetramer **12b** were obtained in high yields, the isolated yields of precursors **12c** and **12d** with larger ring sizes were decreased. [6_n]Cyclophynes **13** were produced by light or laser irradiation, but the isolation failed. Although the isolation and characterization of curved oligoyne-containing macrocycles had been expected to provide important information about the properties of the angle-strained oligoyne system, the isolation of cyclophynes bearing angle-strained oligoynes was unsuccessful.

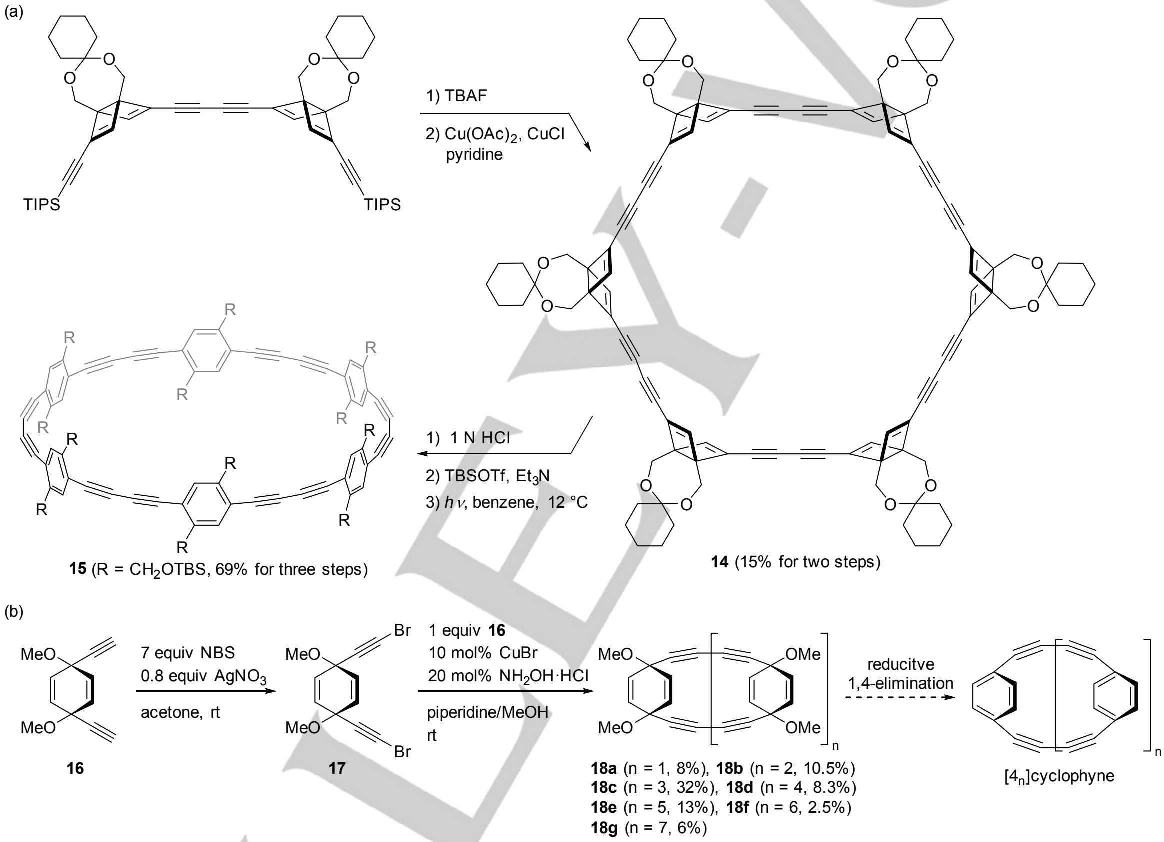

Figure 12. (a) [4_6]cyclophyne **15**. (b) Cyclic (*Z*)-1,4-diethynyl-1,4-dimethoxycyclohexa-2,5-diene oligomers. TBAF: tetra(*n*-butyl)ammonium fluoride, TIPS: triisopropylsilyl, TBS: *tert*-butyldimethylsilyl, NBS: *N*-bromosuccinimide.

Compared with oligoyne-containing *para*-cyclophynes, macrocycles bearing butadiyne moieties are more accessible. To synthesize [4_6]cyclophyne, Ohkita, Tsuji, and a co-worker utilized the isomerization of Dewar benzene (Figure 12a).[95] Cyclohexamer **14** bearing Dewar benzene moieties as a precursor was prepared through Eglinton homocoupling in moderate yield. After changing the protecting groups from acetonides to siloxys, [4_6]cyclophyne **15** was obtained in 69% yield from three steps by photoisomerization. The isosbestic point observed in UV–vis spectra indicated the clean conversion of the precursor **14** to cyclophyne **15** during photoisomerization. The fast rotation of the *p*-phenylene moieties on the NMR time scale was suggested by a ^{1}H and ^{13}C NMR study.

Sankararaman, Hopf, and co-workers proposed other approaches to [4_n]cyclophynes, selecting cyclooligomers of (*Z*)-1,4-diethynyl-1,4-dimethoxycyclohexadiene (**16**) as a precursor (Figure 12b).[96] They obtained cyclodimer **18a** and cyclotrimer **18b** in only 2.5% and 9.1% yields, respectively, employing the Eglinton homocoupling of **16**. They then reported the improved synthesis of cyclooligomer precursors **18** in 80% yield via Cadiot–

Chodkiewicz coupling of **16** and its dibromo derivative **17**.[97] The reductive 1,4-elimination of dimethoxy groups to construct curved phenylene units has not been applied so far.

The calculated bond angles ($\angle_{sp}$) at sp carbons of **8**, **10**, **13**, and **15** are summarized in Figure 13. The bond angles ($\angle_{sp}$) of larger *para*-cyclophyne **10a** are calculated to be less strained than for *para*-cyclophyne **8**. The bond angles ($\angle_{sp}$) of **13** are estimated to be 166.1–167.1° (for **13a**), 169.6–170.3° (for **13b**), 171.6–172.3° (for **13c**), and 173.0–173.5° (for **13d**) by semiempirical AM1 calculations. The calculated cavity size of **15** is about 1.5 nm, and the calculated bond angles ($\angle_{sp}$) of $C\equiv C$–C(sp^2) and $C\equiv C$–C(sp) are 170.8° and 171.2°, respectively.

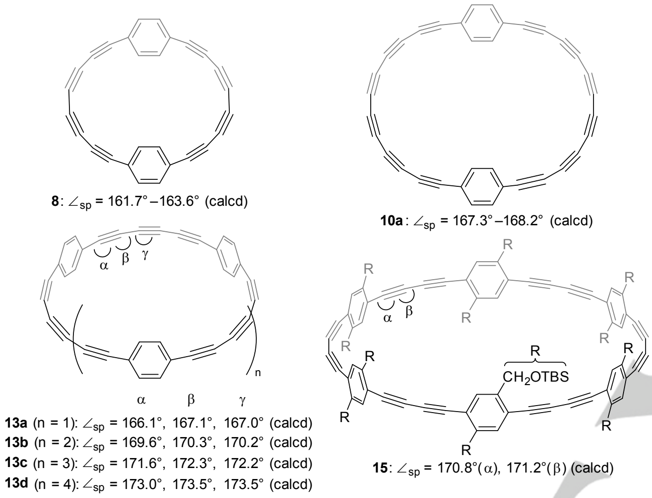

Figure 13. Bond angles at sp carbons in paracyclophynes **8**, **10**, **13**, and **15**.

3.3. Cyclophynes: ethynylene units < phenylene units

To obtain more stable cyclophyne derivatives as well as to reveal the properties and reactivity of angle-strained alkyne units, some research groups developed alkyne-containing CPPs.

Lee, Moore, and co-workers reported the preparation of alkyne-containing CPP **20** ([3]cycloparaterphenyleneacetylene: [3]CPP^{3}A) by applying alkyne metathesis (Figure 14).[98] The molybdenum-catalyzed alkyne metathesis quantitatively and selectively afforded cyclotrimer **19** on the gram scale without chromatographic separation. The reductive aromatization using sodium naphthalenide smoothly proceeded to give the corresponding alkyne-containing CPP **20** in 70% yield. The obtained alkyne-containing CPP can encapsulate C_{70} fullerene in the inner sphere (theoretically estimated diameter: 1.5 nm), forming an intriguing columnar assembly of 1:1 complex $\mathbf{20}\supset C_{70}$ in the solid state. Because of their high association constant (K_a = $1.02 \pm 0.04 \times 10^5$ M^{-1}), the 1:1 complex could be isolated by silica gel column chromatography and could be stored in open air for more than three months. Three alkyne moieties readily react with azide at 50 °C in the absence of a copper catalyst to give triangle-shaped molecule **21** because of their highly strained structures.

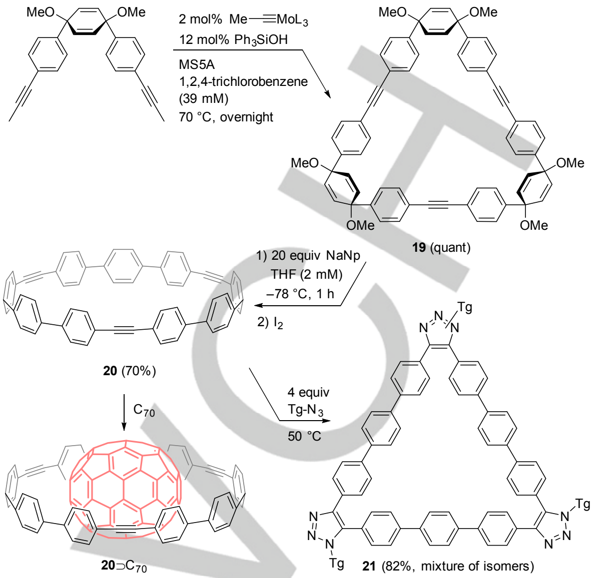

Figure 14. Synthesis of [3]CPP^{3}A **20** and its transformation. L: *tert*-butyl(3,5-dimethylphenyl)amino, NaNp: sodium naphthalenide, Tg–N$_3$: $H_3C(OCH_2CH_2)_3N_3$.

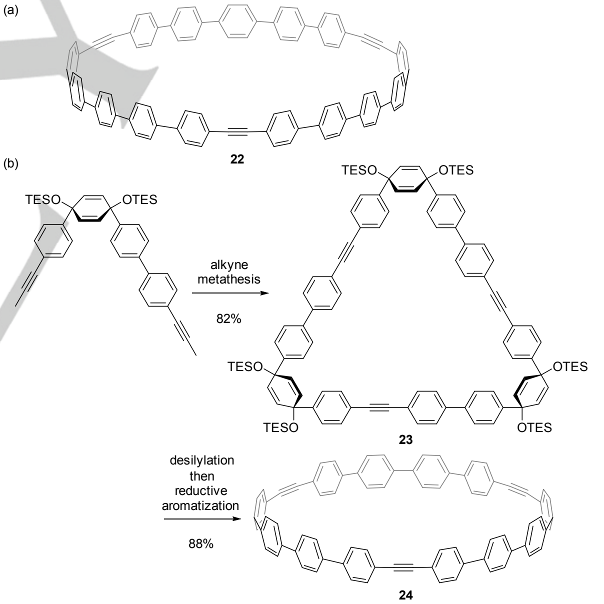

Figure 15. (a) [3]CPP^{5}A **22**. (b) Synthesis of [3]CPP^{4}A **24**. TES: triethylsilyl.

Most recently, Lee and co-workers synthesized alkyne-containing CPP derivative [3]CPP^{5}A **22** and [3]CPP^{4}A **24** by a similar method (Figure 15).[99] Interestingly, the metathesis macrocyclization of unsymmetrical diynes proceeded efficiently, affording the precursor **23** in 82% yield. The reductive aromatization using sodium naphthalenide proceeded efficiently to afford [3]CPP^{n}As in high yields. It is noted that tin-mediated reductive aromatization is not effective in their system even under the improved conditions using H_2SnCl_4 developed by Yamago.[100]

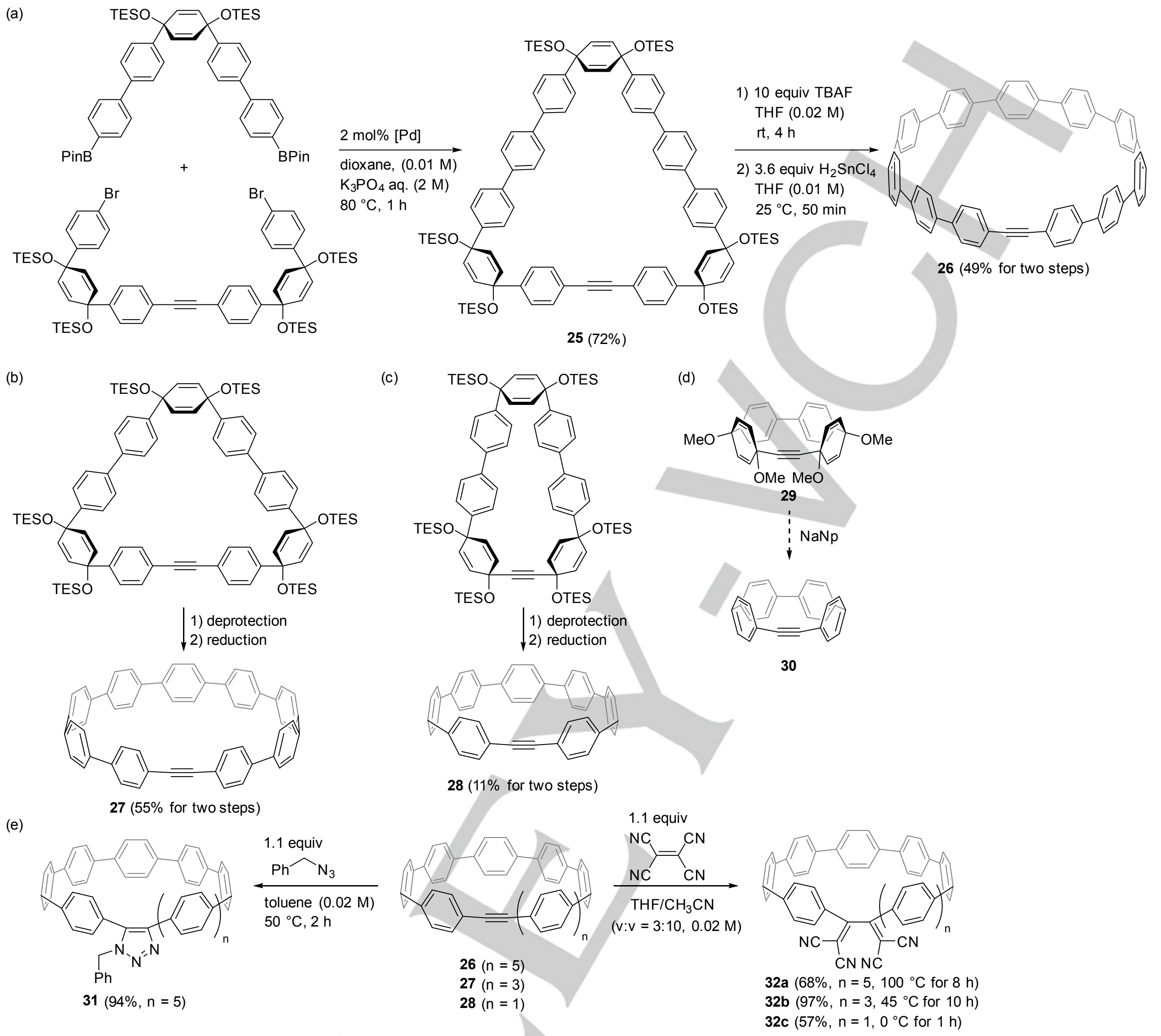

Figure 16. Synthesis of alkyne-containing (a) [11]CPP **26**, (b) [9]CPP **27**, and (c) [7]CPP **28**. (d) Synthetic approach to highly-strained alkyne-containing CPP **30**. (e) Transformation of alkyne-containing CPPs. BPin: 4,4,5,5-tetramethyl-1,3,2-dioxaborolan-2-yl, [Pd]: (2-dicyclohexylphosphino-2’,6’-dimethoxybiphenyl)[2-(2’-amino-1,1’-biphenyl)]palladium(II) methanesulfonate (Buchwald G3 precatalyst).

Alkyne-containing [11]-, [9]-, and [7]CPP derivatives **26**, **27**, and **28** were prepared by Jasti and co-workers (Figures 16a–c).[101] The Suzuki–Miyaura coupling reaction was applied to this end. The coupling reaction efficiently proceeded to afford the precursor **25** in 72% yield. The corresponding precursors of **27** and **28** were prepared in good yields as well. The modified tin-mediated reductive aromatization developed by Yamago and co-workers[100] furnished alkyne-containing CPP derivatives **26** and **27** in good yields (50–57%), though highly strained **28** was obtained in low yield (11%). The same research group reported that the more strained precursor **29** could not be converted to the corresponding alkyne-containing CPP **30** because of large strain energy (473 kJ mol^{-1}) and highly strained alkyne angle (149°) (Figure 16d).[102] The high reactivity of strained alkyne embedded in a CPP skeleton was well supported by the DFT calculation of the Diels–Alder reaction.[103] The theoretical study suggests that the origin of the enhanced reactivity of curved alkynes is attributed not only to the deformation energy but also to the strong interaction energy between the reactants. The DFT calculation also revealed that the frontier molecular orbitals exhibit a significant contribution from the alkyne-centered orbitals, which indicates the high reactivity of angle-strained alkyne. Alkyne-containing [11]CPP derivative **26** undergoes strain-promoted azide–alkyne cycloaddition with benzyl azide to give the corresponding adduct **31** under mild conditions without copper catalyst (Figure 16e). In the case of [2+2]cycloaddition–

retrocyclization (CA–RC) with tetracyanoethene, the reactivity of strained alkyne depends on ring sizes. The [2+2]CA–RC of **28** proceeded at 0 °C within 1 h to give the corresponding adduct **32c** in modest yield, while the [2+2]CA–RC of **26** and **27** giving **32a** and **32b** needed higher temperature and increased reaction time.

The structural information of alkyne-containing CPP derivatives is summarized in Figure 17. The bond angles ($\angle_{sp}$) of alkynes in the complex **20**$\supset C_{70}$ are 164.0–168.3°, determined by X-ray crystallographic analysis (CCDC: 1500189). The minor and major ring axes of **26** (CCDC: 1858070) and **27** (CCDC: 1858071) are 1.54/1.64 nm and 1.27/1.38 nm, respectively, indicating that both molecules are slightly distorted into an ellipsoidal shape. As expected from the failure of isolation of macrocycle **30**, an alkyne in a small ring system is predicted to be highly strained ($\angle_{sp}$ = 149°).

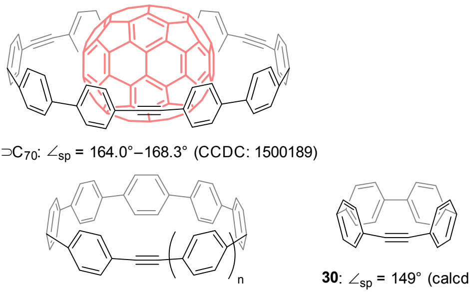

20$\supset C_{70}$: $\angle_{sp}$ = 164.0°–168.3° (CCDC: 1500189)

30: $\angle_{sp}$ = 149° (calcd)

26 (n = 5): $\angle_{sp}$ = 166(1)° (CCDC: 1858070)
27 (n = 3): $\angle_{sp}$ = 160.5(7)°, 162.8(8)° (CCDC: 1858071)
28 (n = 1): $\angle_{sp}$ = 159.4° (calcd)

Figure 17. Bond angles at sp carbons in paracyclophynes (ethynylene units < phenylene units).

3.4. *para*-Cyclophynes: ethynylene units = phenylene units

3.4.1. Synthesis of CPPAs and their supramolecular chemistry

Macrocycles consisting of *para*-phenyleneethynylene, which are so-called CPPA, are one of the most attractive π-conjugated macrocycles (Figure 18). Pioneering work on CPPAs **33** was reported by Oda, Kawase, and co-workers in 1996.[27] The preparation and supramolecular complexation with fullerenes or smaller size CPPAs have been summarized in other review articles.[31,37,38,104] In this section, their method, as well as recent advances in this area, are overviewed.

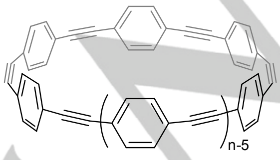

[4]CPPA **33a** (n = 4)
[5]CPPA **33b** (n = 5)
[6]CPPA **33c** (n = 6)
[7]CPPA **33d** (n = 7)
[8]CPPA **33e** (n = 8)
[9]CPPA **33f** (n = 9)

Figure 18. Cycloparaphenyleneacetylenes **33**.

Oda, Kawase, and co-workers first reported the synthesis of [n]CPPA,[27] in which the macrocyclization via low-valent titanium-mediated McMurry coupling[105] afforded a stereoisomeric mixture of cycloparaphenylenevinylenes as a precursor of CPPAs (Figure 19).[106] Macrocycles **34b** and **34c** were efficiently converted to [6]CPPA **33c** and [8]CPPA **33e** through bromination and base-mediated dehydrobromination sequence, although a mixture of inseparable stereoisomers of precursors was used. The transformation of macrocycle **34a** did not afford [4]CPPA **34a** because of its instability under strongly basic conditions. [4]CPPA readily reacted with *tert*-butoxide to form π-conjugated macrocycle **35** having two vinyl ether moieties.[27] The dehydrobromination of **34a** followed by Diels–Alder reaction with furan gave the adduct **36** as a mixture of diastereoisomers. The furan adduct **36** was aromatized by utilizing low-valent titanium reagent to afford angle-strained alkyne-containing macrocycle **37**.

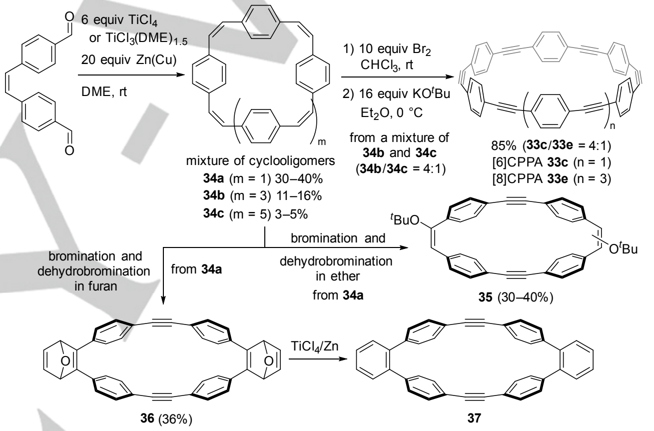

Figure 19. Bromination and dehydrobromination sequence for preparation of [6]CPPA and [8]CPPA and transformation of **34a**. DME: 1,2-dimethoxyethane.

The McMurry coupling of **38** in a mixed solvent system (DME:toluene = 1:1) dramatically improved the macrocyclization efficiency, predominantly producing *ZZEZZE*-cyclohexamer **34b** in good yield while suppressing the formation of cyclotrimer (Figure 20a).[107] This finding then improved the access to [6]CPPA as well. The modified McMurry coupling afforded cyclopentamer **39**, which could be smoothly converted to [5]CPPA **33b** as the smallest CPPA so far reported (Figure 20b).[108] The coupling of dialdehydes **38** and **40** (1:1 ratio) enabled production of the precursor of [7]CPPA **33d** (Figure 20c).[107] [9]CPPA **33f** was obtained by the coupling of *ZZ*-**38** and *ZE*-**38** (3:1 ratio), although separation from the major product [6]CPPA **33c** was necessary (Figure 20d).[107] By employing the McMurry coupling–bromination–dehydrobromination sequence, 1,4- and 2,6-naphthylene-containing [6]CPPA derivatives **41** and **42** were successfully synthesized (Figure 21).[109] To create a deep cavity in the ring system, cyclic [6](1,4)naphthyleneacetylene ([6]CNA) **43** was synthesized by a similar synthetic procedure.[110]

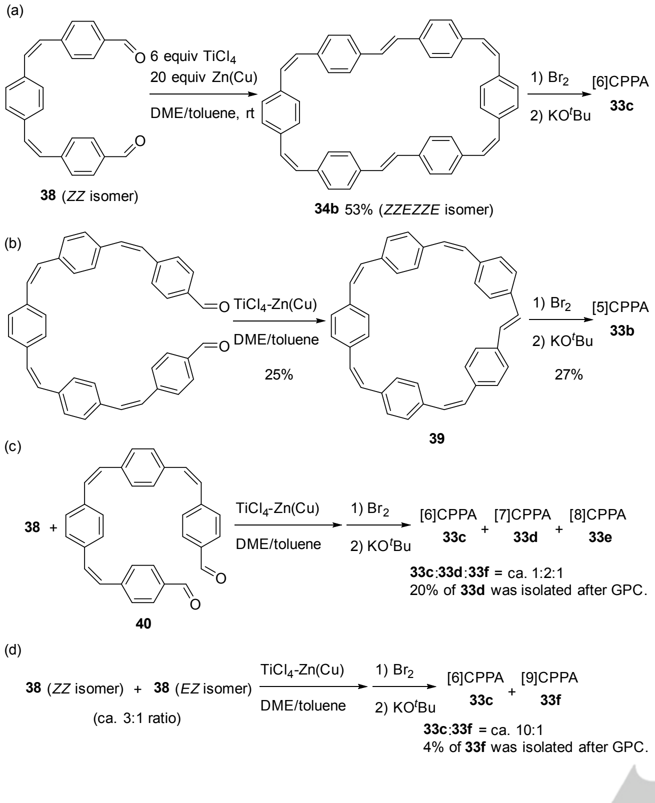

Figure 20. Modified McMurry coupling for preparation of (a) [6]CPPA **33c**, (b) [5]CPPA **33b**, (c) [7]CPPA **33d**, and (d) [9]CPPA **33f**.

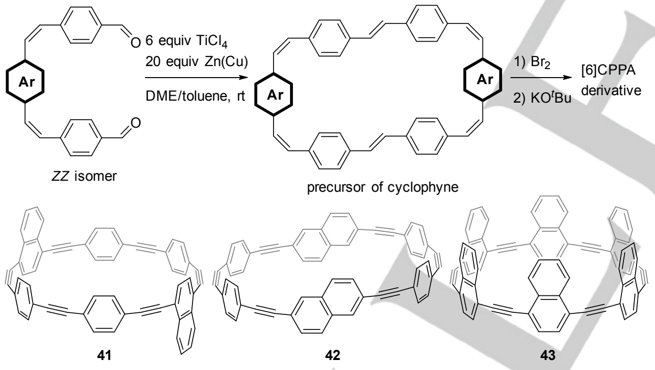

Figure 21. Synthesis of naphthylene-containing CPPA derivatives.

Because of the symmetrical belt-shaped structure of [n]CPPAs, the strong convex–concave π–π interaction in the cavity of nanorings was anticipated. Kawase, Oda, and co-workers succeeded in the encapsulation of hexamethylbenzene[111–113] and fullerenes[28,114] with [6]CPPAs to afford 1:1 complexes (Figure 22). The Gibbs activation energy for dissociation of **33c**⊃C_{60} complex is 41 ± 1.3 kJ mol^{-1} in CD_2Cl_2, which is similar to that of **33c**⊃C_{70} complex (40 ± 0.8 kJ mol^{-1}).[113] From a DFT calculation of **33c**⊃C_{60} complex,[115–117] the center of [6]CPPA is aligned to the center of C_{60}, forming a symmetric structure. The binding energy was estimated to be 117 kJ mol^{-1}. Two *ortho* protons (H_a and H_b) of phenylene moieties in the **33c**⊃C_{70} complex were independently observed by variable temperature NMR measurement in CD_2Cl_2 at –90 °C. Three optimized structures of the **33c**⊃C_{70} complex were estimated by DFT calculations, where C_{70} is standing, lying, or half-lying (Figure 22).[116,117] The inclusion structure, where C_{70} is standing, was estimated to be the most stable (binding energy: 130–134 kJ mol^{-1}). The binding energies of the other two optimized structures were only 8–17 kJ mol^{-1} smaller than the standing structure. As expected experimentally and theoretically, the center of C_{70} is about 0.11 nm above the center of [6]CPPA in the most stable structure.

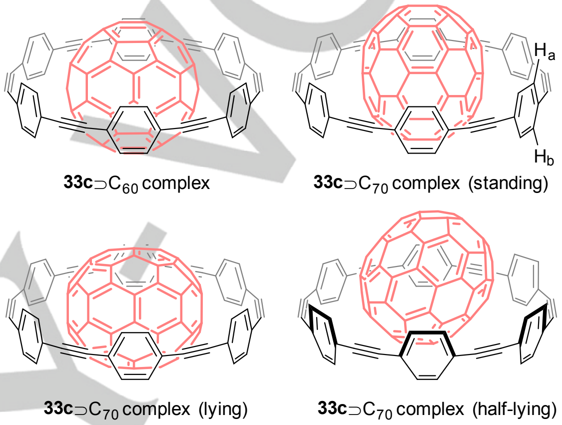

Figure 22. [6]CPPA–fullerene complexes.

By introducing 1,4-naphthylene moieties in [6]CPPA, the binding constants for both C_{60} and C_{70} dramatically increased.[109,110] In the case of **42**, the incorporation of two 2,6-naphthylene moieties changed the CPPA shape ellipsoidally, enhancing the encapsulation toward C_{70}. The encapsulation of [6]CPPA with C_{60} and C_{70} derivatives revealed that the host–guest interaction is affected by the electronic properties of substituents on fullerenes rather than their bulkiness.[114] Further information about the encapsulation properties of CPPA derivatives with fullerenes, including dynamic motion, is summarized in Kawase's account paper.[104]

Based on the strong interaction of CPPAs with the convex π-system, Kawase, Oda, and co-workers anticipated the formation of ring-in-ring complexes. In fact, the ring-in-ring complex of dibenzo[6]CPPA and tribenzo[9]CPPA was detected by NMR measurement (Figure 23).[118] Furthermore, in the presence of C_{60}, a double inclusion complex tribenzo[9]CPPA⊃dibenzo[6]CPPA⊃C_{60} **44** was observed. From the titration experiments, it was revealed that the association constant of [9]CPPA⊃[6]CPPA complex **46** (ca 40 M^{-1}) is much smaller than that of [8]CPPA⊃[5]CPPA **47** complex (9200 ± 1400 M^{-1}) in $CDCl_3$ at 30 °C.[118] The association constant of tribenzo[9]CPPA⊃dibenzo[6]CPPA **45** is 470 ± 80 M^{-1}, which is larger than for **46** due to the π-expanded structure. The difference of association constants can be attributed not only to van der Waals forces but also electrostatic and charge-transfer interactions. This finding points out the difference in electronic properties between planar and curved π-conjugated systems.

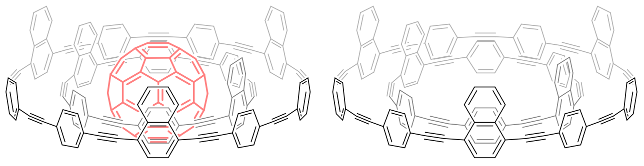
tribenzo[9]CPPA$\supset$dibenzo[6]CPPA$\supset C_{60}$ complex **44** tribenzo[9]CPPA$\supset$dibenzo[6]CPPA complex **45**

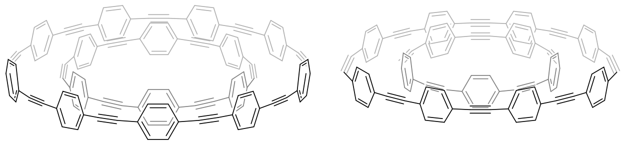
[9]CPPA$\supset$[6]CPPA complex **46** [8]CPPA$\supset$[5]CPPA complex **47**

Figure 23. Ring-in-ring complexes.

Because the benzo-fused CPPA showed better encapsulation ability for fullerenes, CPPAs bearing polyaromatic compounds were considered to be more favorable host molecules for fullerenes. More recently, Miki, Ohe, and co-workers demonstrated the preparation of anthracene-containing CPPAs through an alternative synthetic method and their encapsulation ability.[119] The Sonogashira–Hagihara coupling reaction followed by tin-mediated reductive aromatization produced anthracene-containing [6]CPPA derivatives **48** and **49** (Figure 24). The palladium- and copper-catalyzed cyclotrimerization of 9,10-diethynyl-9,10-dimethoxy-9,10-dihydroanthracene with 1,4-diiodobenzene afforded the precursor **50** of [6]CPPA in 15% yield together with cyclodimer (3%) (Figure 25a). The precursor **51** having electron-rich *n*-butoxy groups was also obtained in 15% yield, indicating that the macrocyclization of small fragments is not efficient enough to provide precursors in high yield. [6]CPPA **48** has not yet been isolated through the conventional tin-mediated reductive aromatization of the corresponding precursor **51** due to the low stability of strained alkynes under strongly acidic conditions (1 N HCl(aq)). In contrast, in the presence of C_{60}, the [6]CPPA–fullerene (**48**$\supset C_{60}$) complex was obtained in 51% yield, though excess amounts of tin(II) chloride were necessary. This finding pointed out that the strong encapsulation of guest molecule C_{60} inhibits strained alkyne moieties of the host molecule from decomposition. The association constant (K_a) was roughly estimated at more than 5.0×10^6 M^{-1} by NMR measurement, which was larger than for the **33c**$\supset C_{60}$ complex. This result also supports the notion that the introduction of polyaromatics in CPPAs enhances the C_{60} encapsulation ability. The electron-rich [6]CPPA derivative **49** also acts as a good host molecule for C_{60}.

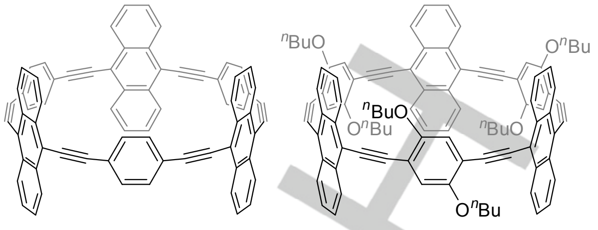

[6]CPPA derivative **48** [6]CPPA derivative **49**

Figure 24. Anthracene-containing CPPAs.

Based on the high encapsulation ability of anthracene-containing CPPA derivatives, Miki, Ohe, and co-workers demonstrated the synthesis of twin [6]CPPA derivatives, in which two [6]CPPAs are hinged by one benzene ring, and its encapsulation of two C_{60} molecules (Figure 25b).[119] The precursors **55** and **56** were synthesized by stepwise cross-coupling of **52** with dihydroanthracene **53** or **54**. The precursor **55** underwent reductive aromatization in the presence of excess amounts of C_{60} to give twin [6]CPPA–fullerene 1:2 complex (**57**$\supset 2C_{60}$), which was detected by MALDI-TOF mass spectrometry. After forming **57**$\supset C_{60}$, the electron density of the host [6]CPPA is decreased by charge-transfer interaction. The second complexation afforded unstable 1:2 complex **57**$\supset 2C_{60}$, which decomposed during purification. In contrast, the reductive aromatization of **56** having electron-rich butoxy groups afforded twin [6]CPPA–fullerene 1:2 complex (**58**$\supset 2C_{60}$) in good yield. Furthermore, electron-rich twin [6]CPPA derivative captured two methanofullerene **mC₆₀** efficiently under identical conditions, affording the **58**$\supset$**2mC₆₀** complex in good yield. The first cathodic process corresponding to the reduction of the fullerene entity of **48**$\supset C_{60}$, **49**$\supset C_{60}$, and **58**$\supset 2C_{60}$ was –1.16 V, –1.29 V, and –1.28 V (vs Fc^+/Fc), respectively. All one-electron reduction peaks were cathodically shifted by 60–180 mV as compared with that of a pristine C_{60} (–1.10 V). This difference in cathodic shifts indicates that there is charge-transfer interaction between C_{60} and electron-rich [6]CPPAs **49** and **58**.

Truhlar and co-worker clarified that the binding energy (181 kJ mol^{-1}) between [6]CPPA and (5,5)-carbon nanotube (CNT) is much larger than that between [6]CPPA and C_{60} (117 kJ mol^{-1}) from DFT calculation.[115] Based on this background, Miki, Ohe, and co-workers carried out the complexation of anthracene-containing CPPAs with CNTs.[120] The cross-coupling of large fragments afforded the precursors **60**–**63** in good yields (Figure 26). In contrast to the synthesis of [6]CPPA derivatives **48** and **49**, CPPA derivatives **64**–**67** were obtained by the modified tin-mediated reductive aromatization using H_2SnCl_4[100] without guest molecules. [9]- and [10]CPPA derivatives **65**–**67** could be stored in a refrigerator in the dark for several months. In contrast, [8]CPPA **64** in the solid state gradually decomposed, probably due to the high reactivity of strained alkynes.

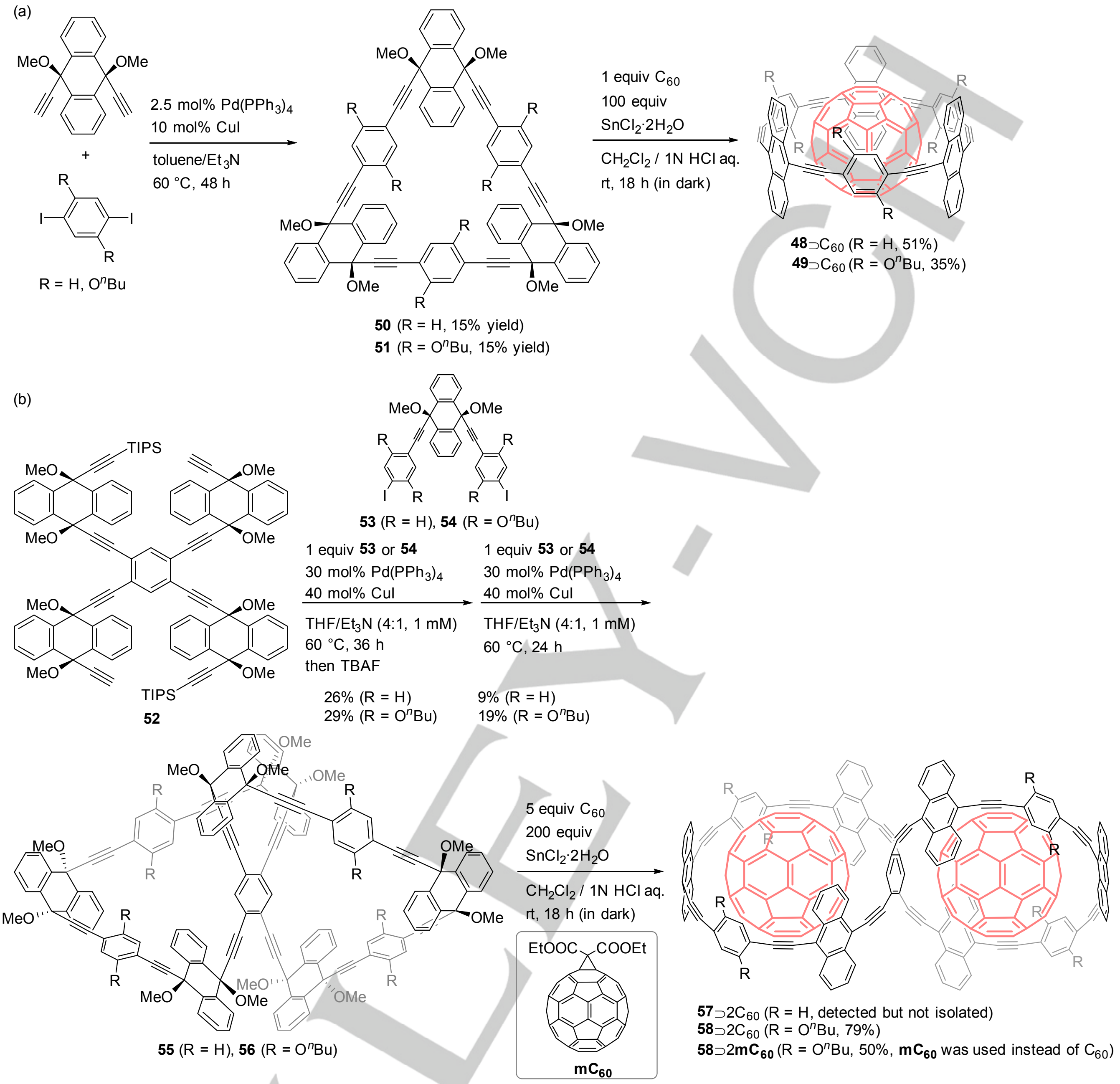

Figure 25. Preparation of inclusion complexes of (a) anthracene-containing [6]CPPA and (b) twin [6]CPPA derivatives with C$_{60}$.

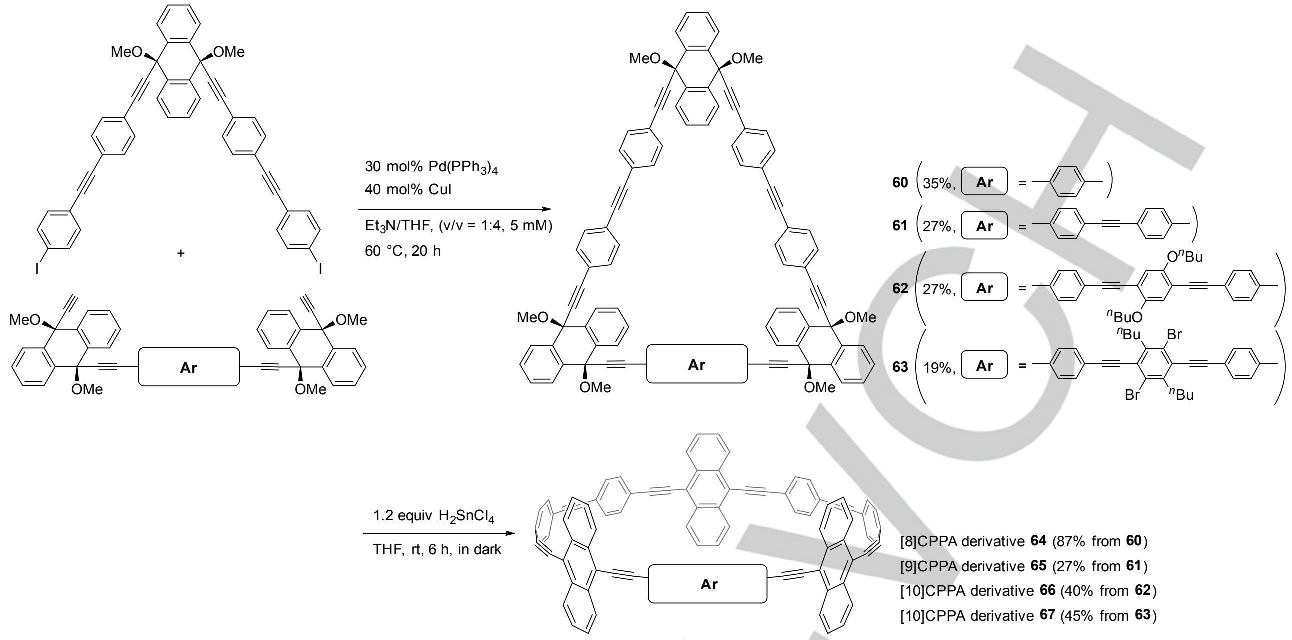

Figure 26. Preparation of anthracene-containing [8]-, [9]-, and [10]CPPA derivatives.

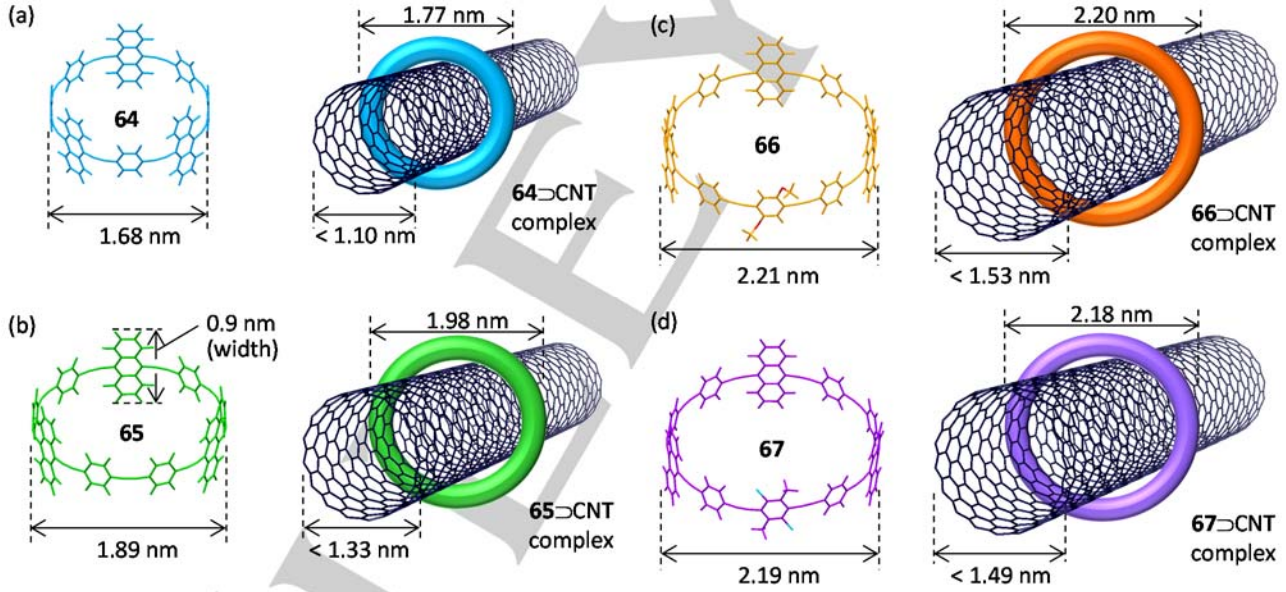

Figure 27. Energy-minimized structure of CPPAs (a) **64**, (b) **65**, (c) **66**, and (d) **67**. Butoxy and butyl groups in **66** and **67** were replaced to methoxy and methyl groups, respectively. Schematic illustration of optimized CPPA⊃CNT complexes. Reproduced with permission from ref. 120. Copyright 2018 Wiley-VCH Verag GmbH & KaA, Weinheim.

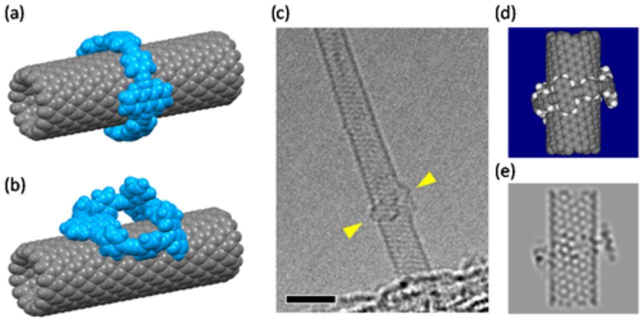

Figure 28. (a) “Tube-in-ring” and (b) “ring-on-tube” structures of CPPA⊃CNT complex of (14,0)CNT and **64** optimized with Forcite program and visualized by Mercury 3.6 software. Both terminals of CNT are capped with hydrogen atoms. (c) High-resolution TEM image of **65**⊃CNT **R** complex. Scale bar, 2 nm. (d) Model structure of the complex of (11,6)-CNT and CPPA **65**. (e) Corresponding TEM image simulation. Reproduced with permission from ref. 120. Copyright 2018 Wiley-VCH Verag GmbH & KaA, Weinheim.

The energy-minimized structures of [8]-, [9]-, and [10]CPPAs were calculated at the B3LYP/6-31G(d) level of theory (Figure 27). The diameters of anthracene-containing CPPAs **64**–**67** were 1.68, 1.89, 2.21, and 2.19 nm, respectively. These values are slightly smaller than those of CPPAs ([8]CPPA **33e**: 1.74 nm, [9]CPPA **33f**: 1.96 nm, based on an AM1 calculation) reported by Kawase and co-workers.[108] Interestingly, calculations showed that the ring sizes of CPPAs **64** and **65** could be expanded by 0.1 nm through complexation, whereas no expansion of **66** and **67** was found. The diameters of the CNTs that can be interlocked by CPPAs **64**–**67** were estimated at 1.10, 1.33, 1.53, and 1.49 nm, respectively. Both “tube-in-ring” complexation and “ring-on-tube” complexation were optimized by force field calculations with the Forcite program (Figure 28a and 28b). The “ring-on-tube” complexation is stabilized by C–H–π interaction as well as π–π interaction of one of three anthracene moieties or one of three phenyl moieties with a curved CNT surface.

The complexation with single-walled CNTs **P** (diameter (ϕ) = 0.7–1.0 nm), **Q** (ϕ = 1.1–1.4 nm), and **R** (ϕ = 1.2–1.6 nm) clarified that CNTs **P**, **Q**, and **R** preferentially interact with [8]CPPA **64**, [9]CPPA **65**, and [10]CPPA **66**, respectively. The good size fit is important for the formation of rotaxane-like structures of CNTs.

High-resolution transmission electron microscopy (TEM) of the **65**⊃CNT **R** complex revealed that CPPAs could interact with CNTs in the “tube-in-ring” manner (Figure 28c). The model structure of the CPPA⊃CNT complex of (11,6)-CNT and **65** showed good agreement with the TEM image (Figure 28d and 28e). The “tube-in-ring” complexation was also supported by scanning probe microscopy, thermogravimetric analysis, and Raman spectroscopy. This “ring toss” method for the preparation of functionalized CNTs, such as water-soluble CNTs, will find application in electronic and biomedical applications.

Table 1. Spectral data of CPPAs.

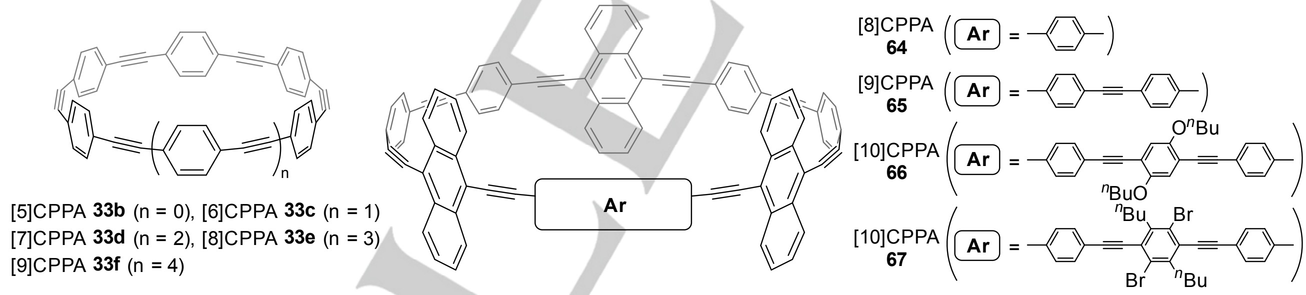

[5]CPPA **33b** (n = 0), [6]CPPA **33c** (n = 1)
[7]CPPA **33d** (n = 2), [8]CPPA **33e** (n = 3)
[9]CPPA **33f** (n = 4)

CPPAs	δ(phenylene) in ^{1}H NMR (ppm)[a]	bond angle ($\angle_{sp}$)[b]	absorbance λ_{max} (nm) [log ε][c]	emission λ_{max} (nm) [Φ][c]	CPPAs	δ(phenylene) in ^{1}H NMR (ppm)[a]	bond angle ($\angle_{sp}$)[b]	absorbance λ_{max} (nm) [log ε][c]	emission λ_{max} (nm) [Φ][c]
[5]CPPA **33b**	7.15	162.5°	346 [5.02]	449, 461	[8]CPPA **64**	7.53[e]	168.9°–170.0°	467 [4.77]	563 [0.005]
[6]CPPA **33c**	7.35	165.5° [164.4°][d]	349 [5.40]	471 [0.27]	[9]CPPA **65**	7.48, 7.60	169.9°–171.2°	467 [5.17]	530, 568 [0.90]
[7]CPPA **33d**	7.36	167.6°	355 [5.41]	418, 448	[10]CPPA **66**	7.56[e]	171.2°–172.2°	467 [5.21]	527, 564 [0.92]
[8]CPPA **33e**	7.40	169.2° [168.6°][d]	355 [5.47]	416, 447 [0.15]	[10]CPPA **67**	7.68[e]	171.2°–172.1°	468 [5.15]	526, 563 [0.81]
[9]CPPA **33f**	7.43	170.4°	354 [5.51]	414, 442					

[a] In CDCl$_3$. [b] Calculated at B3LYP-6-31G(d) level. [c] In cyclohexane for **33**, in CHCl$_3$ for **64**–**67**. [d] Average bond angle determined by X-ray crystallographic data in ref. 111. [e] Averaged values of phenylene units of molecules. In the case of **66**, butoxy-substituted phenylene protons were omitted.

3.4.2. Photophysical properties of CPPAs

The specific properties of CPPA and anthracene-containing CPPAs are summarized in Table 1. In the ^{1}H NMR spectra, all phenylene protons were equally observed, indicating the highly symmetric nature of CPPAs **33**.[104] There are no large differences in chemical shifts of phenylene protons except for [5]CPPA **33b**.[104,108] A significant difference in chemical shifts between the [4n+2] π-electron system in odd-numbered CPPAs and the [4n] π-electron system in even-numbered CPPAs was not observed. Although the bathochromic shift of absorption maximum is not significant, the emission spectra broadened and shifted bathochromically as the ring size decreased. From the DFT calculation, the HOMO–LUMO transition is forbidden and the strong absorption can be assigned to the sum of HOMO–2 to LUMO, HOMO–1 to LUMO, HOMO to LUMO+1, and HOMO to LUMO+2 transitions, resulting in the small difference in absorption maxima of CPPAs.[120] A similar tendency was found in the CPP chemistry.[121] As to emission spectra, the bathochromic shift in smaller rings is explained by the release of the strain energy in the excited state of CPP. The emission of CPPAs is such a case. Compared with the emission spectrum of [6]CPPA, that of [5]CPPA shifted hypsochromically, probably due to the increased strain and rigidity.

In the ^{13}C NMR spectra, the sp carbon was observed at a lower field like the sp^{2} carbon, as the ring size of CPPA became smaller. This result supports the notion that the contribution of quinoid form increases as the ring size of CPPA decreases. This tendency is also similar to CPPs.[121]

The solid-state structures of [6]CPPA **33c** and [8]CPPA **33e** with guest molecules were determined using X-ray crystallographic analysis (CCDC: 153427 and 153428).[111] The bond angles at sp carbons are in the range of 162.5–165.6° (average: 164.4°) and 164.3–171.4° (average: 168.6°), respectively. The structure of 1:1 complex of [6]CPPA **33c** with methanofullerene mC_{60} was also determined using X-ray analysis (CCDC: 199147).[28] In the solid state, methanofullerene is captured on the bowl-shaped [6]CPPA. The bond angles ($\angle_{sp}$ = 162.2–166.2° (average: 164.5°)) are similar to those of [6]CPPA with hexamethylbenzene (CCDC: 153427).

As to anthracene-containing CPPAs **64**–**67**, no significant influence of ring size in ^{1}H NMR chemical shift of phenylene protons, absorption maximum, and emission maximum was observed.[120] Although the molar extinction coefficients (ε) of CPPAs **64**–**67** are larger than 10^{5} cm^{-1} M^{-1}, the quantum yield (Φ = 0.005) of [8]CPPA is much smaller than those of the others (Φ = 0.81–0.92). The absorption and emission spectra of [8]CPPA **64** ($\angle_{sp}$ = 168.9–170.0°) and [9]CPPA **65** ($\angle_{sp}$ = 169.9–171.2°) have been reported (Figure 29).[120] From the time-dependent (TD)-DFT calculation, the shoulder signal of around 550 nm in the absorption spectrum of [8]CPPA **64** is assigned as vertical transitions, including the HOMO–LUMO transition, which is forbidden in **65** but allowed in **64**. Because linear oligo(*p*-phenyleneethynylene)s exhibit high ε and Φ values, the larger CPPAs may not show specific strain-induced photophysical properties. This difference in the photophysical properties between [8]CPPA ($\angle_{sp}$ < 170°) and [9]CPPA ($\angle_{sp} \geq$ 170°) supports the notion that the arbitrarily defined borderline of angle ($\angle_{sp}$ = 170°)[27] between strained and unstrained alkynes seems to be quite reasonable.

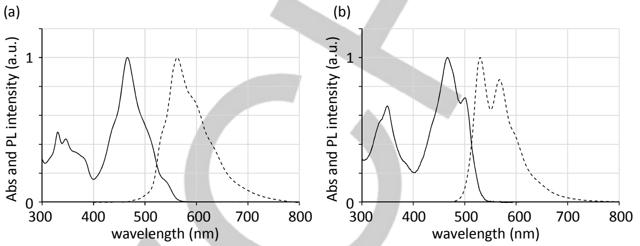

Figure 29. UV-vis (solid) and photoluminescence (dotted) spectra of (a) [8]CPPA **64** and (b) [9]CPPA **65**. Reprinted with permission from ref. 120. Copyright 2018 Wiley-VCH Verag GmbH & KaA, Weinheim.

3.5. Related π-conjugated macrocycles bearing angle-strained alkynes

To clarify its high reactivity and specific photophysical properties, angle-strained alkyne-containing macrocycles with various π-conjugated spacers instead of *para*-phenylene were also investigated. The representative macrocycles are summarized in this section.

3.5.1. *ortho*-Phenylene and *meta*-phenylene spacers

Dehydroannulenes are a family of π-conjugated macrocycles consisting of oligoenes and at least one alkyne. By introducing several alkynes in the macrocyclic system, planar π-conjugated molecules have been designed and synthesized for investigation of their aromaticity and application to electronic materials. Dehydroannulene analogues, such as dehydrobenzoannulenes, in which oligoethynylene, oligovinylene, or a mixture of ethynylene and vinylene are bridged by *ortho*-phenylene moieties, are also attractive molecules as optoelectronic materials and precursors of new two- or three-dimensional carbon networks.[35,122] So far, researchers have created a variety of dehydroannulene derivatives with angle-strained alkyne moieties. Their highly strained mono- and oligoethynylene structures were anticipated by DFT calculations and confirmed by X-ray crystallographic analyses. The representative molecules having angle-strained alkynes are summarized.

Cyclooctatetraene is one of the [4n]annulenes with a tub-shaped conformation. Dehydro[8]annulenes, such as cycloocta-1,5-diene-3,7-diyne (**68**), would presumably be planar, but its isolation has not been reported (Figure 30a). Stevenson and co-workers reported the generation of radical anion of **68** from 1,4-dibromocyclooctatetraene (Figure 30b).[123] Benzo-fused derivative **69** was synthesized through photoinduced bromination of biphenylene and base-mediated dehydrobromination (Figure 30c); however, **69** decomposed within a few minutes at 0 °C due to its low stability.[124] A sharp olefinic singlet peak (δ = 5.07 ppm in CDCl$_3$) was observed at –20 °C, but it gradually disappeared, which means a short lifetime for **69** under ambient conditions. Rapid purification followed by cycloaddition with dienes afforded the corresponding adducts.

5,6,11,12-Tetradehydrodibenzo[*a*,*e*]cyclooctene (**70**), a dehydrobenzo[8]annulene, so-called "Sondheimer diyne," was first synthesized by Wong, Sondheimer, and co-worker in 1974 (Figure 30d).[125] The angle-strained alkyne structure confirmed by X-ray crystallographic analysis was then reported.[126] The bond angles ($\angle_{sp}$) are 155.3–156.4° in the solid state. A much better synthetic method for dehydrobenzo[8]annulene **70** and its derivatives was reported by Orita and co-workers (Figure 30e).[127] The sequential inter- and intramolecular Wittig–Horner-type olefinations and base-mediated elimination of sulfinic acid afforded functionalized dehydrobenzo[8]annulenes in good yields. The same group reported the facile transformation of dehydrobenzo[8]annulenes to pentalenes.[128] The photoinduced elimination of CO from cyclopropenone is also applicable to the generation of dehydrobenzo[8]annulene **70**. The *in situ* generated **70** was efficiently trapped by azide to form bistriazole-fused macrocycle **73** (Figure 30f).[129] This method enabled the conjugation of azide-grafted bovine serum albumin with azide-grafted biotin under physiological conditions. Most recently, Sondheimer diyne was used as an intercalator of DNA.[130] The intercalation enhanced the crosslinking efficiency between azide-grafted base pairs. The related macrocycle **71** was synthesized by Romers, Wong, Sondheimer, and co-workers.[131] The structures of two independent molecules were determined by X-ray analysis, where one is planar and another is slightly tilted (CCDC: 1139955). The bond angles at sp and sp^2 carbons are 151.9–156.1° (average: 154.0°) and 143.9–146.2° (average: 145.0°), respectively. Phenanthrene-fused dehydrobenzo[8]annulene derivative **72** (CCDC: 1268933) was synthesized through a bromination–dehydrobromination sequence.[132] The bond angles at sp carbons are similar to those of **70**. Despite its highly strained structure, dehydrobenzo[8]annulene **72** is stable at high temperature (decomposition temp.: 183 °C). Fukazawa, Yamaguchi, and co-worker reported a new approach to dehydrobenzo[8]annulene through sequential electrocyclization reactions (Figure 30g).[133] Copper-mediated coupling and valence isomerization of dehydrobenzo[16]annulene afforded phenanthrene-fused dehydro[8]annulene **74** in moderate yield.

By replacing the monoyne moieties in dehydro[8]annulenes with diyne and tetrayne moieties, π-expanded dehydroannulenes were synthesized (Figure 31a). Diederich and co-workers synthesized dehydro[12]annulene **75**[134,135] and dehydro[20]annulene **76**[136] by Hay coupling (Figure 31b). The X-ray crystallographic analysis of **75** revealed the planar structure (CCDC: 1229799) and the bond angles of 164.5° and 166.9° at sp carbons, **75** being less strained than dehydrobenzo[8]annulenes. The absorption edge (660 nm (1.87 eV)) and the paratropic character observed in ^{1}H NMR spectrum suggest the antiaromaticity of **75**. The strong intramolecular charge-transfer interactions between peripheral electron-donating *N*,*N*-diisopropylanilino groups and the electron-deficient dehydroannulene core of **76** were suggested by UV–vis absorption spectrometry.

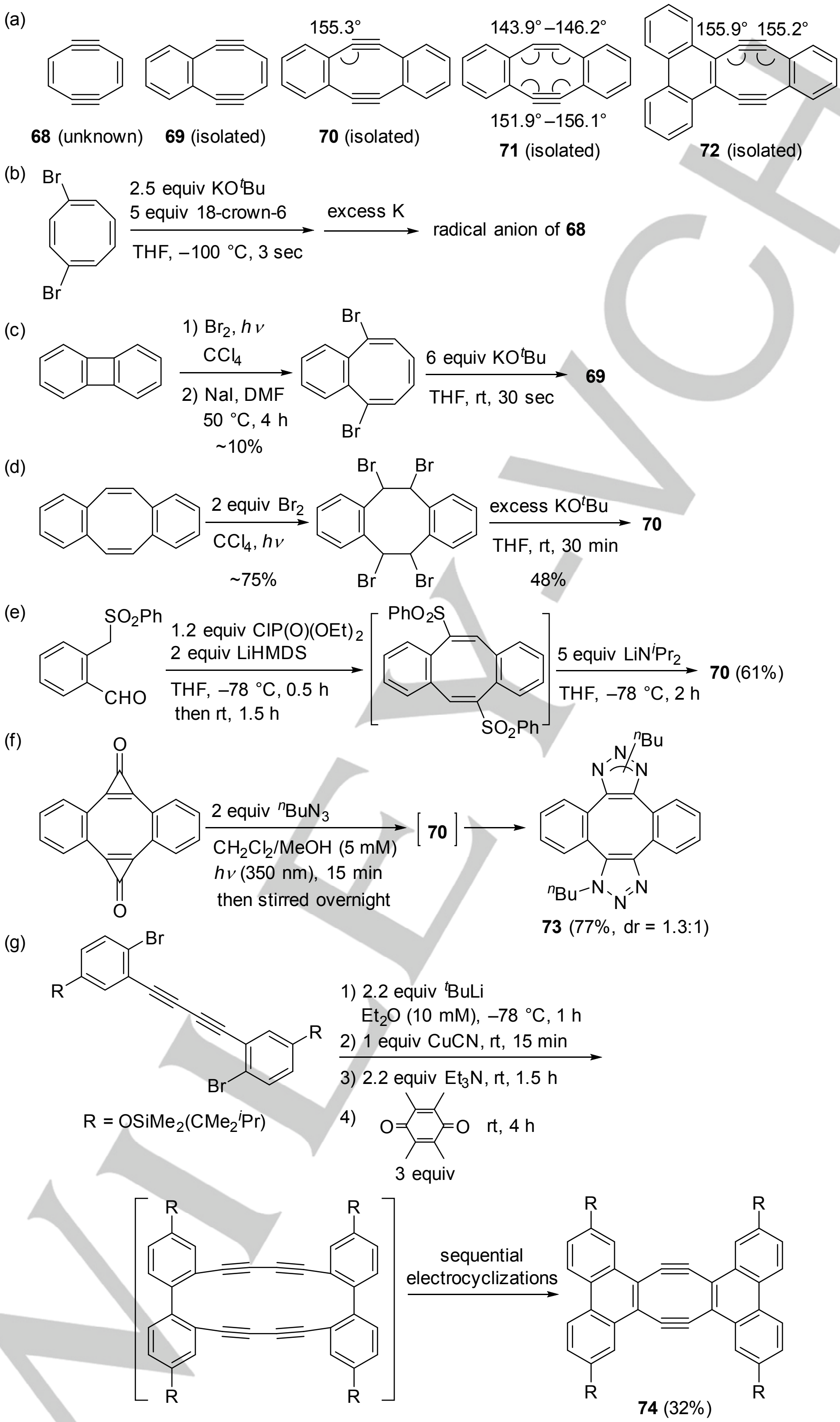

Figure 30. Dehydro[8]annulene and dehydro[8]benzoannulene derivatives: synthesis and transformation. LiHMDS: lithium bis(trimethylsilyl)amide.

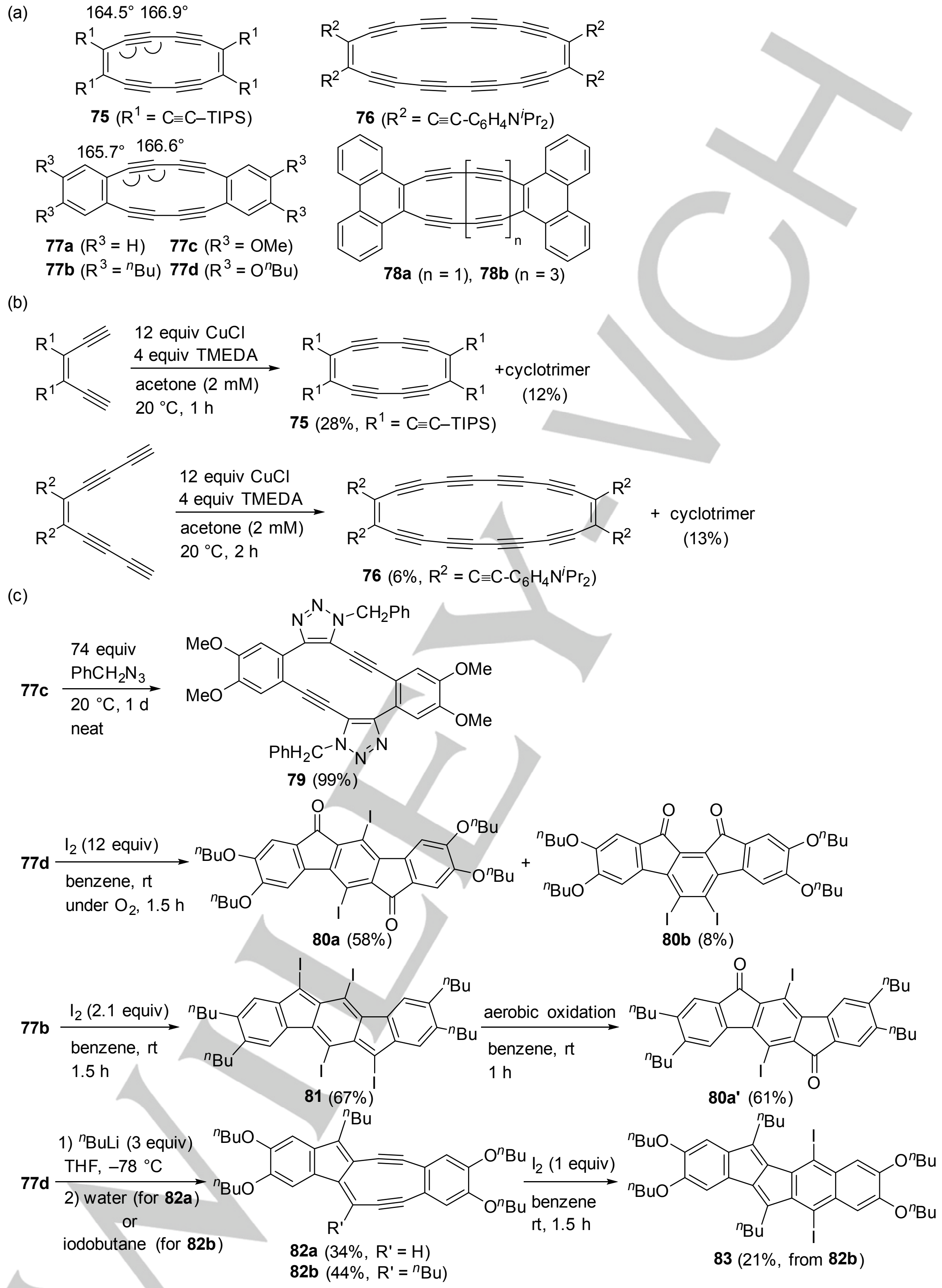

Figure 31. (a)(b) [12]- and [20]dehydroannulenes and dehydrobenzannulene derivatives and (c) their transformation.

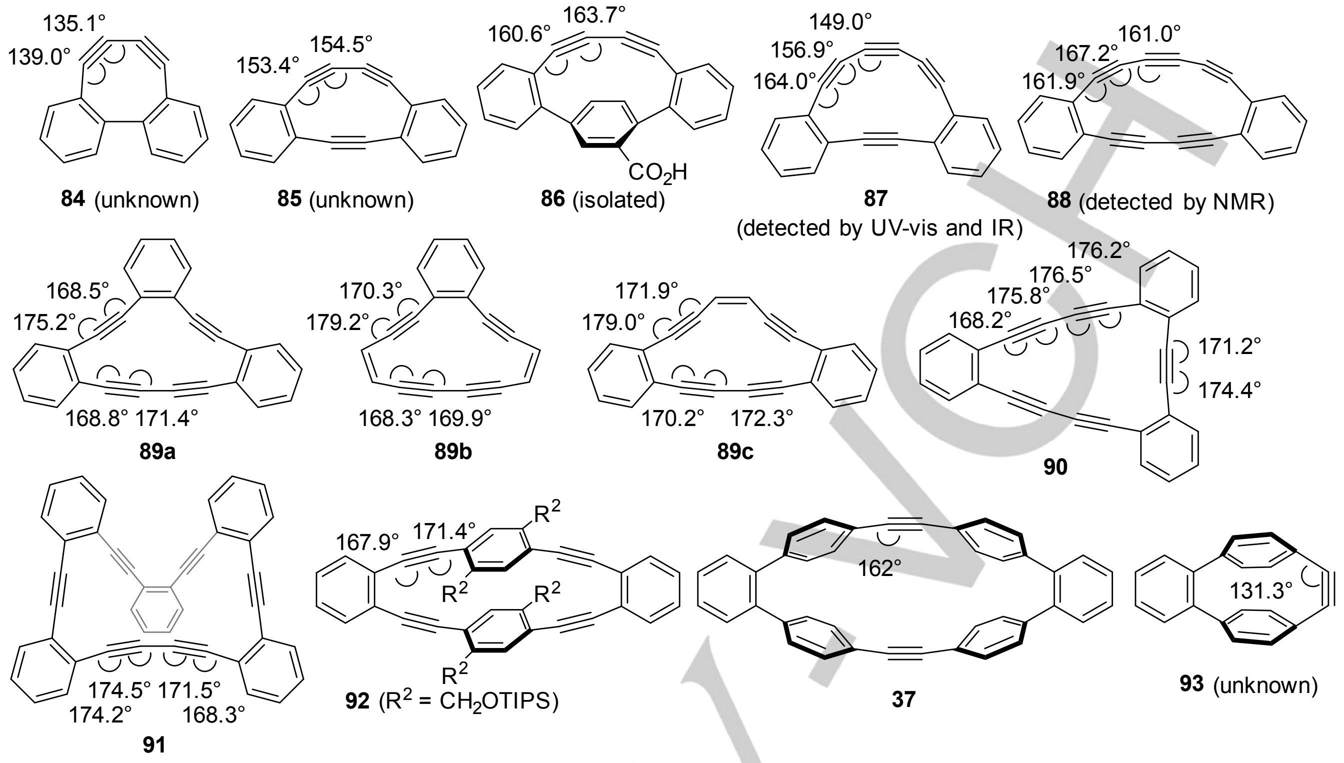

Figure 32. Representative dehydrobenzoannulenes containing *o*-phenylenes. Bond angles of **84**, **85**, **87**, **88**, **89a**, and **93** were given by DFT calculation.

Dehydrobenzo[12]annulene **77a** was synthesized by Eglinton, Raphael, and co-workers using copper-mediated coupling,[137,138] and the strained structure was confirmed later by X-ray crystallographic analysis of **77b** ($\angle_{sp}$ = 165–167°).[139] Its symmetrical and planar π-conjugated structure induced the formation of self-assemblies, such as nanofibers and gels.[140–145] As expected from the highly strained structure, the strain-promoted double azide–alkyne cycloaddition of **77c** takes place regioselectively to give adduct **79** (Figure 31c).[146] The electrophilic cyclization of **77d** using an excess amount of iodine under oxygen atmosphere gave two types of diiododiones, **80a** and **80b**.[147] The electrophilic cyclization of **77b** using two equivalents of iodine gave tetraiodide **81**, which smoothly converted to **80a'** under aerobic conditions.[139] The electrophilic cyclization of **77d** using *n*-butyllithium proceeded to give the bicycle[7.3.0] ring system **82** in moderate yield.[148] By treating **82b** with iodine, diiodobenzonaphthopentalene **83** was obtained through the electrophilic cyclization of the strained nine-membered ring. In contrast to **75**, dehydrobenzo[12]annulene **77a** does not exhibit paramagnetic properties and its absorption maximum was observed at around 450 nm (2.74 eV).

The copper-mediated cyclodimerization furnished phenanthrene-fused dehydro[12]annulene **78a**.[149] Although benzo-fused dehydro[20]annulene was not isolated,[150] phenanthrene-fused dehydro[20]annulene **78b** was synthesized by a similar copper-mediated cyclodimerization.[151]

Because of highly strained bond angles at sp carbons (135.1° and 139.0°), tetradehydrodibenzocyclooctene **84** has not been isolated so far (Figure 32).[152,153] Instead, the derivatization by Diels–Alder reaction with isobenzofuran afforded the corresponding adduct **94** (Figure 33a). Although dehydrobenzo[10]annulene **85** has less-strained alkynes than **84**, its isolation has not been reported. By considering that the bond angles ($\angle_{sp}$) of **85** are similar to those of **70**, the low stability of **85** might be caused by the high reactivity of angle-strained diyne.[154] By replacing the monoyne moiety in **85** with the *para*-phenylene moiety, Fallis and co-workers synthesized less-strained macrocycle **86** employing intramolecular Eglinton coupling.[155] The angle-strained alkyne structures were determined using X-ray crystallographic analysis (CCDC: 133376). The synthesis of dehydrobenzo[12]annulene **87** was reported by Tobe and co-workers.[154,156] The bond angles ($\angle_{sp}$) in the triyne component are 149.0°, 156.9°, and 164.0° estimated by DFT calculation. The monoyne between phenylene moieties is slightly deformed to the inside of the annulene ring by 7.2–7.6°, making monoyne and triyne moieties curve inward and outward, respectively. Because of its high reactivity, dehydrobenzo[12]annulene **87** was detectable only by spectrometric analyses in a matrix at low temperature. The photoirradiation of **95** in furan afforded the corresponding adduct **96**, which indicated that dehydrobenzo[12]annulene **87** is a highly reactive intermediate (Figure 33b). The generation of less-strained macrocycle dehydrobenzo[14]annulene **88** was confirmed by NMR measurements, but it has not been isolated.[156,157] Dehydrobenzo[14]annulene **89a** containing three *ortho*-phenylene moieties was synthesized by Vollhardt, Youngs, and co-workers employing Cu-mediated Eglinton coupling.[158,159] Dehydrobenzo[14]annulene **89a** is photosensitive, but it is stable enough to be isolated in high yield (83%) by column chromatography on silica gel. In the solid state, two monoyne moieties are curved inward, while a diyne moiety is curved outward (CCDC: 1315186). Related macrocycles **89b** and **89c** (CCDC: 1277747), including *cis*-alkene(s) instead of *o*-phenylene(s), were reported by Haley and co-workers.[160–162] These macrocycles are similar to **89a** having strained monoynes and a diyne. Because of its stability and planarity, Haley, Tobe, Hisaki, and Miyata, and other research groups independently explored the synthesis of related dehydrobenzo[14]annulenes, their transformation, and their application as fluorescent material and supramolecular assembly.[163–174] [16]DBA **90** was synthesized by Haley and co-worker.[175–178] X-ray analysis revealed that the diyne moiety is slightly strained. Orita, Otera, and co-workers reported the other pathway to **90**.[178] Youngs and co-workers prepared angle-strained diyne-containing macrocycle **91** by Hay coupling.[179] The bond angles at a diyne moiety are slightly curved ($\angle_{sp}$ = 168.3–174.5°) by the X-ray crystallographic analysis (CCDC: 1170130). Ohkita, Tsuji, and co-workers synthesized π-expanded dehydrobenzoannulene derivative **92** through Dewar benzene photoisomerization.[180] X-ray crystallographic analysis of **92** showed 167.9–171.4° bond angles ($\angle_{sp}$) (CCDC: 1296163), which indicates that the *para*-phenylene insertion into diyne moieties of **77** leads to a less-strained structure. Macrocycle **37** consisting of two *ortho*-phenylenes and two diphenylacetylene moieties was synthesized by Wong.[181] Oda, Kawase, and co-workers then independently reported an alternative pathway (Figure 19).[27] Although there is no information about the angle at the alkyne moieties in the literature, theoretical calculation estimates the bond angle ($\angle_{sp}$) at around 162°. As expected from the highly strained structure of **37**, the alkyne moieties act as a good dienophile to give a cycloadduct efficiently upon treatment with cyclopentadienone.[182] The generation of strained alkyne-containing molecule **93** bearing a highly strained alkyne was examined by Wong.[181] The sequential dehydrobromination of dibromide **97** or transformation of selenadiazole **99** accompanying nitrogen gas generation at high temperature leads to the generation of **93** (Figure 33c). Because of its highly strained structure, **93** was not isolated but could be trapped by dienes to afford the corresponding adducts **98** and **100**. Taking the bond angles ($\angle_{sp}$) into account, a strained alkyne whose bond angle is less than 155° is considered to be too reactive to be isolated.

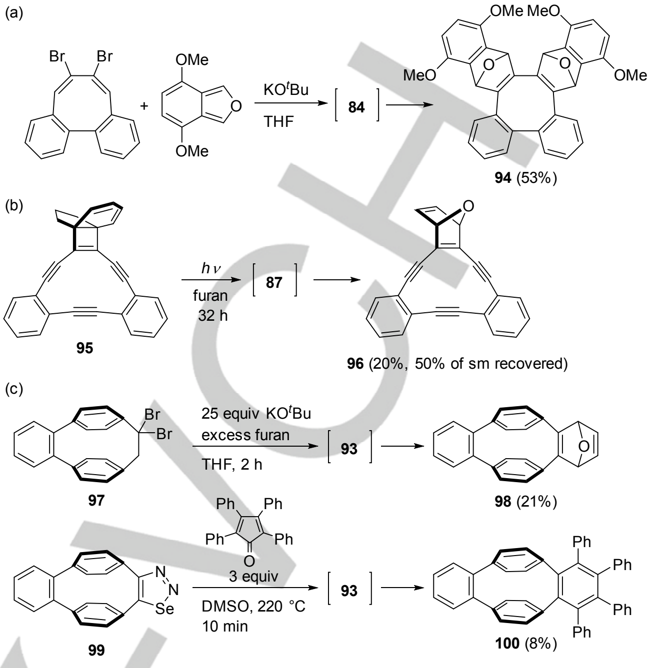

Figure 33. Diels-Alder reaction through the generation of dehydrobenzoannulenes (a) **84**, (b) **87**, and (c) **93**.

To construct angle-strained alkyne-containing macrocycles, a *meta*-phenylene unit is also one of the useful linkers (Figure 34). Ohkita, Tsuji, and co-workers reported a macrocycle **101** consisting of both *para*- and *meta*-phenylenethynylene units through the photoisomerization of Dewar benzene moieties.[183] In the solid state, the macrocycle forms a parallelogram-like shape, and therefore, two of the four *meta*-phenylenediethynylene moieties are strained ($\angle_{sp}$ = 168.7–179.9°) (CCDC: 134167). The *para*-phenylene moieties can rotate along the macrocycle. Despite the sterically hindered side chains, the interconversion between diastereoisomers is faster than the NMR time scale at room temperature.

Some of the small-sized *meta*-cyclophanes having curved alkyne moieties are strained. Oda, Kawase, and co-workers synthesized [2.2.2]metacyclophane-1,9,17-triyne (**102**)[184] and [2.2.2.2]metacyclophane-1,9,17,25-tetrayne (**103**)[185] by utilizing the synthetic sequence of McMurry coupling and bromination followed by dehydrobromination. Although the strained macrocycle **102** is sensitive to silica gel, colorless crystalline material was obtained after column chromatography (alumina) at 0 °C. X-ray analyses of **102** and **103** showed that the bond angles ($\angle_{sp}$) are 158.4–158.7° (CCDC: 1109524) and 167.6–169.9° (CCDC: 1215943), respectively. The angle-strained alkynes in **102** smoothly underwent cycloaddition with cyclopentadienes at room temperature to afford 1:2 adduct **113** in 76% yield (Figure 35a). Because the bond angles ($\angle_{sp}$) in the monoadduct were estimated to be more strained (152° and 163°) by AM1 calculation, the monoadduct was not isolated at all. In contrast, less-strained cyclophane **103** does not undergo Diels–Alder reaction with cyclopentadiene. Cyclotetramer **104**, including *m*-

phenylenediethynylene, was synthesized by Tobe and co-workers using Eglinton coupling.[186] Cyclotetramers are strain free, which is confirmed by AM1 calculation. By utilizing their symmetrical and planar structure, Tahara, Tobe, De Feyter, and co-workers succeeded in the preparation of two-dimensional self-organized materials.[187,188] More strained cyclotrimers have not been synthesized so far.

Tobe and co-workers prepared the strained dehydrobenzo[15]annulene **105** bearing a *meta*-phenylene unit using an intramolecular coupling reaction (CCDC: 1149315).[189] The diyne moiety is strain free, although one of the bond angles at the monoynes is smaller than 170°. Fallis and co-workers synthesized the more strained dehydrobenzo[11]annulene derivative **106** according to their synthetic procedure of *para*-phenylene-containing macrocycle **86**.[190] Compared with **105**, the diyne moiety of **106** is highly strained ($\angle_{sp}$ = 153.5° and 164.1°) (CCDC: 147868) because the length of the *m*-phenylene linker is shorter than the diyne. Despite the highly strained structure, Diels–Alder reaction of **105** with cyclopentadiene did not occur either at room temperature or at reflux temperature for 24 h. The reaction proceeded in a sealed tube at 120 °C, affording the corresponding 1:1 adduct **114** (Figure 35b). A second addition was not observed due to the unstrained linear structure of the remaining alkyne. Recently, a macrocycle **107** containing both *ortho-* and *meta*-phenyleneethynylene moieties was synthesized.[191] Although the mechanism is unclear, the most strained alkyne of macrocycle **107** underwent intermolecular dimerization to afford macrocycle **115** (Figure 35c). The copper-free click reaction of the highly strained alkyne of **107** also proceeded to afford the corresponding triazole-containing macrocycle **116** in good yield. Haley and co-workers synthesized a series of bis(dehydrobenzoannuleno)benzenes **108** and **109** using Pd-catalyzed or Cu-mediated homocoupling reactions.[61–63] The bond angles ($\angle_{sp}$) at alkyne moieties in **108** and **109** are similar to those of dehydrobenzo[14]annulene **89a** and dehydrobenzo[15]annulene **105**. By introducing donor/acceptor substituents on corner benzene rings in **108** and **109**, the fluorescence wavelength could be fine-tuned. A macrocycle **110** having both *ortho-* and *meta*-phenyleneethynylene moieties was synthesized, where bond angles at all alkyne moieties are strain free ($\angle_{sp}$ = 172–179°).[192] Tobe and co-workers applied the photoinduced elimination of indane to the synthesis of macrobicycles **111a** ($C_{60}H_6$), **111b** ($C_{60}Cl_6$), **112a** ($C_{78}H_{18}$), and **112b** ($C_{78}H_{12}Cl_6$).[193–195] Interestingly, the ion peak of $C_{60}H_6^-$ together with that of fullerene anion (C_{60}^-) was detected during photoirradiation to **111**, implying the possibility of fullerene synthesis from a macrobicycle. The π-expanded C_{78} was also detected by a similar photoinduced transformation.[196] For the preparation of oligoyne-containing macrobicycle **111a**, Rubin and co-workers independently applied photoinduced carbon monoxide-elimination of a cyclobutendione-containing macrocycle.[197,198] In negative-ion mode of laser desorption mass spectrometry, prominent ions corresponding to **111a** and C_{60} were observed.

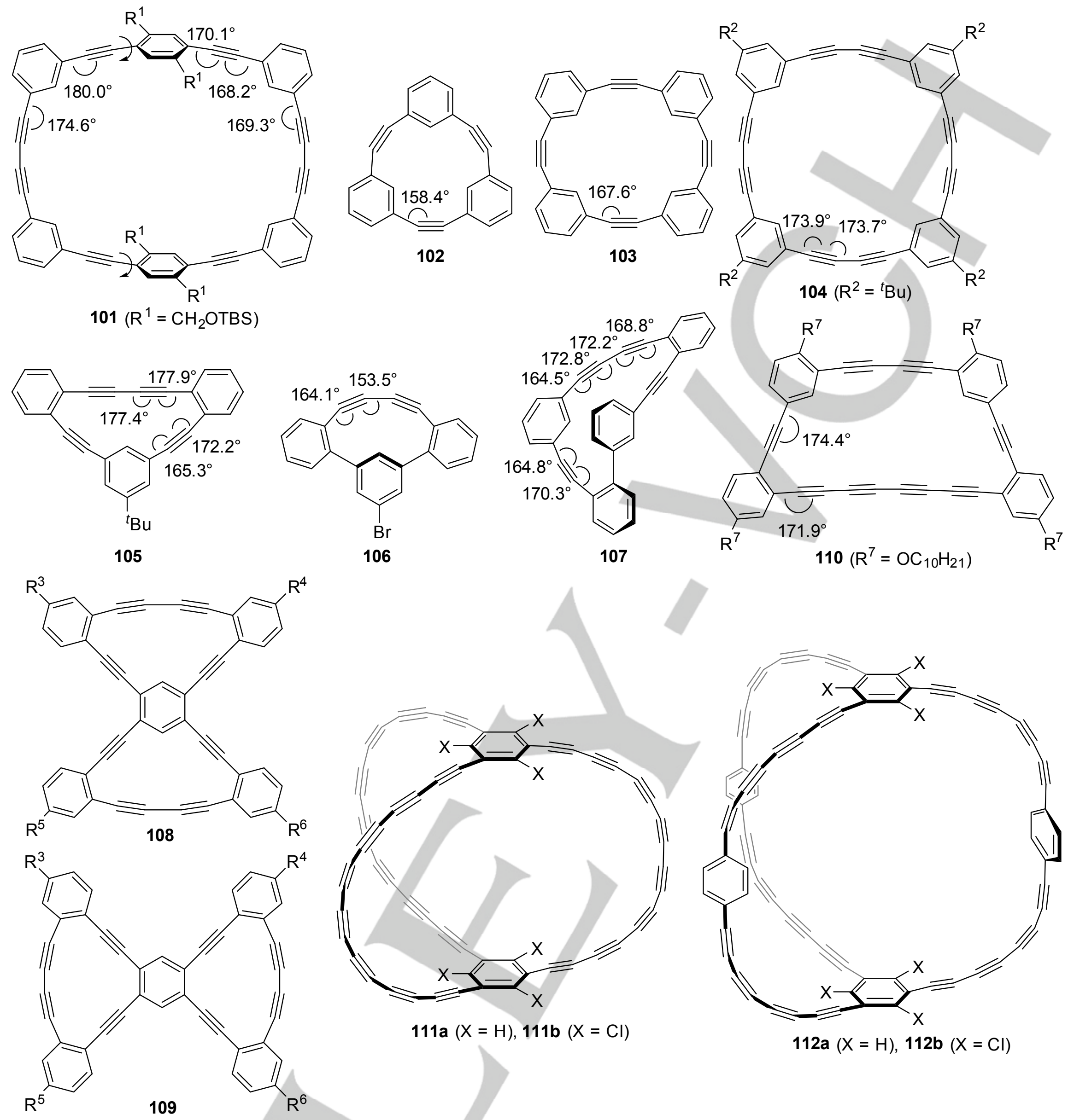

101 (R^1 = CH$_2$OTBS)

102

103

104 (R^2 = ^{t}Bu)

105

106

107

110 (R^7 = OC$_{10}$H$_{21}$)

108

109

111a (X = H), **111b** (X = Cl)

112a (X = H), **112b** (X = Cl)

Figure 34. Representative strained macrocycles having *meta*-phenyleneethynylene moieties.

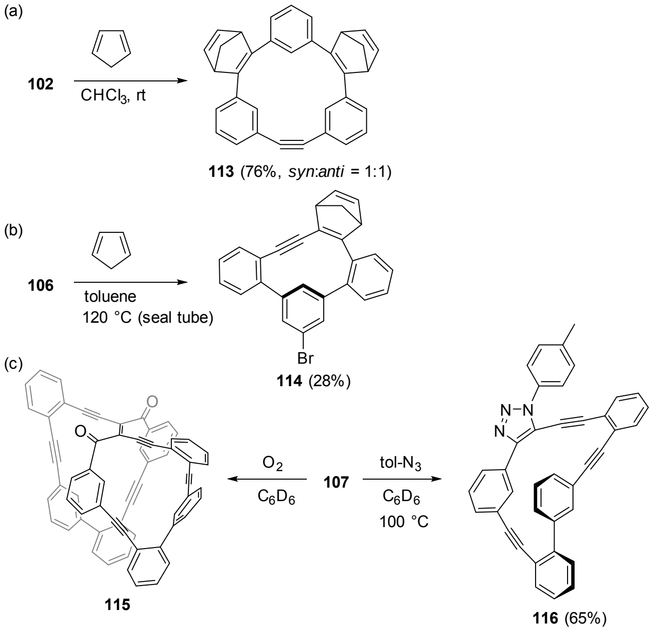

Figure 35. Transformation of strained macrocycles having *meta*-phenyleneethynylene.

3.5.2. Pyridine spacer

Related to *meta*-phenylene-containing macrocycles, macrocycles bearing pyridine and angle-strained alkyne moieties were also reported. Representative examples are summarized in Figure 36.

The synthesis of macrocycle **117** consisting of four *para*-phenyleneethynylene units and four pyridine spacers was reported by Yamaguchi, Yoshida, and co-workers.[199] The AM1 calculation suggested that the structure of pyridinophanes **117** is strain free. The related macrocycles **118** consisting of four *meta*-phenyleneethynylene units and four pyridine spacers were also reported.[199] Although the macrocycles **118** are estimated to be strain free by calculation, X-ray analysis revealed that the bond angles ($\angle_{sp}$ = 169.0–177.7°) became smaller by complexation with two copper(II) compounds (CCDC: 1150129). Compared with acyclic compounds, macrocycles **117** and **118** exhibit unusually strong fluorescence (Φ = 0.18–0.59), probably because of their rigid structures. By utilizing the cross-coupling and reductive aromatization sequence, Miki, Ohe, and co-workers synthesized pyridinophane **119** having strained alkynes.[200] The bond angles ($\angle_{sp}$ = 167–171°) are larger than that of [6]CPPAs, which was estimated by DFT calculation. The absolute quantum yield of **119** (Φ = 0.47), which is similar to that of **118**, suggests that the strained structure does not decrease the quantum yield significantly. The Yoshida and Tobe groups reported strained pyridinophanes **120**[201] and **121**[202,203] containing monoynes and butadiynes, respectively. Pyridinophanes **120** and **121** were synthesized by Sonogashira–Hagihara coupling and Eglinton homocoupling, respectively. The bond angle ($\angle_{sp}$) of **120** was around 169–171°, as determined by X-ray crystallographic analysis (CCDC: 203785 and 203876). Tobe and co-workers reported the laser irradiation-induced generation of octayne-bridged pyridinophane **122**.[204] The photoinduced transformation of azafullerene $C_{58}N_2$ from highly reactive pyridinophane **122** was confirmed spectroscopically. Haley and co-workers synthesized dehydrobenzopyrid[15]annulenes **123a** and **123b** containing strained alkynes.[205,206] The X-ray crystallographic analysis of **123a** and **123b** indicated that the butadiyne bridge is not curved ($\angle_{sp}$ = 175–179°, CCDC: 665933), but the monoyne moieties are curved ($\angle_{sp}$ = 163–173°, CCDC: 665934). Dehydrobenzopyrid[15]annulenes **123a** and **123b** bearing a proton-accepting pyridine ring showed dynamic proton-induced emission switching properties. Baxter and co-workers reported terpyridine-containing macrocycle **124**.[207] The bond angles ($\angle_{sp}$) of a butadiyne moiety are strained (165.4° and 170.1°), but two of the four monoyne moieties are not significantly curved ($\angle_{sp} \geq$ 174°) (CCDC: 913133).

Fallis and co-worker reported the template-directed synthesis of phenanthroline-containing macrocycle **125** (Figure 37).[208] The copper(II) template formation followed by Eglinton coupling facilitates the desired macrocyclization, and side reactions such as polymerization were efficiently suppressed. The helical structure was proposed by molecular modeling, although the structural details of strained angles were not reported.

Other macrocycles, including alkyne and pyridine moieties, were reported by Baxter, Schlüter, Abe, and Inouye, and other groups.[209–221] Bipyridine and terpyridine spacers are also utilized, but these macrocycles are all strain free.

3.5.3 Heteroaromatics as a spacer: furan, pyrrole, tetrathiafulvalene, and carbazole

Strained macrocycles having furylene and diethynylfuran moieties are rare. A few examples of alkyl-tethered macrocycles or metal-containing macrocycles are known.[222–225] Macrocycles having a diethynylpyrrole moiety are scarcely found in the literature. Because of their redox-active property, many tetrathiafulvalene-containing macrocycles have been developed so far; however, these are unstrained and shape-consistent macrocycles. Macrocycles having a diethynylcarbazole moiety have been intensively investigated, probably because of their stability and application to functional materials.

The Sonogashira–Hagihara coupling reaction can provide cyclooligomers containing 3,6-carbazolylacetylene moieties (Figure 38a).[226] Although the cross-coupling of 3,6-diethynylcarbazole **126a** and 3,6-diiodocarbazole **127** afforded polymer (**path A**); cyclotetramer **129** was obtained from **126a** and diiodide **128** in 14.3% yield together with cyclooctamer (5.4% yield) under Pd- and Cu-catalysis (concentration: ca 5 mM) (**path B**). Zhang and Moore found that alkyne metathesis of 3,6-diethynylcarbazole derivative **130** afforded cyclotetramer **129** in 84% yield (**path C**).[227,228] Because of their nanoporous structure in the solid state,[229] this shape-persistent cyclotetramer **129** and its derivatives were widely applied to molecular engineering, such as self-assembled materials and sensing.[230] Although alkyne metathesis dramatically improves the macrocyclization efficiency, this method could not be applied to the synthesis of thermodynamically less stable strained macrocycles. Glaser coupling reaction of 3,6-diethynylcarbazole **126b** afforded strained cyclotrimer **131** in 6% yield together with a detectable amount of cyclotetramer **132**, although the structural data were not provided (Figure 38b).[231] Self-assembled layers of **131** and **132** were observed on the surface of graphite.[232] Although **131** forms a single layer self-assembly regardless of the existence of coronene, the cavity inside **132** can be filled with coronene in the self-assembled layer.

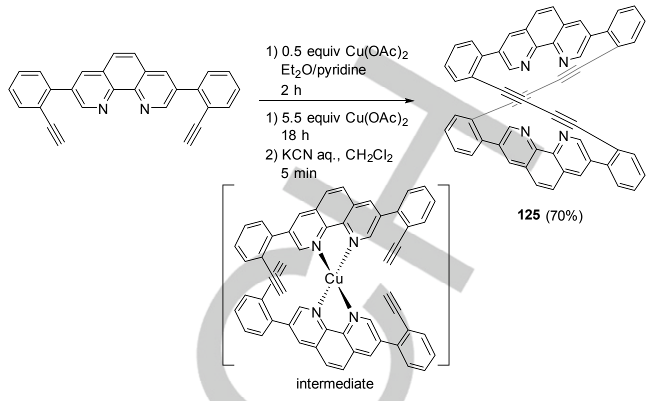

125 (70%)

Figure 37. Copper-template-directed synthesis of helical macrocycle.

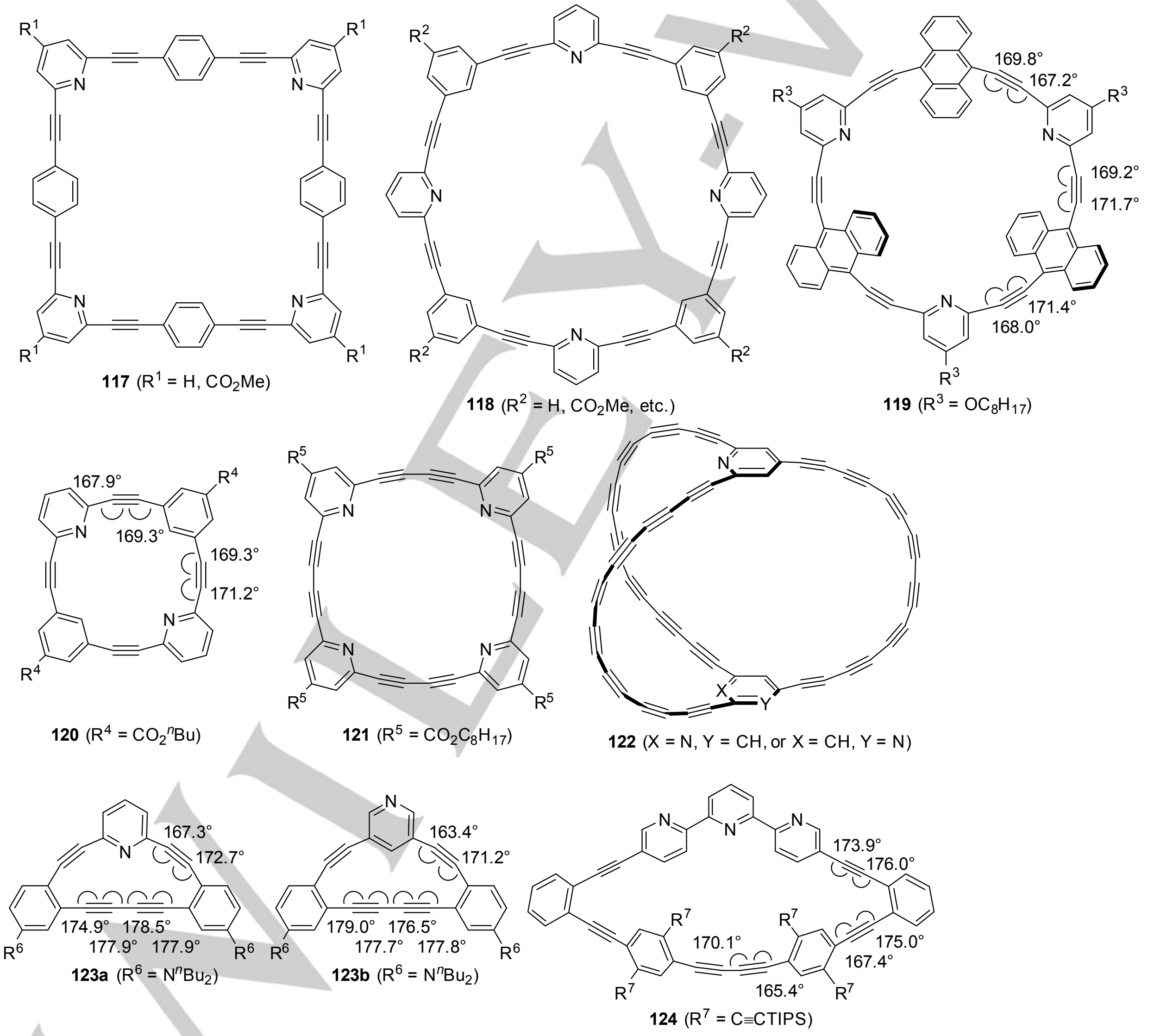

117 (R^1 = H, CO$_2$Me)

118 (R^2 = H, CO$_2$Me, etc.)

119 (R^3 = OC$_8$H$_{17}$)

120 (R^4 = CO$_2{}^n$Bu)

121 (R^5 = CO$_2$C$_8$H$_{17}$)

122 (X = N, Y = CH, or X = CH, Y = N)

123a (R^6 = N^{n}Bu$_2$)

123b (R^6 = N^{n}Bu$_2$)

124 (R^7 = C≡CTIPS)

Figure 36. Strained alkyne-containing pyridinophanes.

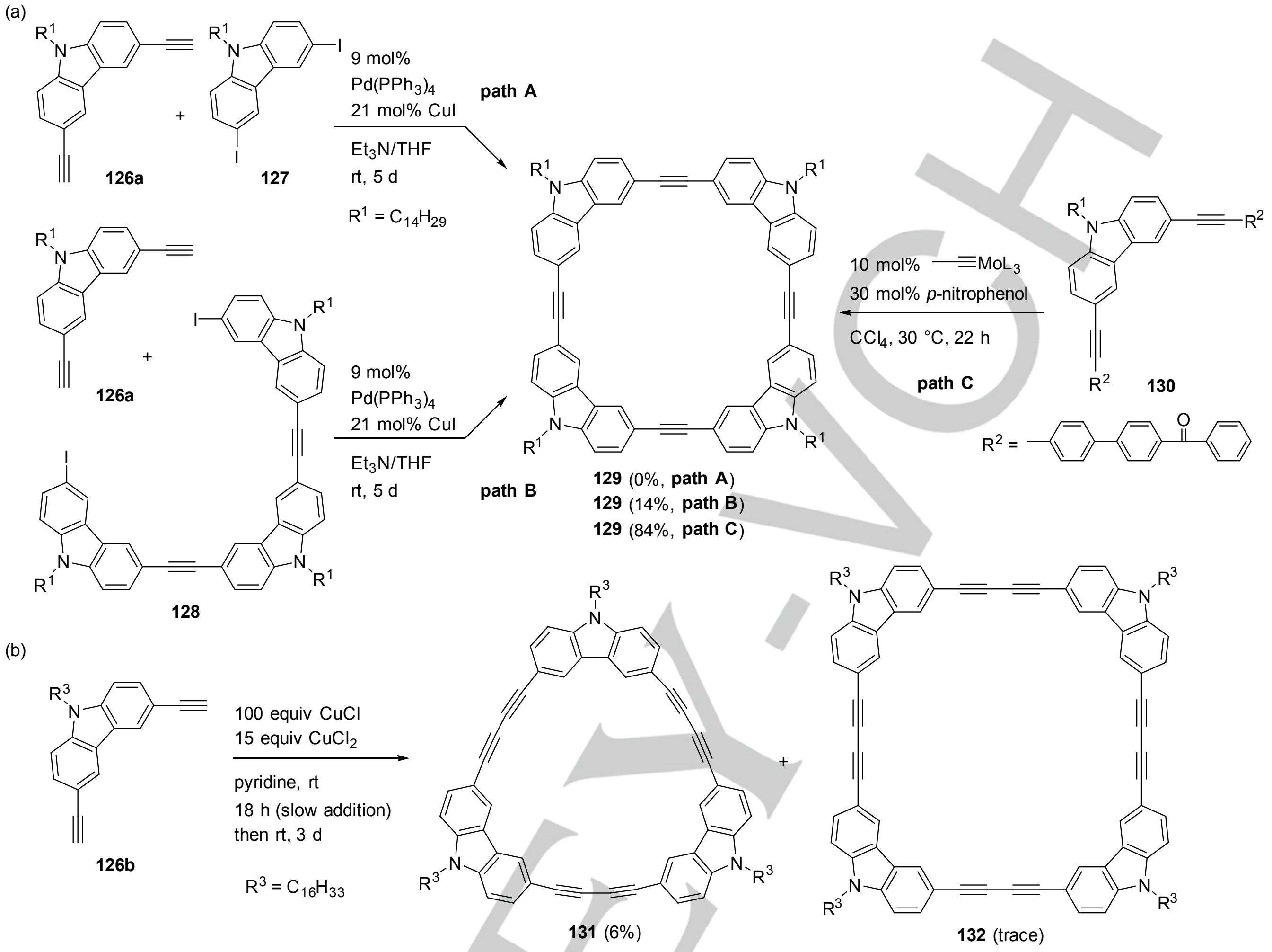

Figure 38. Preparation of carbazole-containing macrocycles. L: *tert*-butyl(3,5-dimethylphenyl)amino.

The Eglinton coupling of 1,8-diethynylcarbazole afforded cyclodimer **133a**, cyclotrimer **133b**, and cyclotetramer **133c** in 35%, 4.9%, and 7.6% yields, respectively (Figure 39).[233] The bond angles ($\angle_{sp}$) of cyclodimer **133a** (CCDC: 816648) and cyclotrimer **133b** (CCDC: 816649) are 168.2–174.9° and 170.2–178.7°, respectively. The fluorescence quantum yield of **133a** (Φ = 0.426) is higher than those of **133b** and **133c**. Diyne moieties in **133** can be converted to pyrroles and thiophenes, affording the corresponding macrocycles **134** and **135** in good yields.[233,234] Interestingly, the oxidation of **135** led to the formation of core-modified porphyrin, whose Q-like bands are extremely redshifted. Strained cyclodimer **133a** can be accessible to furan- and selenophene-containing porphyrinoids.[235]

As to 2,7-diethynylcarbazole-containing macrocycle, Höger, Lupton, and co-workers reported the giant macrocycle **136** to demonstrate exciton localization in π-conjugated macromolecules (Figure 40).[236,237] The template-assisted macrocyclization through Sonogashira–Hagihara coupling proceeded smoothly to give **136** containing the main macrocycle (ring) and the template (spoke), although the structural data are unavailable.

Müllen and co-workers synthesized 2,7-disubstituted carbazole-containing giant macrocycle **137** through template-directed macrocyclization (Figure 41).[238] This molecule formed a 1:1 host–guest complex with hexa-*peri*-hexabenzocoronene on highly oriented pyrolytic graphite (HOPG). Scanning tunneling microscopy visualized the well-aligned two-dimensional assembly of 1:1 complex on HOPG with a hexagonal pattern.

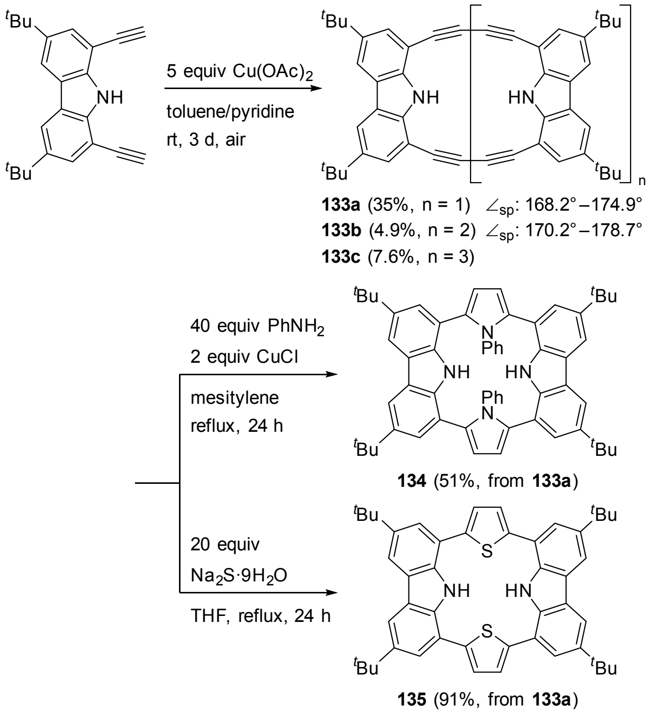

133a (35%, n = 1) ∠$_{sp}$: 168.2°–174.9°
133b (4.9%, n = 2) ∠$_{sp}$: 170.2°–178.7°
133c (7.6%, n = 3)

134 (51%, from **133a**)

135 (91%, from **133a**)

Figure 39. Cyclooligomers of 1,8-diethynylcarbazole and their transformation.

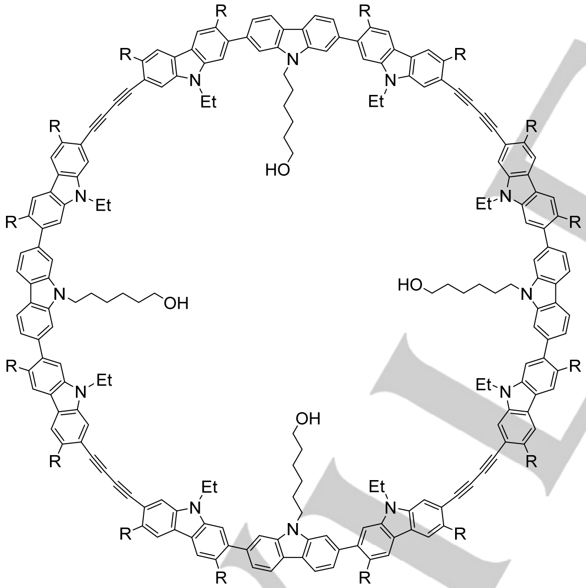

137

Figure 41. π-Conjugated carbazole macrocycle **137**. R = $C_{12}H_{25}$.

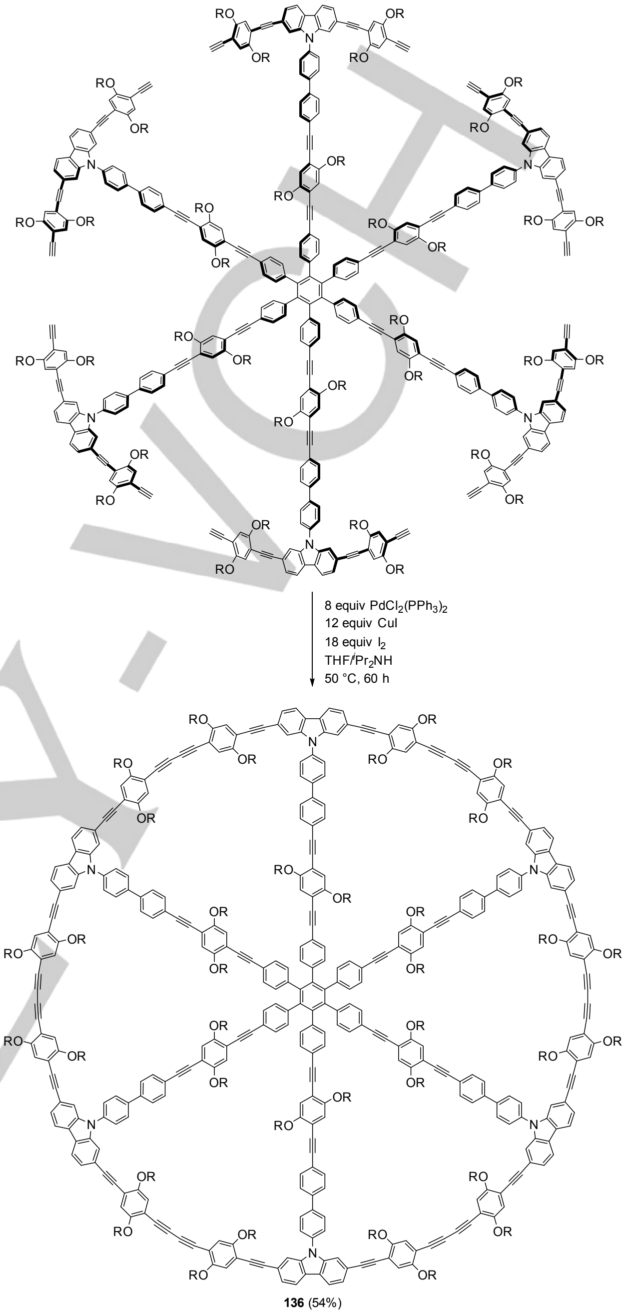

136 (54%)

Figure 40. Giant π-conjugated spoked-wheel macrocycle. R = C_8H_{17}.

3.5.4. Thiophene spacer

Compared with macrocycles bearing furan and pyrrole, thiophene-containing macrocycles have been more intensively investigated because of its stability and attractive electronic properties.[239] Oda, Kawase, and co-workers reported the synthesis of thiophene-containing strained macrocycle **139a** through McMurry coupling of **138a** using the $TiCl_3(DME)_{1.5}$/Zn(Cu) system (Figure 42).[240] The coupling reaction mainly afforded cyclotrimer (10–15%) together with a trace amount of strained cyclodimer **139a**. The planar structure of **139a** was confirmed by X-ray crystallographic analysis. The bond angles ($\angle_{sp}$) are 165–166° in the solid state with *cis*-configuration of the two alkenes. Iyoda and co-workers reported that a modified procedure ($TiCl_4$/Zn system) more efficiently gave the thiophene-containing macrocycles **139b–139f**.[241–248] The series of thiophene-containing macrocycles **139** exhibited large molar extinction coefficients ($2.49–6.39 \times 10^5$ M^{-1} cm^{-1}) at 447–488 nm and moderate fluorescence around 559–606 nm (Φ = 0.069–0.11). Furthermore, larger macrocycles show remarkably large maximum two-photon absorption cross section (δ_{max} = 15100–107800 GM), probably due to the increment of π-conjugation.[242] Some of the macrocyclic oligothiophenes were applied to fluorescence switching, field-effect transistor activity switching, and electrical conductivity switching.[245] The macrocyclic oligothiophene (30mer) dramatically strengthens interaction between chromophores in comparison with natural light-harvesting antenna LH2 of purple photosynthetic bacteria.[249]

Cyclo[n](3,4-dibutyl-2,5-thienyleneethynylene)s **140a–140c** were synthesized through bromination of macrocycle **139c–139e** followed by dehydrobromination (Figure 43a).[239,241,244] Iyoda and co-workers developed two alternative synthetic routes to cyclo[n](3,4-dibutyl-2,5-thienyleneethynylene)s, such as (1) the intramolecular Sonogashira–Hagihara coupling (Figure 43b)[239,246] and (2) the double-elimination reaction[239,250] developed by Orita and Otera (Figure 43c). The intramolecular Sonogashira–Hagihara coupling of linear oligomer **141a** and **141b** afforded cyclooctamer **140b** and cyclodecamer **140c**, respectively. The double-elimination procedure through the coupling of **142** and **138f** gave cyclododecamer **140d**. X-ray crystallographic analyses revealed that the bond angles ($\angle_{sp}$) of **140a** (CCDC: 1426417) and **140b** (CCDC: 1038258) are 167.0–171.4° and 168.0–179.8°, indicating that **140a** and **140b** are circular and ellipsoidal shapes in the solid state, respectively. Interestingly, cyclo[8](3,4-dibutyl-2,5-thienyleneethynylene) **140b** as well as its precursor **139d** encapsulated fullerene to form Saturn-like 1:1 inclusion complexes **140b**$\supset C_{60}$ (CCDC: 1038260) and **139d**$\supset C_{60}$ (CCDC: 1038259) (Figure 44).[246] Macrocycle **139d** having a planar structure formed a two-dimensional network on the surface of HOPG, where the reversible photoisomerization took place. The strong interaction between the convex surface of fullerene and sulfur atoms enabled the formation of a 1:2 complex of two fullerene molecules with the large macrocycle.[251]

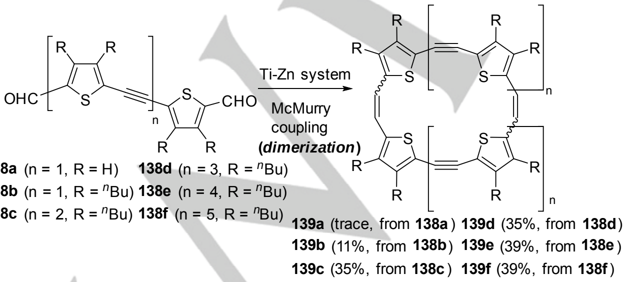

Figure 42. Synthesis of thiophene-containing macrocycles through McMurry coupling.

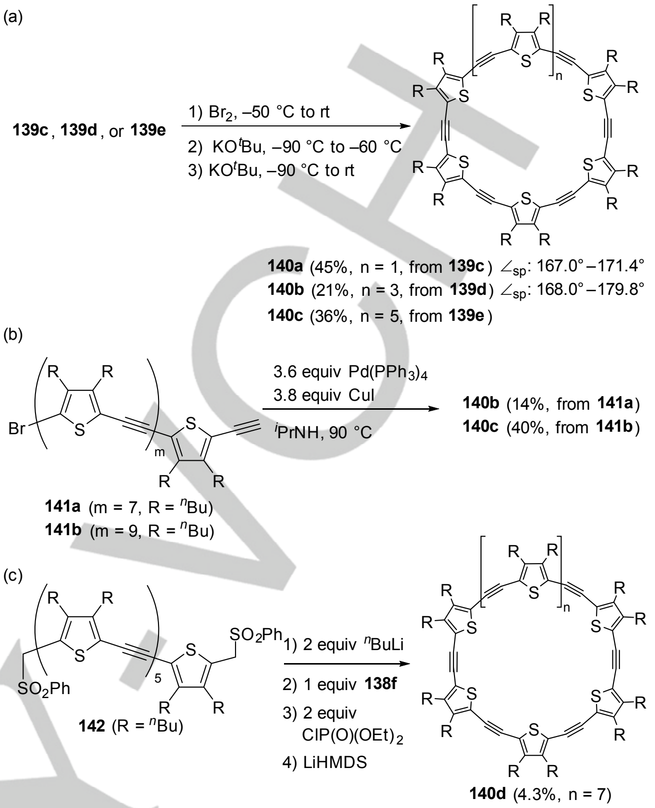

Figure 43. Synthesis of cyclo[n](3,4-dibutyl-2,5-thienyleneethynylene)s.

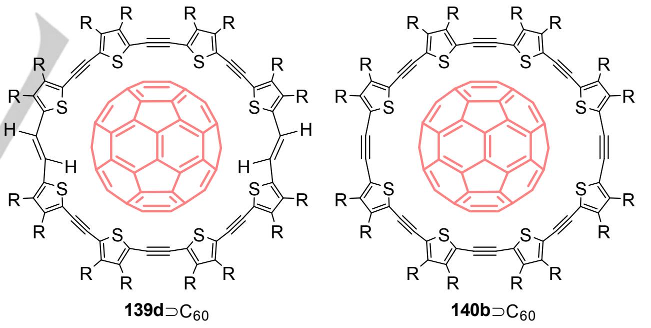

Figure 44. Inclusion complexes of fullerene with macrocycles **139d** and **140b**.

The largest giant macrocycle **143** having diethynylthiophene moieties was reported by Mayor and co-worker (Figure 45).[252] Because of the large molecular size (diameter: ≈12 nm), this molecule is assumed to be strain free. The absorbance maximum (λ = 461 nm) is in good agreement with the theoretical value (462 nm) estimated for the linear oligomers.

Bäuerle and co-workers reported the synthesis of strained thiophene-containing macrocycle **145** through oxidant-induced elimination of platinum complexes (Figure 46).[253] The formation of dinuclear platinum(II) complex from diyne proceeded smoothly to afford macrocycle **144** in excellent yield. The strained macrocycle **145** was obtained in good yield through ligand coupling upon I_2-mediated oxidation of platinum complex **144**. The bond angles ($\angle_{sp}$) of **145** are 160–168°, and its longest and shortest S–S distances are 1.10 nm and 0.81 nm, respectively (CCDC: 201462). The thiophene formation from diyne using sodium sulfide gave cyclo[8]thiophene **146**.

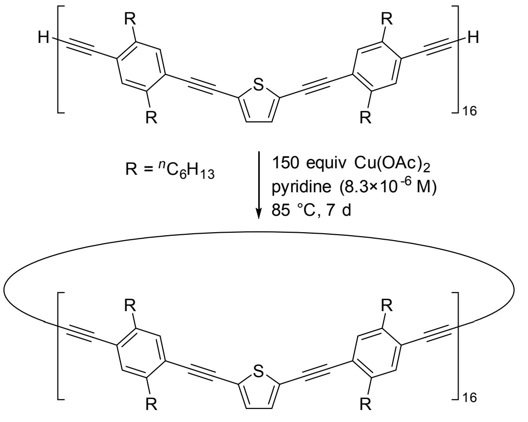

143 (38%)

Figure 45. Giant macrocycle containing 2,5-diethynylthiophene.

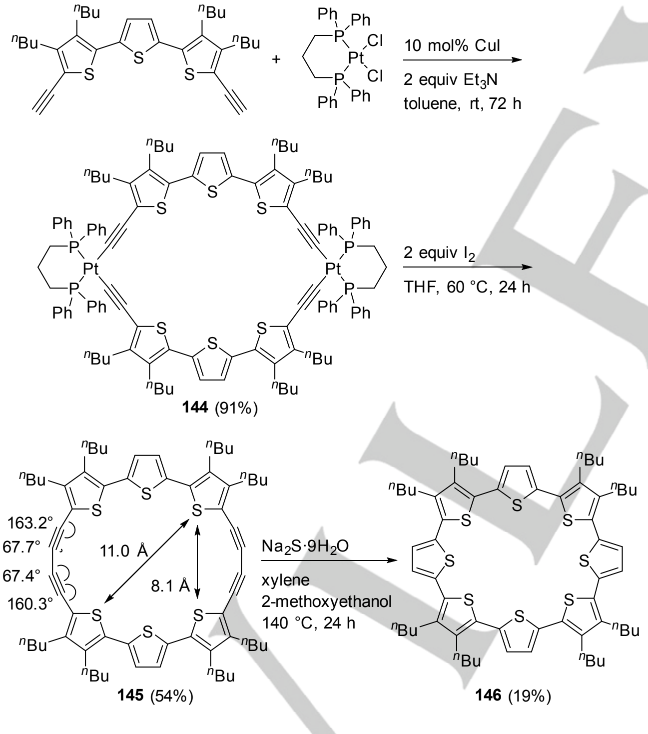

Figure 46. Strained macrocycle through reductive elimination of platinum complexes.

Thiophene-fused dehydroannulenes were also reported. Representative examples are shown in Figure 47. Although thiophene-fused dehydroannulene **147** (CCDC: 1205022)[254,255] confirmed by X-ray analysis is strain free, its derivatives **148**[256,257] seem to be slightly strained. The X-ray data (CCDC: 1119562 (**148b**)) are not sufficient to discuss the bond angles of alkynes. Haley and co-workers synthesized π-expanded thiophene-fused macrocycles **149**, but these series are strain free.[258] Haley and co-workers synthesized thiophene-fused strained dehydroannulenes **150** using intramolecular Eglinton diyne formation.[162,259,260] Both dehydrothieno[14]annulene **150a** (CCDC: 698377) and benzo-fused analogue **150b** (CCDC: 698376) are planar structures, which were confirmed by X-ray crystallographic analyses. Related macrocycles **150c** and **150d**, including *cis*-alkenes, were synthesized by Haley and co-workers.[162] The curved structures of **150** are similar to that of dehydrobenzo[14]annulene **89a**. Thiophene-fused dehydrobenzo[15]annulene analogues **151** were also synthesized by Haley and co-workers.[261]

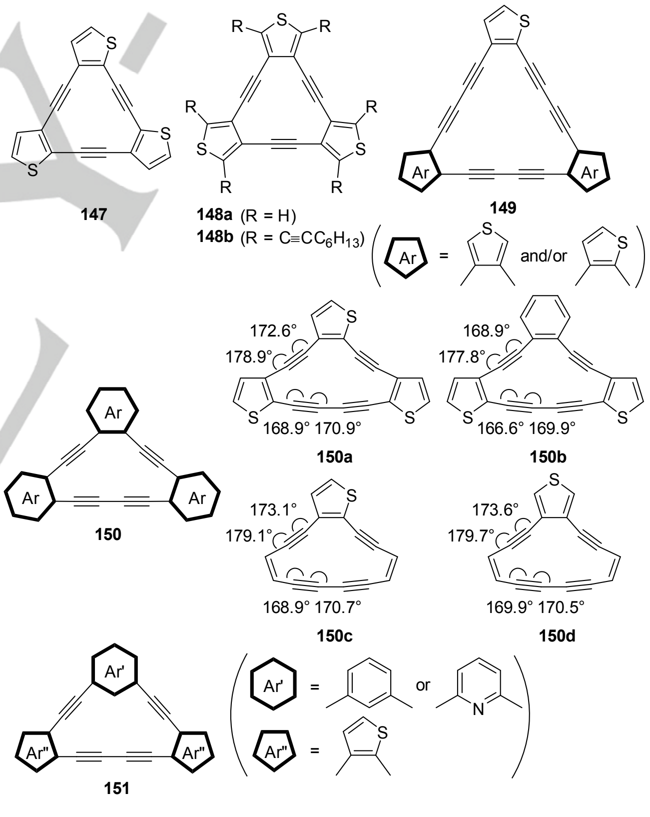

Figure 47. Thiophene-fused dehydroannulenes.

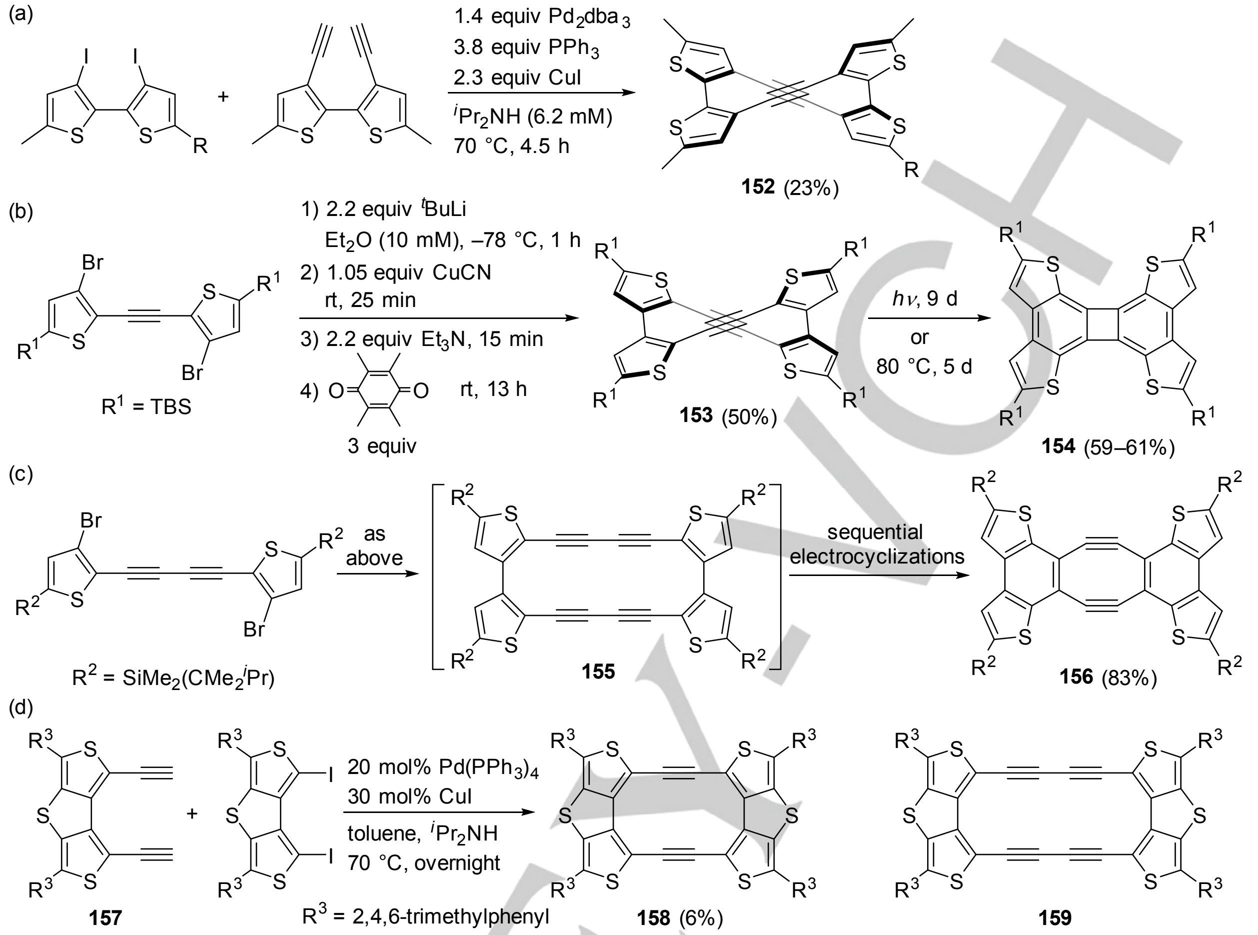

Figure 48. Twisted and planar bithiophene-containing macrocycle.

Marsella and co-workers synthesized bithiophene-containing twisted macrocycle **152** in moderate yield using a Sonogashira–Hagihara coupling reaction (Figure 48a).[262,263] Fukazawa, Yoshizawa, Yamaguchi, and co-workers reported similar thiophene-fused macrocycle **153** by copper-mediated homocoupling (Figure 48b).[264] X-ray crystallographic analyses indicate the bond angles ($\angle_{sp}$) of **152** (CCDC: 194064) and **153** (CCDC: 937080) are 176.0–179.0° and 173.9–178.9° with strain-free structures, respectively. Macrocycle **153** is readily transformed to thiophene-fused biphenylene **154** under photoirradiation or mild heating conditions.[265,266] The interesting sodium metal-mediated transformation of macrocycle **153** gave thiophene-fused heptalene.[266] The diyne-containing macrocycle **155** was not isolated through the copper-mediated homocoupling because the similar valence isomerization shown in Figure 30g proceeded smoothly to give thiophene-fused dehydrobenzo[8]annulene **156** (Figure 48c).[133] Nishinaga and co-workers synthesized planar dehydro[12]annulene **158** using Sonogashira–Hagihara coupling (Figure 48d).[267] The copper-mediated homocoupling of diyne **157** also proceeded to afford dehydro[16]annulene derivative **159** in moderate yield. The aromaticity of [4n] π-systems was reported very recently.[268]

3.5.5. Biphenyl, binaphthyl, fluorene, phenanthrene, and triphenylene spacers

Diethynylbiphenyl could be used as a good spacer to construct angle-strained alkyne-containing macrocycles involving macrocycle **107**. 2,2′-Diethynyl-1,1′-biphenyl-containing macrocycle **160**, which is the benzo-fused analogue of bithiophene-containing macrocycles **152** and **153**, was synthesized in the 1970s (Figure 49a).[269] The bond angle of **160** at *sp* carbons ($\angle_{sp}$ = 173.8°) determined by X-ray crystallographic analysis indicated that it is twisted but unstrained.[270] Kawase, Oda, and co-workers synthesized 3,3′-diethynyl-1,1′-biphenyl-containing macrocycle **161** (Figure 49b).[271] Based on X-ray crystallographic analyses, the bond angles of macrocycle **161** ($\angle_{sp}$ = 160–161°) are much smaller than those of **160**. The chiral D_2 symmetric structure of **160** was implied, but optically pure macrocycle has not yet been isolated. More strained macrocycles **161** with axial chirality are in equilibrium between *meso*- and *dl*-forms in solution, but only the *meso*-isomer of **161b** was obtained. Because of the steric hindrance of methoxy groups, the energy barrier between *dl* and *meso* in **161b** is larger than that in **161a**.

As mentioned in Section 3.5.1 (Figure 30g), the cyclodimer of 2,2′-diethynyl-1,1′-biphenyl is readily converted to dehydrobenzo[8]annulene **74** through sequential electrocyclization reactions. Similarly twisted π-extended macrocycle **162** (CCDC: 1249521) and related macrocycles were also reported (Figure 49c).[272–276] The racemization barrier of **162** through a planar structure was predicted to be 31 kJ mol^{-1}.[272] Macrocycle **162** is known to decompose explosively to give carbon materials with concomitant CH_4 and H_2 gas generation under vacuum at 245 °C.

Tobe and co-workers synthesized the more strained 2,2′-diethynyl-1,1′-biphenyl-containing macrocycle **163** using Eglinton coupling (Figure 50).[277] X-ray analysis revealed that two crystallographically independent molecules are included in the unit cell (CCDC: 1003171). The bond angles at sp carbons α, β, γ, and δ in the two molecules are 166.7° (α), 159.3° (β), 160.8° (γ), 169.7° (δ) and 168.8° (α), 161.5° (β), 162.0° (γ), 170.9° (δ). Because of its highly strained structure, the transannular cyclization induced by electrophilic bromine proceeded smoothly to afford dibromodibenzopicene **164** in good yield. The heating of **163** in furan gave dibenzopicene derivative **165**, indicating the generation of a benzyne intermediate. The large strain energy imposed on the diyne moiety leads to the intramolecular [4+2] cycloaddition.

Lee and co-workers reported the synthesis of macrobicycle **166** containing monoyne and diyne moieties (Figure 51).[278,279] The phenyl ring at the center of the molecule is perpendicular to the basal bowl-shaped π-system due to the steric demand. Although the structural data were not reported, the dynamic structural change of the curved π-system would lead to the formation of a supramolecular capsule with both planar coronene and bowl-shaped corannulene.[278,279] Baldridge, Siegel, and co-workers found that dehydro[10]annulene derivative **167b** (18%) was formed together with decapentynylcorannulene **167a** (10%) in the transformation of perchlorocorannulene (Figure 52).[280] The X-ray data (CCDC: 673329) supported the planar [10]annulene-type structure comprised of two cumulenyl or alkynyl linkages.

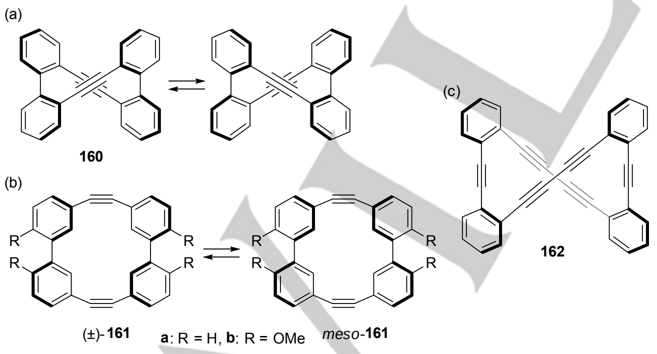

Figure 49. Biphenyl-containing macrocycles. One of chiral isomers is shown.

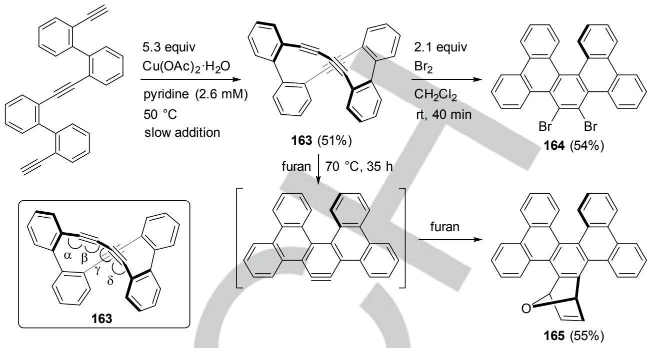

Figure 50. Twisted biphenylophane and its transformation.

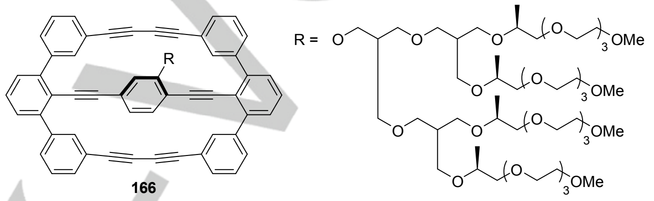

Figure 51. Macrobicycle **166**.

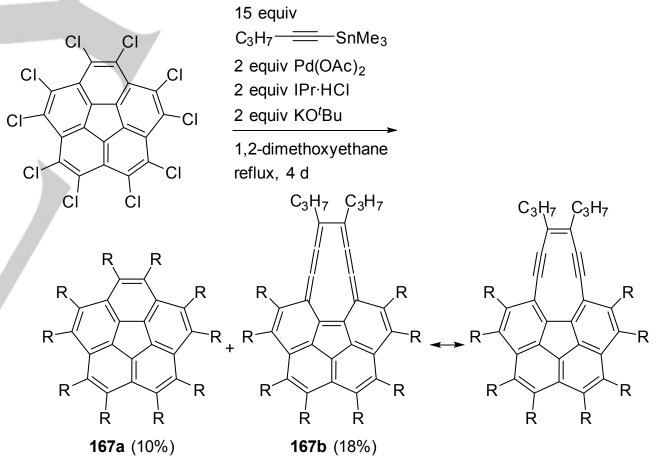

Figure 52. Isomerization of decapentynylcorannulene. IPr·HCl: 1,3-bis(2,6-diisopropylphenyl)imidazolium chloride. R = $C\equiv C–C_3H_7$.

The 1,1′-binaphthyl moiety was used as a spacer to construct chiral macrocycles. 3,3′-Diethynyl-1,1′-binaphthyl was utilized to synthesize strain-free macrocycles, some of which are applied to a sensor.[281–284] Diederich and co-workers synthesized binaphthyl-containing macrocycles **168** for sugar detection (Figure 53).[281–283] The molecular dynamics simulation (no information about bond angles) showed that these molecules are strain free. The smaller macrocycle **168a** is suitable for the recognition of monosaccharides, whereas the wider rectangular-shaped macrocycle **168b** provided a good fit to disaccharides. The association constant between smaller triangle-shaped macrocycle **169** and monosaccharide is about half the value of **168a**.

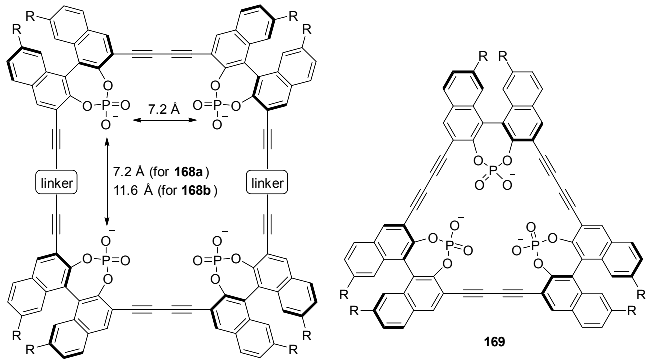

168a (linker = non) **168b** (linker = *p*-phenylene)

Figure 53. Binaphthyl-containing macrocycles. R = OCH_2Ph.

The introduction of a chiral spacer leads to the chiroptically active macrocycles bearing angle-strained alkynes. Despite the attractive chiral structure, a limited number of macrocycles have been reported so far.

Orita, Otera, and co-workers synthesized dehydroannulene derivatives **170** and **171** through an intramolecular Orita–Otera reaction or intramolecular Eglinton homocoupling (Figure 54a and 54b).[285] The twisted π-conjugated structure, as well as the curved structure of alkynes ($\angle_{sp}$ = 169–174°) of **171**, were confirmed by X-ray crystallographic analysis (CCDC: 689743). Macrocycle **170** is similarly twisted but less strained than **171**, which is suggested by DFT calculation. Carbon double-helicates **172**–**174** were prepared using intramolecular Sonogashira–Hagihara coupling (Figure 54c).[286–288] From DFT calculations, the bond angles ($\angle_{sp}$) of **172**–**174** are estimated to be 173.9–175.0°, 175.2–177.8°, and 169.7–174.5°, respectively.[288,289] In the solid state, bond angles ($\angle_{sp}$) of **172b** (CCDC: 165479) are around 171–177°, which is in good agreement with the data obtained by the DFT calculations. The two *meta*-phenylene rings are somewhat tilted from planarity due to the repulsion between protons at the double *ortho*-position. Chemical shifts of acetylenic carbon atoms in **172a**, **173**, and **174** were observed at 90.4–92.1, 92.1–94.2, and 91.4–92.3 ppm, indicating that **173** is more strained than the others in solution.

Rissanene, Herges, and co-workers reported the synthesis of the triply twisted Möbius annulene **176** (Figure 55).[290] Its precursor **175** was obtained using Pd- and Cu-catalyzed Cadiot–Chodkiewicz coupling of dibromide and mono-protected diyne. The intramolecular Eglinton homocoupling in a dilute solution for over one month afforded the desired macrocycle **176** in 11% yield. X-ray crystallographic analysis (CCDC: 938919) showed that the bond angles ($\angle_{sp}$) are 168.8–178.0°, suggesting that a part of the alkynes are strained. This molecule is the first example of triply twisted Möbius annulene. DFT calculations on the triply twisted annulene **176** and related macrocycles were recently reported from other research groups.[291–294]

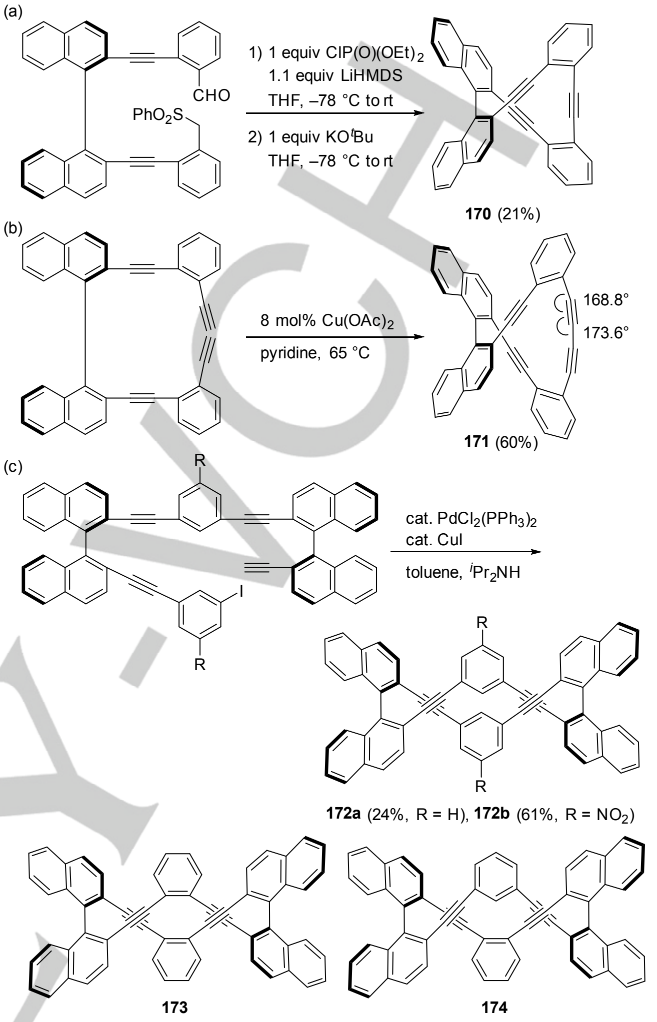

Figure 54. 2,2'-Diethynyl-1,1'-binaphthyl-containing macrocycles.

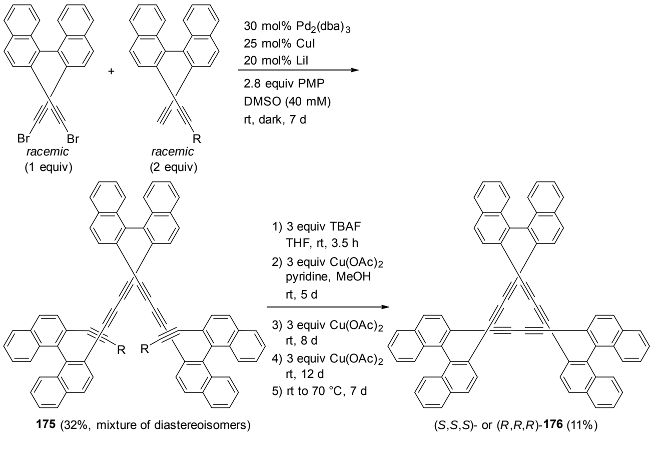

Figure 55. Triply twisted Möbius annulene. PMP: 1,2,2,6,6-pentamethylpiperidine. R = dimethyl(1,1,2-trimethylpropyl)silyl.

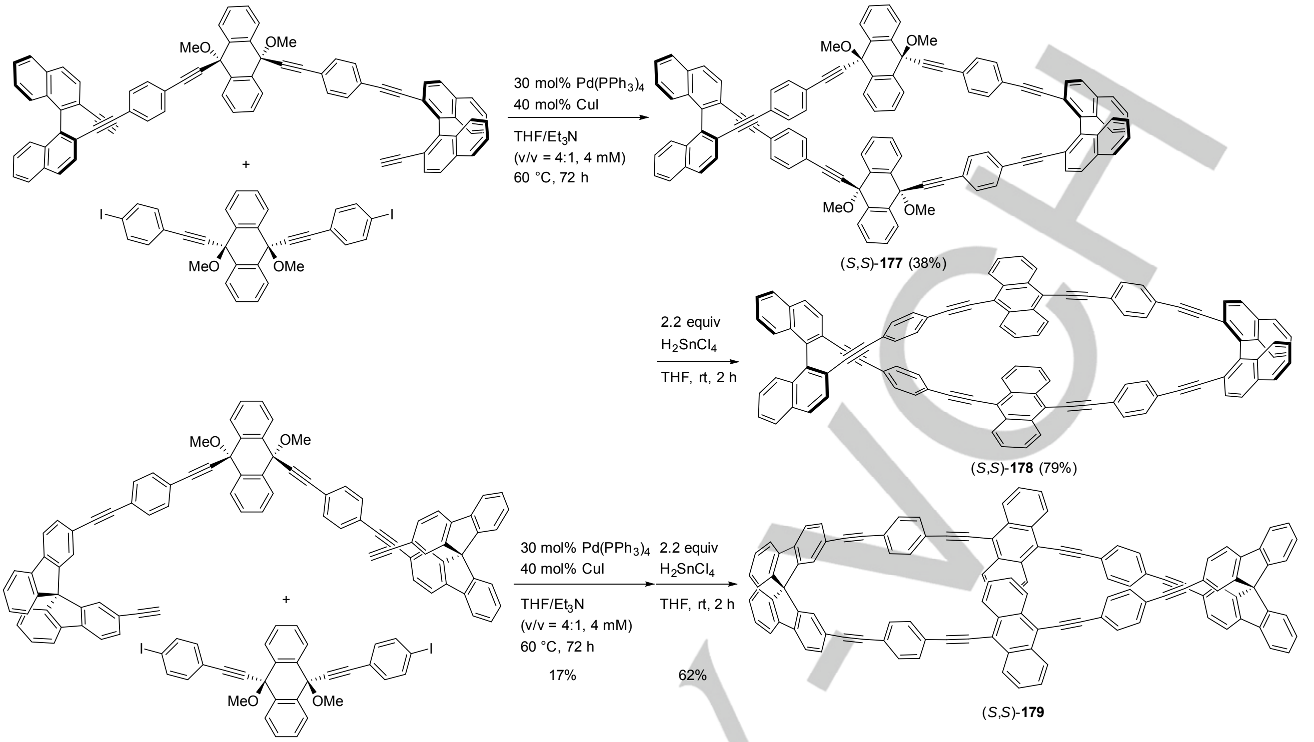

(*S*,*S*)-**177** (38%)

(*S*,*S*)-**178** (79%)

(*S*,*S*)-**179**

Figure 56. Carbon double helices consisting of chiral 2,2’-diethynyl-1,1’-binaphthyl and 9,9’-spirobifluorene moieties.

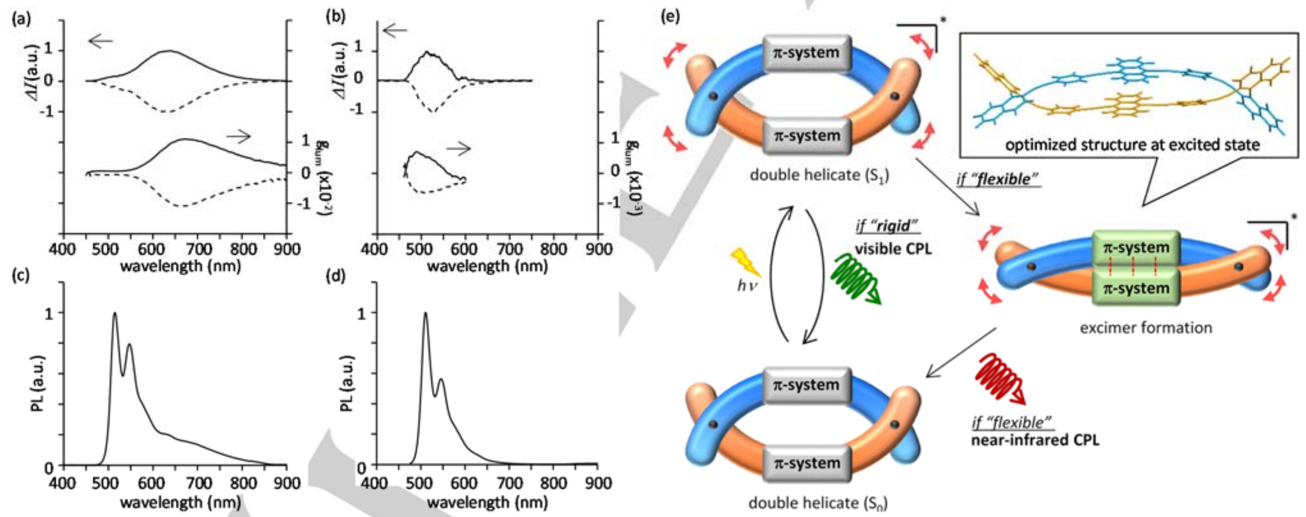

Figure 57. Circularly polarized luminescence spectra of (a) **178** and (b) **179**. (*S*,*S*)-isomer: solid line; (*R*,*R*)-isomer: dashed line. In CHCl$_3$ (1.0 × 10^{-6} M). Photoluminescence spectra of (c) **178** and (d) **179**. (e) Circularly polarized luminescence from carbon double helices. Reproduced with permission from ref. 295. Copyright 2018 Wiley-VCH Verag GmbH & KaA, Weinheim.

Miki, Ohe, and co-workers recently reported the 2,2′-diethynyl-1,1′-binaphthyl-containing carbon double helices (Figure 56).[295] The precursor (*S*,*S*)-**177** was synthesized using macrocyclization under Sonogashira–Hagihara coupling conditions. The modified tin-mediated reductive aromatization provided the carbon double helix (*S*,*S*)-**178** in good yield. The carbon double helices **179** having 9,9′-spirobifluorene was synthesized in a similar manner. DFT calculations showed the bond angles ($\angle_{sp}$) of **178** and **179** are 173–175° and 175–176°, respectively, indicating that neither molecule is highly curved at the ethynylene units. The rigid carbon double helix **179** emitted strong photoluminescence around 500–650 nm (Φ = 0.93, Figure 57d); however, weak circularly polarized luminescence was observed (luminescence dissymmetry factor: g_{lum} = 0.00071, Figure 57b). In contrast, the flexible carbon double helix **178** emitted photoluminescence (Φ_{total} = 0.49) around 500–650 nm along with photoluminescence through intramolecular excimer formation (600–850 nm, $\tau \geq 20$ ns) (Figure 57c). Interestingly, strong circularly polarized luminescence (g_{lum} = 0.011) through intramolecular excimer formation was observed in the near-infrared region (Figure 57a). TD-DFT calculation suggested that ethynylene moieties grafted to binaphthyl spacers are strained in the tightly interlocked excimer structure of **178** ($\angle_{\mathrm{sp}}$ = 165.9–173.8°) (Figure 57e).

By utilizing a planar bridged biphenyl, such as carbazole, fluorene, phenanthrene, and triphenylene, the macrocyclization efficiency is usually improved. The majority of these macrocycles are shape-consistent without angle-strained alkynes. Carbazole-containing macrocycles are mentioned above (see Section 3.5.3).

Almost all of the fluorene-containing macrocycles are strain free. Kim, Wu, and co-workers synthesized 3,6-diethynylfluorene-based macrocycles **180** by Stille-coupling (Figure 58a).[296] Although cyclotetramer **180b** and cyclopentamer **180c** are strain free, cyclotrimer **180a** is slightly strained. Macrocyclic polyradical species are efficiently generated upon treatment with tin(II) reductant.

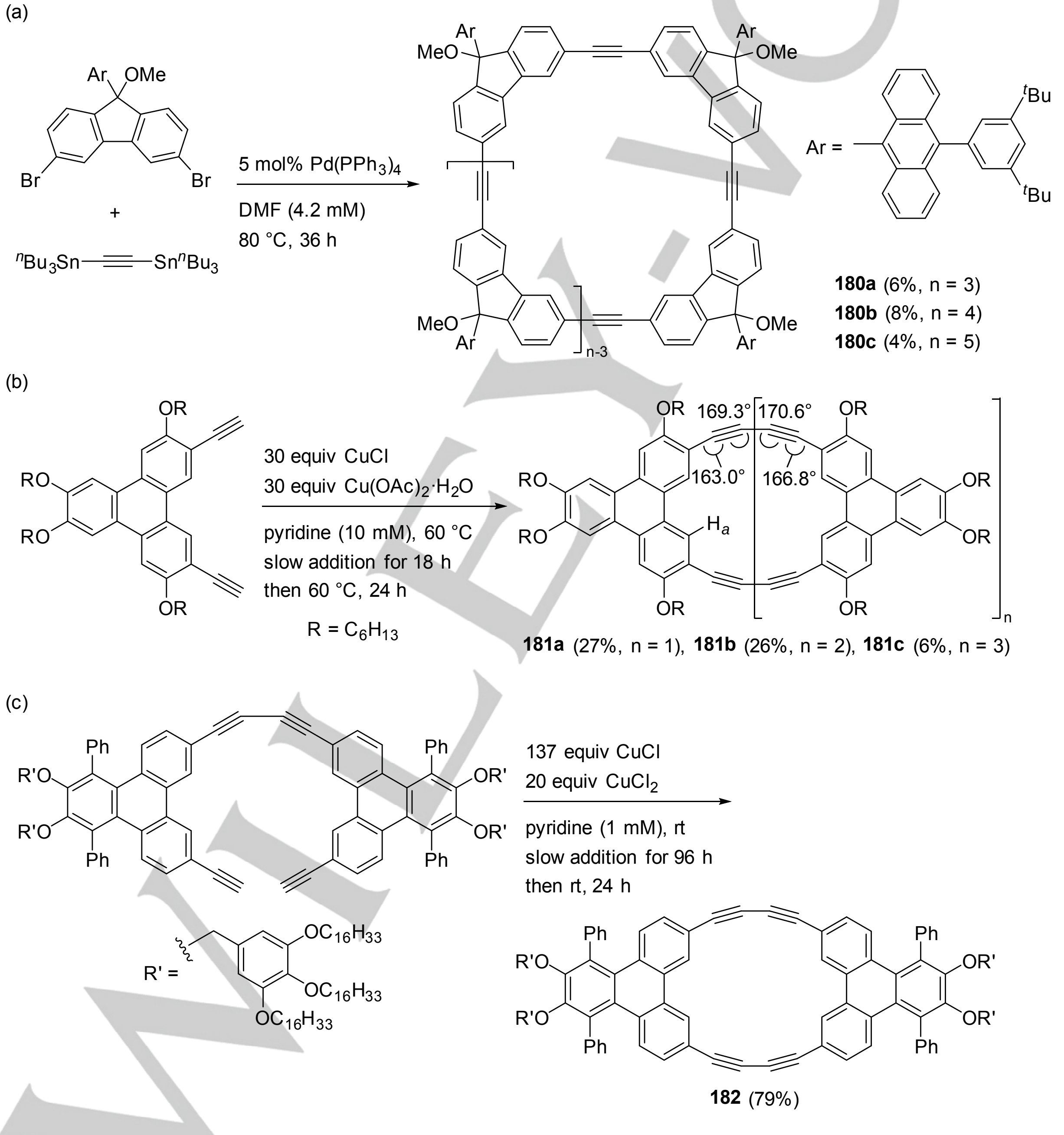

Figure 58. Fluorene-, triphenylene-containing macrocycles. Bond angles of cyclodimer **181a** are shown.

Reported phenanthrene-containing macrocycles are almost strain free. Dehydrobenzoannulene derivatives, such as **72**, **74**, and **78**, and dithienothiophene-containing macrocycle **156** (*vide supra*) are representative examples containing angle-strained alkynes in their π-system. Cammidge and co-workers synthesized triphenylene-fused macrocycles **181** by Eglinton coupling (Figure 58b).[297,298] Cyclodimer **181a** is planar-shaped and contains angle-strained alkynes. The protons H_a in the cavity are observed at downfield (9.23 ppm), indicating that cyclodimer is formally a [4n] π-electron antiaromatic system. Interestingly, cyclodimer **181a** forms a nematic mesophase on heating, although strong inter- and intracolumnar interactions were confirmed by X-ray analysis (CCDC: 769122). The copper-mediated intramolecular coupling of linear dimer improves the macrocyclization efficiency, where the similar cyclodimer **182** could be synthesized in excellent yield (Figure 58c).[299] A systematic alignment on HOPG was observed by microscopic observation.

3.5.6. Anthracene spacer

9,10-Anthrylene moieties of 9,10-anthryleneethynylene-containing CPPA derivatives **48**, **49**, **57**, **58**, and **64**–**67**, and 9,10-anthryleneethynylene-containing carbon double-helicates **178** and **179** play a pivotal role in attractive interaction. By utilizing the interaction of π-expanded anthracene rings, macrocycles exhibit a strong encapsulation property as well as near-infrared circularly polarized luminescence through intramolecular excimer formation.

9,10-Anthryleneethynylene-containing strained macrocycles have been intensively studied by Toyota and co-workers. 9,10-Anthryleneethynylene-containing macrocycles **183** were synthesized using Eglinton homocoupling (Figure 59a).[300] The bond angles ($\angle_{sp}$) of **183a** are 171.1–177.8°, which were determined by X-ray crystallographic analysis (CCDC: 756295), indicating that the alkynes are not highly curved. The larger macrocycles **183b** and **183c** are strain free. Two 9,10-anthrylene rings similarly rotate by ≈40° relative to the basal macrocyclic plane. The calculation of **183a** showed that the rotation energy is as small as 8 kJ mol^{-1} per unit.

Toyota and co-workers reported 1,8-anthrylene–ethynylene-containing macrocycles.[301–307] The intramolecular Sonogashira–Hagihara coupling followed by Eglinton coupling afforded monoyne- and diyne-containing macrocycles **184** and **185**, respectively (Figure 59b). While **184** and **186** show interesting dynamic behaviors such as swinging and pedaling, these macrocycles are strain free (Figure 60).[304,307,308] The selected examples of strained macrocycles are depicted in Figure 61. Fan-blade-shaped macrocycle **187** was synthesized as a racemic mixture by Eglinton coupling.[309–312] The pure enantiomer could be resolved using chiral high performance liquid chromatography. DFT calculations pointed out that the macrocyclic structure is slightly distorted because of the steric repulsion between a hydrogen atom and a methoxy group inside the macrocyclic ring. The monoyne moiety is slightly strained, although the diyne moiety is strain free. The free energy of activation $\Delta G^{\ddagger}$ for enantiomerization is estimated at 122 kJ mol^{-1} by kinetic analysis. Fan-blade-shaped macrocycle **188** having a dodecyl group could form a self-assembled network on graphite.[312] All molecules in each domain of self-assembly have the same two-dimensional chirality. A theoretical calculation of cyclotrimer **189** suggested a small energy difference (0.5 kJ mol^{-1}) between C_2- and C_s-symmetric structures. The C_2-symmetric structure in the solid state was determined by X-ray crystallographic analysis (CCDC: 611249).[313] The bond angles ($\angle_{sp}$ = 165.6–174.3°) in the solid state are consistent with those ($\angle_{sp}$ = 166.7–174.4°) estimated by DFT calculation. In contrast, cyclotrimer **190** favored the much more stable C_s-symmetric structure than C_2-symmetric structure, which was evaluated by DFT calculation. The bond angles ($\angle_{sp}$ = 166.0–171.0°) estimated by DFT calculation are similar to those of cyclotrimer **189**. Macrocycle **191** bearing two monoynes and two diynes was prepared by Pd-catalyzed monoyne formation and Cu-mediated diyne formation.[301] Anthracene rings in the molecule are almost planar as depicted by the rhombus-shaped structure with approximately D_2 symmetry. Diynes of **191** are slightly curved ($\angle_{sp}$ = 169.7–175.7°) in the solid state, but monoynes are not strained ($\angle_{sp}$ = 173.2–176.7°) (CCDC: 630820). Cyclic pentamers **192** and **193** possess strained alkynes.[314,315] In DFT calculations, the acetylenes in **192** and **193** are estimated to be curved up to $\angle_{sp}$ = 168.0° and 165.5°, respectively.

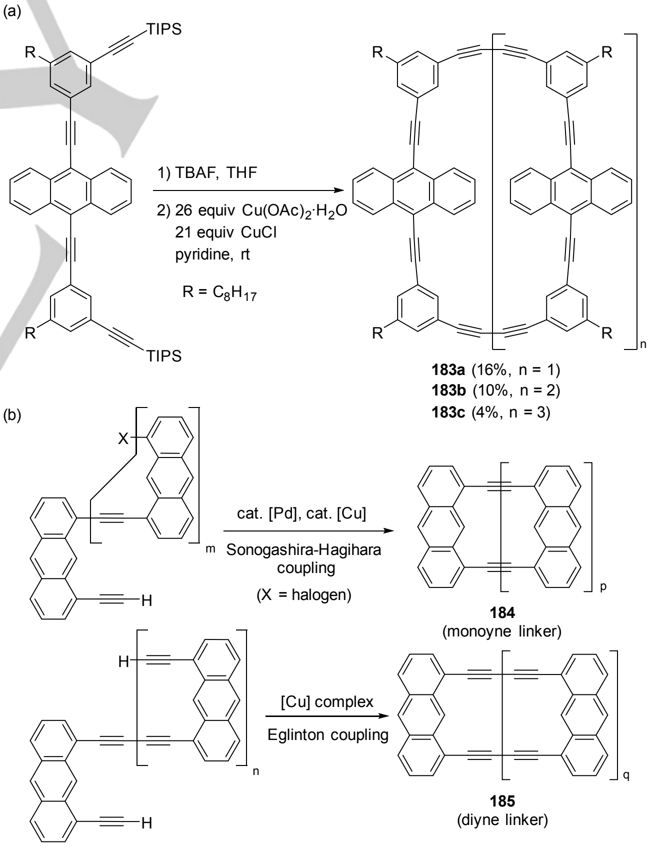

Figure 59. Strained 9,10-anthryleneethynylene-containing macrocycles.

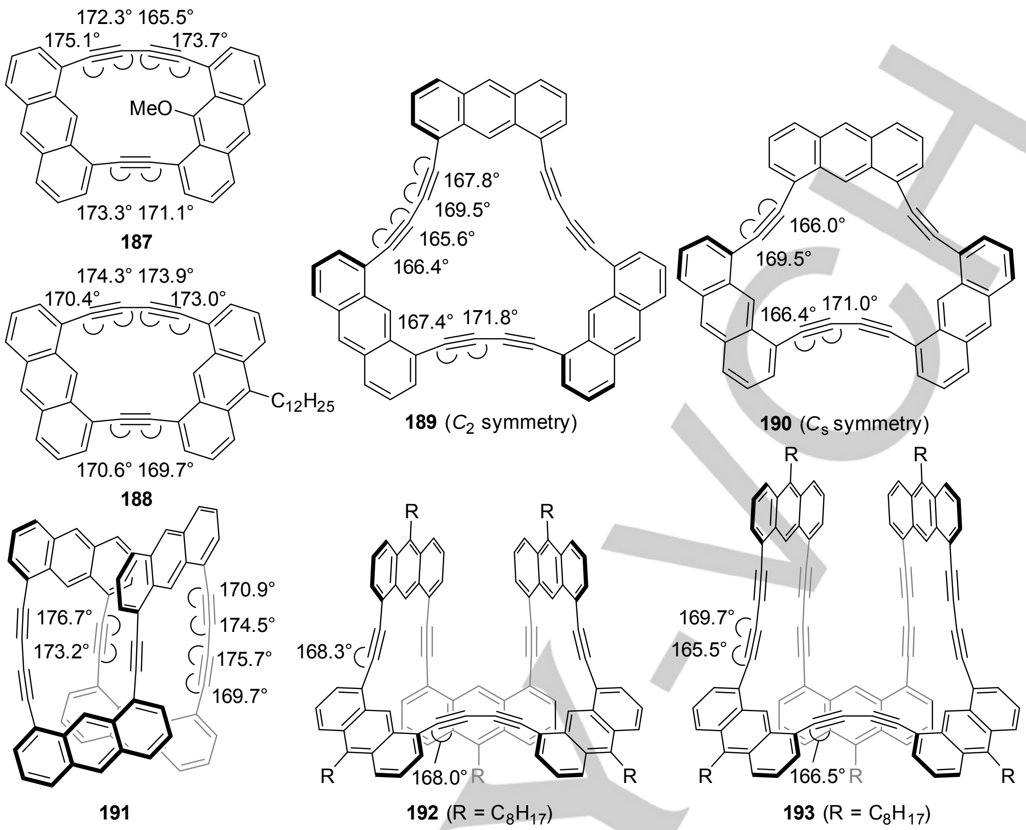

Figure 61. Strained 1,8-anthrylene-ethynylene-containing macrocycles. Bond angles were determined by X-ray (**187**–**189** and **191**) and DFT (**190**, **192**, and **193**), respectively.

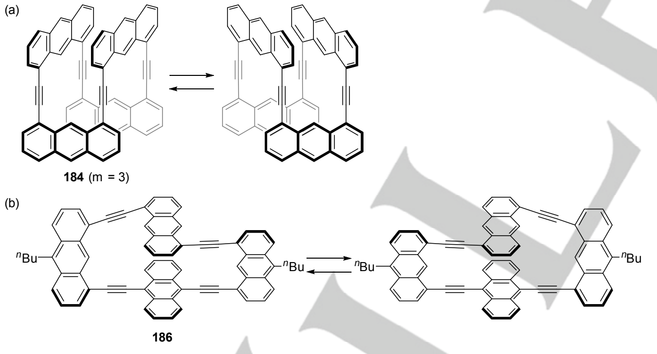

Figure 60. 1,8-Anthryleneethynylene-containing macrocycles showing dynamic (a) swinging and (b) pedaling behaviors.

3.5.7. Porphyrin spacer

Anderson and co-workers reported an intelligent method to synthesize macrocycles consisting of porphyrins and strained alkynes (Figure 62).[64] Because there is an account paper on porphyrin-containing macrocycles,[64] the representative macrocycles are overviewed in this section.

The ring size could be perfectly controlled by template molecules that can coordinate to the center metal of porphyrins. The first breakthrough was made by the template-assisted synthesis of π-conjugated porphyrin cyclooctamer **194d** in 2007.[316] The other size of macrocycles, such as cyclopentamer **194a**, cyclohexamer **194b**, cycloheptamer **194c**, and cyclododecamer **194e**, were successively synthesized using appropriate templates in the Glaser coupling reaction.[317–320] For example, templates **196** and **197** were used for the synthesis of **194a** and **194b**, respectively. The bond angles at alkynes in cyclopentamer **194a** are estimated at 169.8° and 173.0° by DFT calculation, whereas complexation with corannulene-based template **196** slightly warped the alkynes ($\angle_{sp}$ = 166–170°).[317] The bond angles at sp carbons in the complex of **194b** with template **197** were determined as 168–171° by X-ray crystallographic analysis (CCDC: 860774),[321] which are in good agreement with values obtained by calculation.[322] Free cyclohexamer **194b**, whose bond angles are 171.7° and 174.3° (DFT calculation), is strain free, indicating that the coordination of template molecules changes the ring structure. Cyclododecamer **194e** could be synthesized from linear porphyrin tetramer **199** and template **197** by removal of two templates from the supramolecular Vernier complex **200** (Figure 63).[320,323] The Vernier-template route is applicable to the synthesis of larger porphyrin macrocycles, such as 24-porphyrin nanoring.[324,325] Cyclohexamer **195** bearing a porphyrin–alkyne alternative structure could be synthesized using template **198** under Sonogashira–Hagihara coupling conditions.[326] The bond angles at *sp* carbon of **195** are slightly strained in the structure without a template ($\angle_{sp}$ = 169.1–170.9°) and with a template ($\angle_{sp}$ = 170.0°), which are estimated by DFT calculations. Cyclooctamer **203** was obtained by the coupling reaction of linear octamer **201** with template **202** (Figure 64).[326] Template-free cyclooctamer **203** is strain free ($\angle_{sp}$ = 172.4°), but alkyne moieties in **203** (with template) are more strained. The combination of Glaser coupling and Sonogashira–Hagihara coupling enables obtaining porphyrin macrocycles **204** and **205** containing monoyne or diyne moieties upon treatment with templates **197** and **198**, respectively (Figure 65).[322] The insertion of an ethynylene moiety into porphyrin nanoring **195** dramatically enhanced the affinity to the template **198**, increasing the binding constant by a factor 3 × 10^9. The bond angles of **204** and **205** are similar to those of **194b** and **195**, respectively.

Template-assisted macrocyclization has most recently applied to the preparation of tube-shaped,[327,328] ball-shaped,[329] caterpillar-like,[330] and Russian doll-like[331] supramolecular assemblies. The evaluation of aromaticity in porphyrin nanoring systems,[332,333] as well as the preparation of heterometalated porphyrin nanorings through the site-selective demetalation–metalation strategy,[334] are also hot topics in this area.

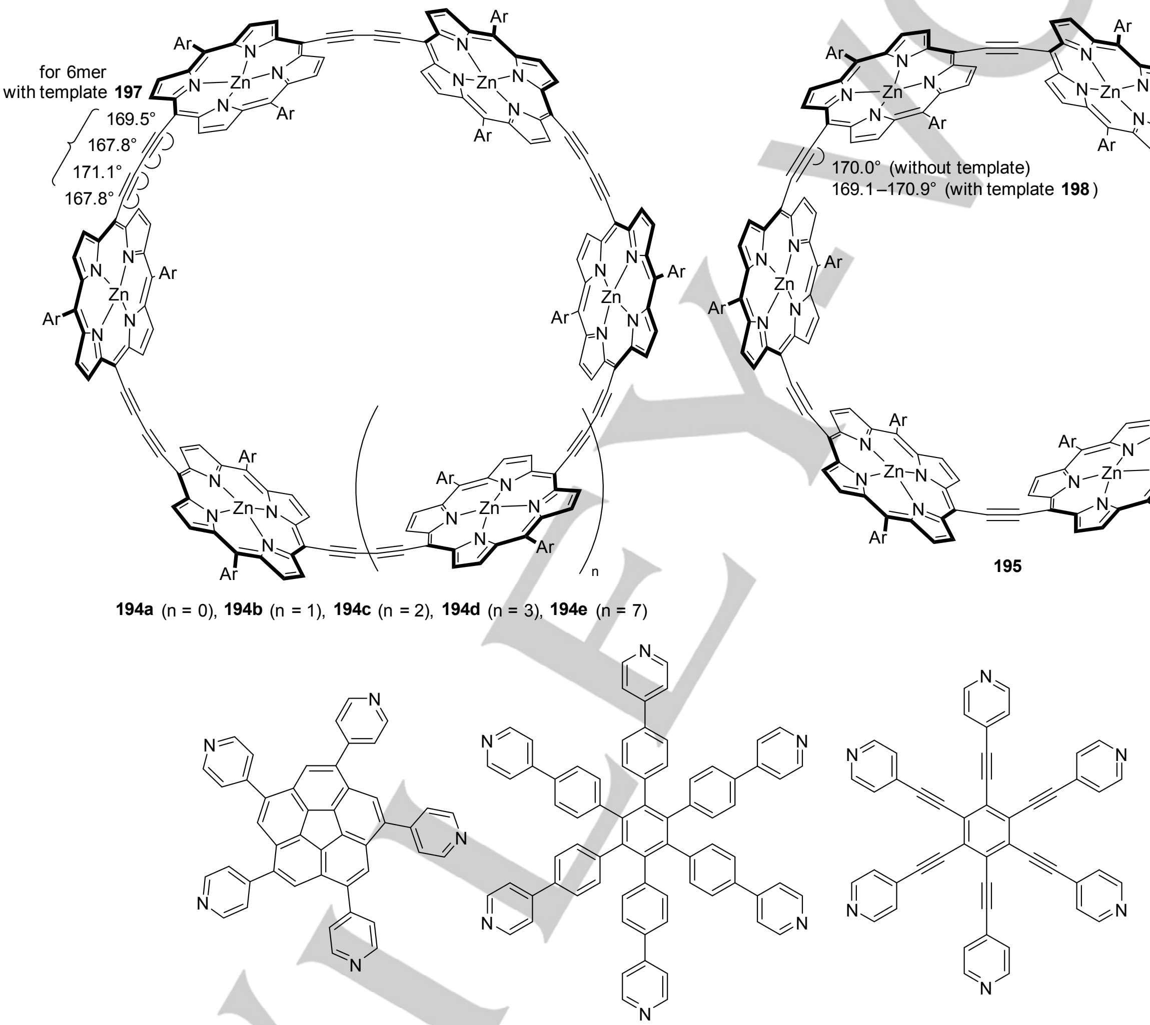

194a (n = 0), **194b** (n = 1), **194c** (n = 2), **194d** (n = 3), **194e** (n = 7)

195

196

197

198

Figure 62. Macrocyclic porphyrin oligomers and templates. Ar groups in marocycles are 3,5-dioctyloxyphenyl, 3,5-di-*tert*-buthylphenyl, or 3,5-bis(trihexylsilyl)phenyl.

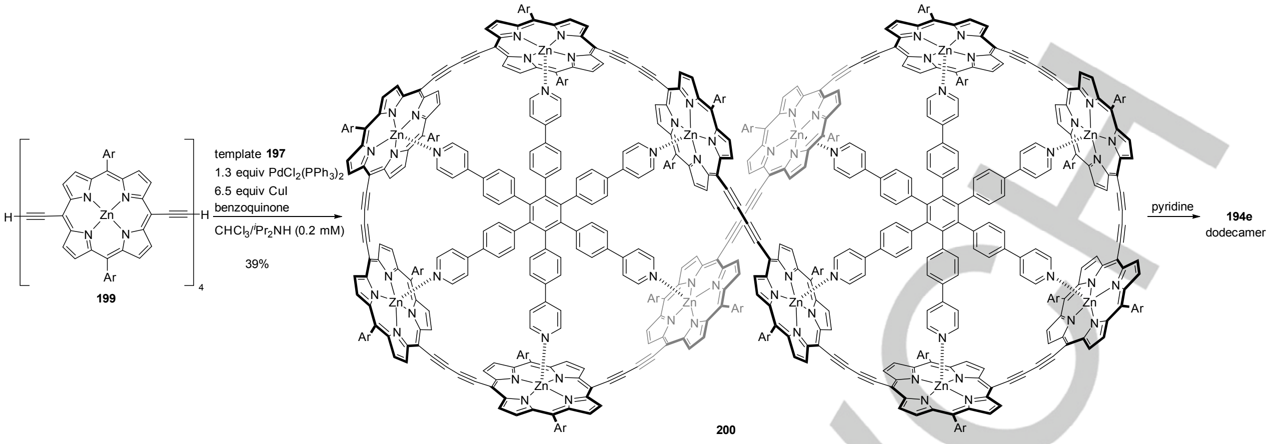

199

200

Figure 63. Supramolecular Vernier complex. Ar = 3,5-di-*tert*-buthylphenyl.

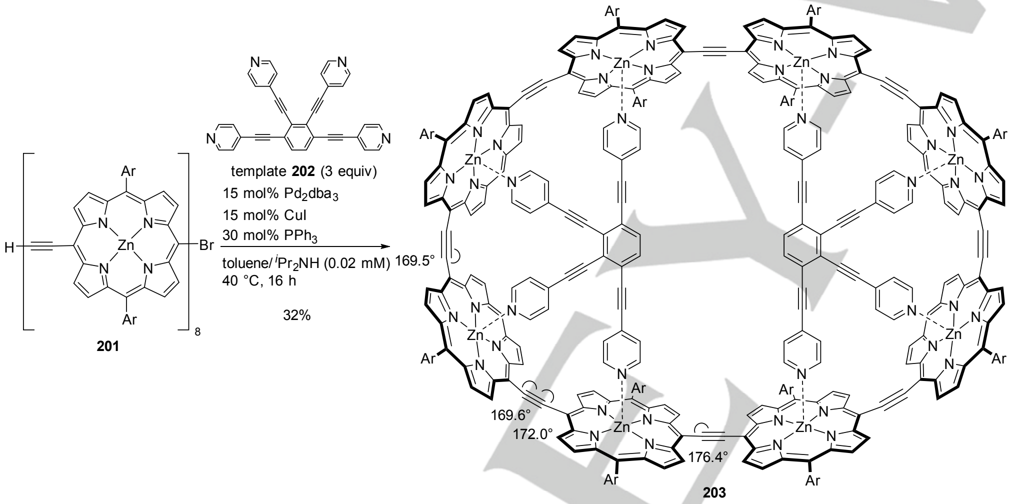

201

203

Figure 64. Template-assisted macrocyclization through Sonogashira-Hagihara coupling. Ar = 3,5-bis(trihexylsilyl)phenyl.

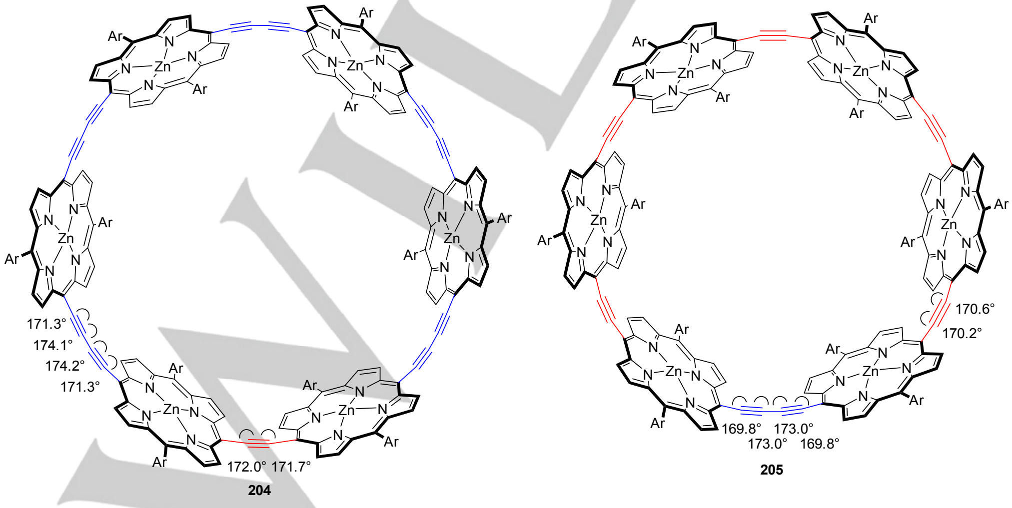

204

205

Figure 65. Unsymmetrical porphyrin nanorings with both ethyne and butadiyne likers.

3.5.8. [2.2]Paracyclophane spacer

[2.2]Paracyclophane is a spacer for through-space π-electron delocalization. Several angle-strained alkyne-containing macrocycles having [2.2]paracyclophane moieties have been reported so far. Haley, Hopf, and co-workers synthesized [2.2]paracyclophane-containing macrocycles **206** and **207** by copper-mediated or palladium-catalyzed homocoupling (Figure 66).[335,336] From the spectroscopic analyses, global transannular π-electron delocalization, including [2.2]paracyclophane, was confirmed. From the X-ray analysis of non-benzo-fused macrocycle (CCDC: 160412), [14]DBA-like paracyclophane-containing macrocycle **206** is strain free. The [14]DBA structure of **207** is quite similar to [14]DBA **89a**, confirmed by X-ray crystallographic analysis (CCDC: 289410). "Step"-shaped and "propeller"-shaped larger hybrid macrocycles were also synthesized.[337] The structures of these hybrid macrocycles are similar to **206** and **207**. Hopf and co-workers synthesized [12]DBA- and [14]DBA-like paracyclophane-containing macrocycles using copper-mediated Hay coupling.[338] The homodimerization of 4,12-diethynyl[2.2]paracyclophane gave a mixture of chiral macrocycle **208** and achiral macrocycle **209** in 67% yield. The copper-mediated cyclization of 4,12-diethynyl[2.2]paracyclophane with *o*-diethynylbenzene afforded the corresponding macrocycle **210** together with homodimer of *o*-diethynylbenzene. [14]DBA-like paracyclophane-containing macrocycles **211** and **212** were synthesized from the corresponding precursor.[338] Both macrocycles are slightly less strained than [12]DBA and [14]DBA, respectively. The cobalt-mediated transformation of triacetylene **213** gave cobalt complex **214** in good yield.[338] Because the alkyne moiety is strained, the cyclotrimerization did not proceed.

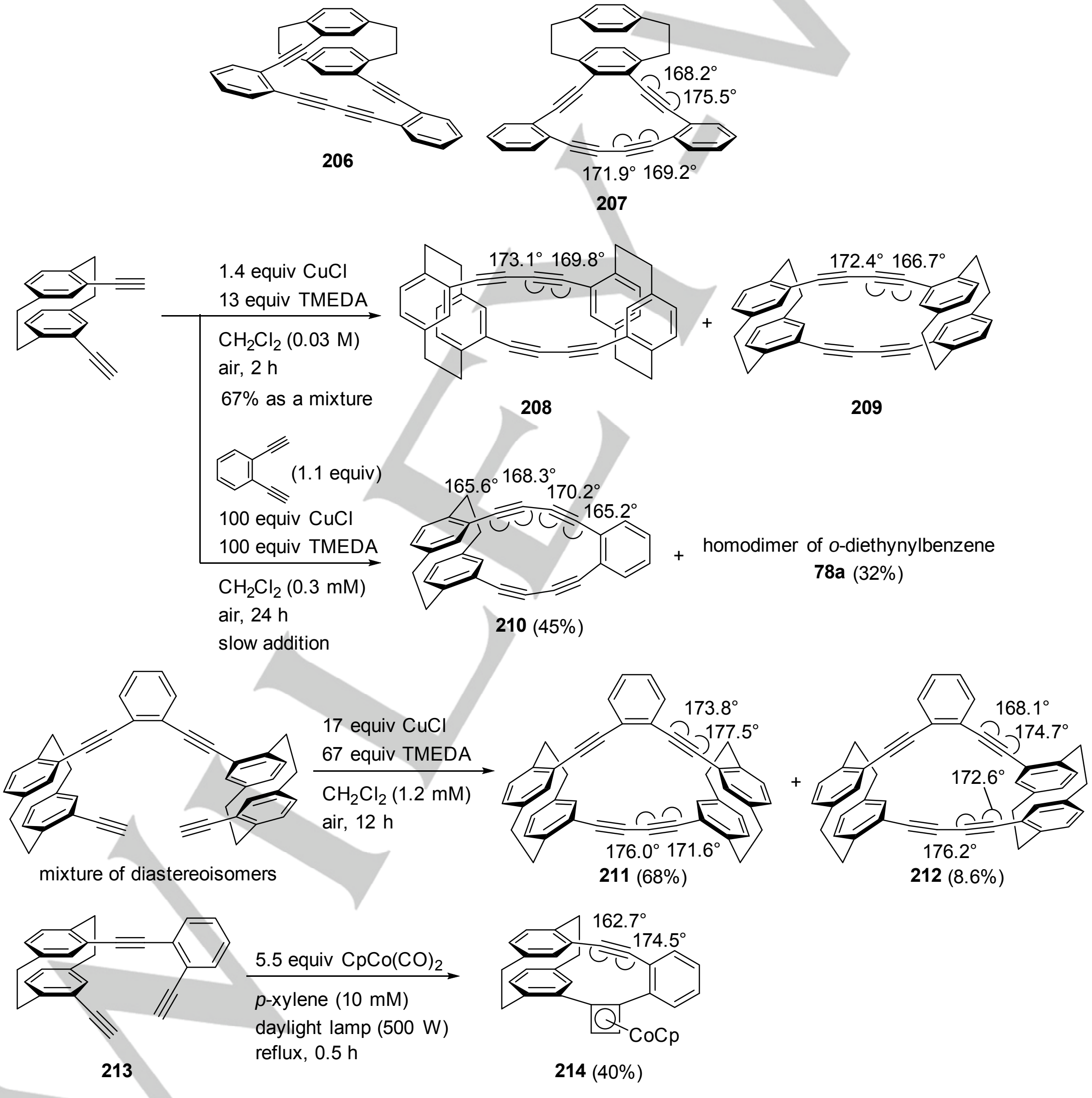

Figure 66. [2.2]paracyclophane-containing macrocycles.

3.5.9. Cyclobutadienyl- and cyclopentadienylmetal complexes as a spacer

Cyclobutadienyl- and cyclopentadienylmetal complexes have been used as a spacer in angle-strained π-conjugated macrocycles.[339] Bunz and co-workers synthesized cyclooligomers of (1,2-diethynylcyclobutadienyl)(cyclopentadienyl)cobalt complex and 1,2-diethynylferrocene (Figure 67).[340,341] Because of planar chirality, cyclooligomers **215** and **216** were obtained as a mixture of diastereoisomers. Upon treatment of **215a** with fluoride, the deprotection of trimethylsilyl groups proceeded smoothly to afford **215b**. The bond angles ($\angle_{\mathrm{sp}}$) of *trans*-**215a** (CCDC: 1248671) and *trans*-**216** (CCDC: 1294802) are 171.6–177.5° and 171.0–178.7°, respectively. Bunz and co-workers synthesized [14]DBA analogues **217**–**220** using intramolecular alkyne-coupling of metallocene-containing diynes.[342,343] From X-ray crystallographic analyses, both cobalt- and iron-containing [14]DBA analogues **218** (CCDC: 157835) and **220** (CCDC: 157834) have similar structures to [14]DBA **89a**. ^{1}H NMR measurement revealed that cyclobutadienyl moieties in **217** and **218** and cyclopentadienyl moieties in **219** and **220** are more aromatic than the benzene ring in **89a** according to the ring-current criterion. π-Expanded macrocycles **221**–**224** containing cobalt and iron complexes were synthesized.[344–347] Because of the square-shaped cyclobutadienyl ligand, cobalt complexes **221** (CCDC: 154093), **222** (CCDC: 176513), and **224** (CCDC: 176515) containing π-expanded cyclobutadienyl ligands are strain free. In contrast, pentagon-shaped cyclopentadienyl ligand distorts the macrocyclic structure of **223**, in which both monoyne and diyne moieties are strained (CCDC: 176514).

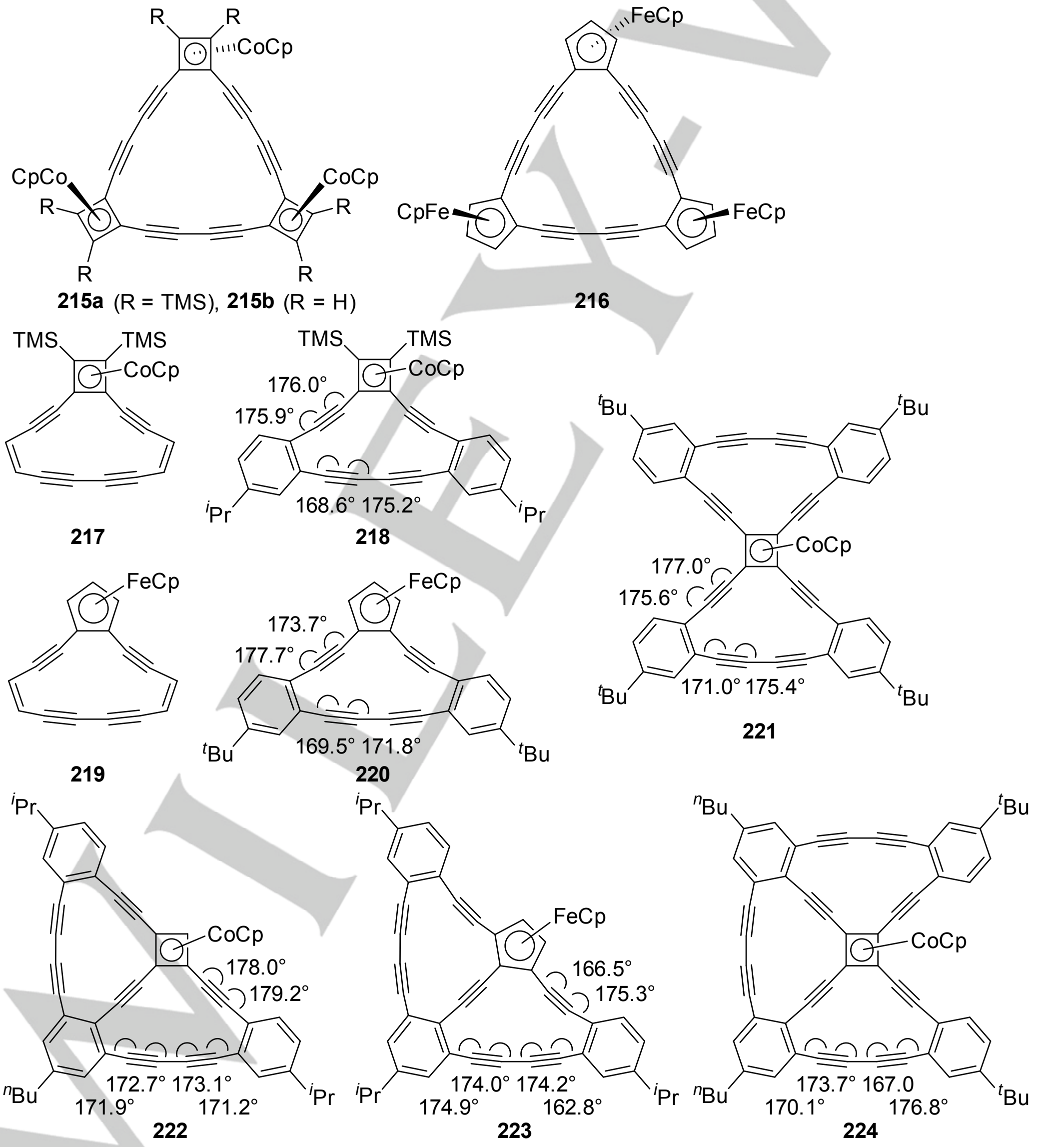

Figure 67. Metallocene-containinig macrocycles. TMS = trimethylsilyl.

3.5.10. π-Expanded radialenes and radiaannulenes

Radialenes consisting of exocyclic double bonds are not stabilized by π-conjugation, but researchers pursued them because of their unique reactivity as well as attractive symmetrical structures (Figure 68).[348] In the 1990s, the groups of both Diederich and Tykwinski reported various π-expanded radialenes and radiaannulenes. Among them, angle-strained macrocycles are highlighted in this section. For shape-persistent π-expanded radialenes refer to account and review articles.[349–352]

Diederich and co-workers synthesized diyne-containing π-expanded radialenes **226** using Hay coupling of 1,1-diethynylethene **225** (Figure 69a).[353] Although there is no structural information about bond angles, cyclotrimer **226a** would be categorized as a strained macrocycle. When the triisopropylsilylethynyl group was used as R^1 substituent in **225** instead of an arylethynyl group, the macrocyclization did not take place.[134] The cyclodimerization and cyclotrimerization of **227** proceeded to give **228a** and **228b** in moderate yields (Figure 69b). This cyclization was further applied to a substrate containing arylethynyl substituents, affording the corresponding macrocycle **226b** in 10% yield. The photophysical properties are much affected by the substituents. The molar extinction coefficients are increased by electron-donating substituents, whereas those of macrocyclic cross-conjugation in **228** bearing silyl substituents are not affected. The donor–acceptor polarization induces a bathochromic shift of the absorption maxima. The aromaticity of π-expanded radialenes was demonstrated experimentally and theoretically.[354]

Tobe and co-workers reported the synthesis of π-expanded radialene derivatives **229** by Eglinton coupling of diethynylmethylenebicyclo[4.3.1]decatriene derivative **229** (Figure 69c).[66] Although no structural information was described, [3]radialene **7a** seems to be strained. All cyclooligomers **7** were converted to the corresponding cyclocarbons through photoinduced indane elimination.

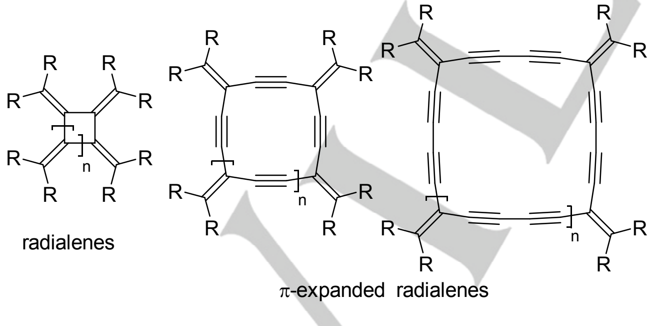

Figure 68. Radialenes and π-expanded radialenes.

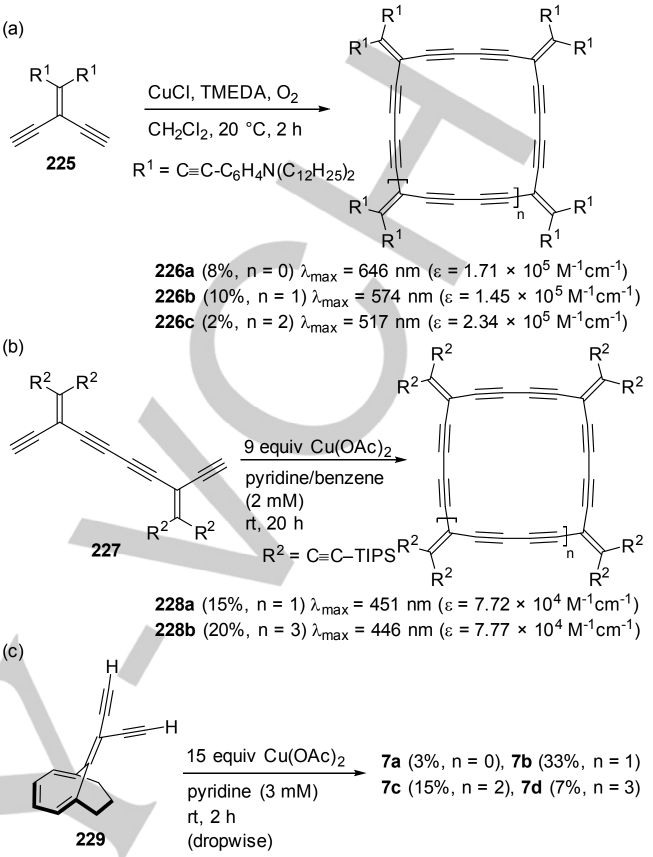

226a (8%, n = 0) λ_{max} = 646 nm ($\varepsilon = 1.71 \times 10^5$ $M^{-1}cm^{-1}$)
226b (10%, n = 1) λ_{max} = 574 nm ($\varepsilon = 1.45 \times 10^5$ $M^{-1}cm^{-1}$)
226c (2%, n = 2) λ_{max} = 517 nm ($\varepsilon = 2.34 \times 10^5$ $M^{-1}cm^{-1}$)

228a (15%, n = 1) λ_{max} = 451 nm ($\varepsilon = 7.72 \times 10^4$ $M^{-1}cm^{-1}$)
228b (20%, n = 3) λ_{max} = 446 nm ($\varepsilon = 7.77 \times 10^4$ $M^{-1}cm^{-1}$)

7a (3%, n = 0), **7b** (33%, n = 1)
7c (15%, n = 2), **7d** (7%, n = 3)

Figure 69. Synthesis of diyne-containing π-expanded radialenes.

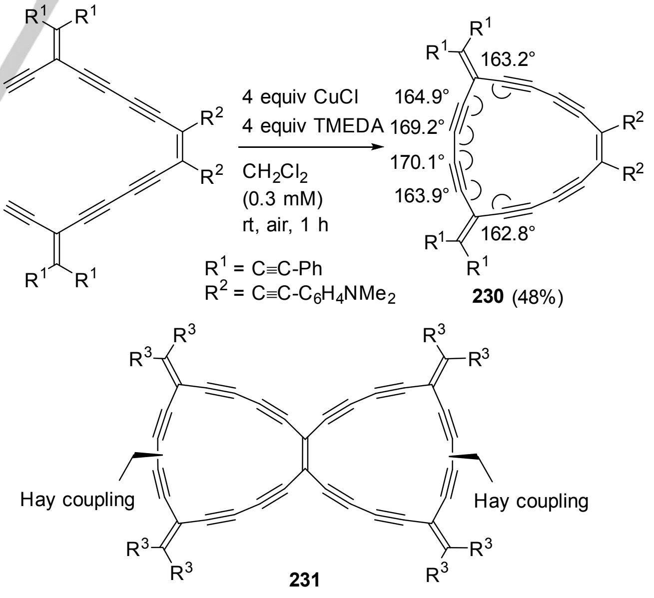

Figure 70. Synthesis of radiaannulenes.

To explore the unprecedented electronic properties of acetylenic carbon sheets, Diederich and co-workers synthesized radiaannulenes, whose structure contained both 1,1-diethynylethene and 1,2-diethynylethene moieties (Figure 70).[355,356] The intramolecular Hay coupling afforded angle-strained alkyne-containing radiaannulene **230**. X-ray crystallographic analysis revealed that the bond angles ($\angle_{sp}$= 163–170°) of nearby *exo*-methylene moieties are smaller than those ($\angle_{sp}$ = 174–179°) around *cis*-alkene (CCDC: 208124). Bicyclic radiaannulenes were also synthesized by the intramolecular Hay coupling.[355,356] Remarkably, bicyclic radiaannulene **231** bearing eight 3,5-di-*tert*-butylphenylethynyl groups at R^3 substituents was obtained in 88% yield. It was shown that radiaannulenes can act as powerful electron acceptors. Bicyclic radiaannulene **231** can be reversibly reduced at –0.83 V (THF, vs Fc^+/Fc), which indicates that **231** is a better electron acceptor than fullerene C_{60}.

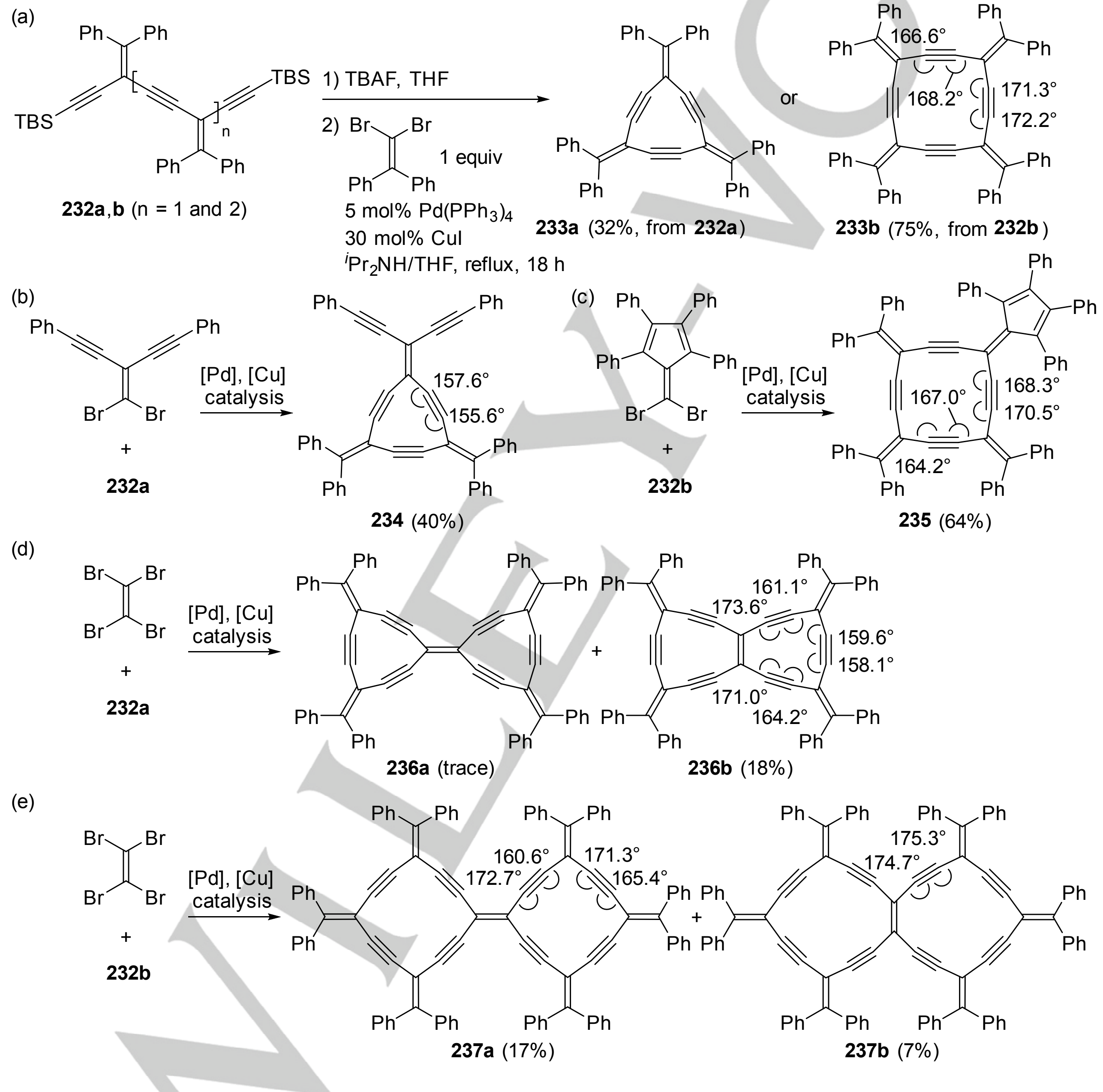

Figure 71. Monoyne-containing π-expanded radialenes and radiaannulenes.

Tykwinski and co-workers prepared monoyne-containing π-expanded radialenes **233** by Sonogashira–Hagihara coupling of **232** (Figure 71a).[350,357] The strained planar structure of **233b** was determined using X-ray crystallographic analysis (CCDC: 652685).[350,358] The introduction of a larger substituent on an *exo*-methylene moiety caused the puckering of π-expanded [4]radialene **235** (38.5°) like cyclobutane rings, which was observed in X-ray crystallographic analysis (CCDC: 952887) (Figure 71c).[359,360] Although a PM3 calculation suggests that the bond angle at the sp carbon of **233a** is smaller than 160°, **233a** was isolated in 32% yield through the Sonogashira–Hagihara coupling. By introducing phenylethynyl groups, the crystal structure of π-expanded [3]radialene derivative **234** could be analyzed (CCDC: 942887) (Figure 71b).[359] This synthetic method could be applied to the preparation of cyclopentamer (45% yield), but is not applicable to cyclohexamer (<5%) due to the competitive polymerization. Bicyclic radiaannulene was obtained using tetrabromoethene instead of 1,1-dibromo-2,2-diphenylethene (Figure 71d).[360] Bisradialene **236a** was not obtained due to its highly strained structure, whereas less-strained **236b** was isolated in 18% yield. X-ray crystallographic analysis revealed that **236b** has an almost planar structure and contains highly strained alkyne next to two *exo*-methylene moieties (CCDC: 652688). Both bisradialene **237a** and bicyclic radiaannulene derivative **237b** were obtained from **232b** and tetrabromoethene (Figure 71e).[358] The core structure of both compounds is nonplanar, but the position of strained alkyne moieties in **237a** (CCDC: 652687) is slightly different from that in **233b**, probably because of the disorder of the cocrystallite formed from **237a** and **237b**.

Sankararaman and co-workers reported the preparation of dehydrobenzo[13]annulene analogues **239** and **240** by deprotection of **238** followed by intramolecular Eglinton coupling (Figure 72).[361] Both benzo-fused precursors **238** bearing saturated and unsaturated cross-conjugation are smoothly converted to bis-dehydro[13]annulenes. Interestingly, non-benzo-fused precursor **241** gave bis-dehydro[18]annulenes **242**. Both structures were determined by X-ray crystallographic analysis (CCDC: 622536 (**239**) and 621595 (**242**)). Bis-dehydro[13]annulenes **239** and **240** are less strained than [12]annulene **75** and dehydrobenzo[12]annulene **77a** due to their one sp^2 carbon-inserted structures. In the structure of **242**, the benzenoid rings and annulene skeletons are not positioned on the same plane due to the steric demand ($\angle_{sp} > 175°$). Although **239** bearing saturated cross-conjugation exhibits fluorescence around 400–500 nm, the fully cross-conjugated annulenes **240** and **242** are nonfluorescent, probably because the nonradiative decay effectively competes with the emission pathway. These results are apparently different from highly emissive bis-dehydrobenzo[15]annulene **108** and bis-dehydrobenzo[14]annulene **109** reported by Haley.[61–63]

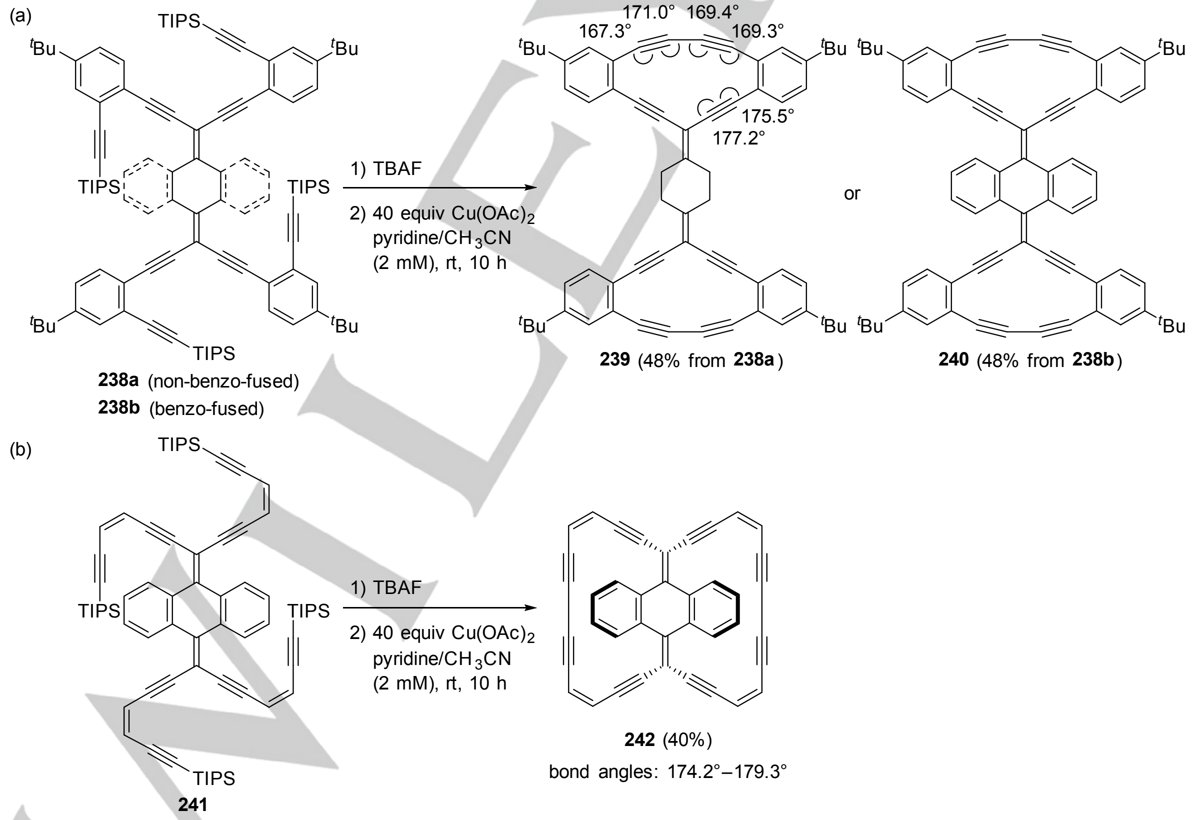

Figure 72. Cross-conjugated bis-dehydroannulenes.

During the investigation of cumulene synthesis, Chauvin and co-workers found the interesting over-reduction of polyyne **243** affording angle-strained alkyne-containing macrocycle (Figure 73).[362] By controlling the tin-mediated reduction conditions and careful quenching by sodium hydroxide, cyclic dibutatrieneacetylene **245** was obtained in 16% yield together with linear butatrieneacetylene **244**. The strained structure of **245** was confirmed by X-ray crystallographic analysis (CCDC: 951899).

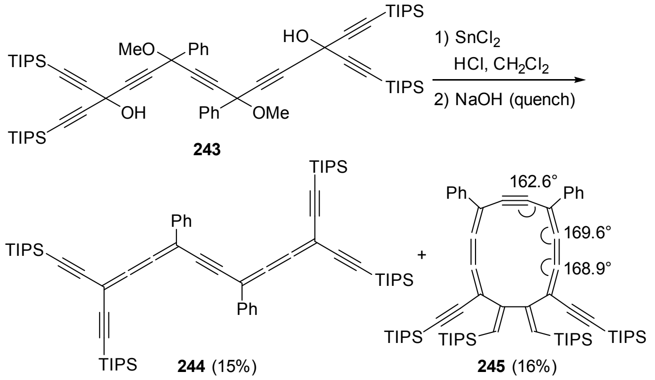

Figure 73. Synthesis of cyclic and non-cyclic dibutatrieneacetylenes through tin-mediated reduction.

4. Conclusion and outlook

In the 20th century, a limited number of π-conjugated macrocycles bearing angle-strained alkynes such as cycloparaphenyleneacetylene and dehydrobenzannulenes were discovered. These molecules were incidentally found in the course of synthesis of cyclocarbons. In the last two decades, many new and structurally attractive macrocycles, including cycloparaphenylenes, carbon nanobelts, thiophene-containing giant macrocycles, and porphyrin nanorings, could be synthesized owing to newly developed sophisticated synthetic methods. Because of their curved π-conjugated system of angle-strained alkyne-containing macrocycles, unique photophysical, electronic, and supramolecular properties have been unveiled. Based on these properties, curved macrocycles have been applied to electronics, molecular sensors, and molecular imaging in cells. Considering that the angle-strained cycloalkynes such as cyclooctyne have been utilized in bioorthogonal chemistry in this past decade, the upcoming application of curved macrocycles emerges not only in electronic materials but also in biochemistry.

Bond angles at sp carbon in strained macrocycles are summarized in Figures 74 and 75. The deformation at sp carbons is mainly caused by the ring strain, especially in a small ring system. In less-strained ring system, steric hinderance and/or intramolecular/transannular interactions can induce the deformation of ethynylenes. It is noted that the structural features as well as properties of π-conjugated system are generally specified by not only bond angles but also bond distances and torsion angles. For isolation of macrocycles, 155–160° seems to be the lower limit of the bond angle at monoyne sp carbon, although this limitation heavily depends on the molecular structures. Because phenylene moieties are tougher against strain than ethynylene, it is important to clarify the relationship between ratio of phenylenes/ethynylenes and bond angle at the sp carbon. These factors should affect the photophysical and electronic properties as well as their stability. The utilization of heteroaromatics as a spacer in a π-conjugated macrocyclic system changes these properties dramatically. Not only by utilizing promising synthetic methods shown in this review but also by exploring new synthetic methods, we believe that new curved π-systems bearing angle-strained alkynes will successively emerge.

Acknowledgment

This work was supported by a Grant-in-Aid for Scientific Research on Innovative Areas “Middle molecular strategy: Creation of higher bio-functional molecules by integrated synthesis (No. 2707)” (18H04404) of The Ministry of Education, Culture, Sports, Science, and Technology, Japan. We are thankful to Professor Yoshito Tobe in Osaka University and National Chiao Tung University for helpful suggestion on the manuscript preparation.

Conflict of interest

The authors declare no conflict of interest.

Keywords: strained alkyne • macrocycle • π-conjugated system

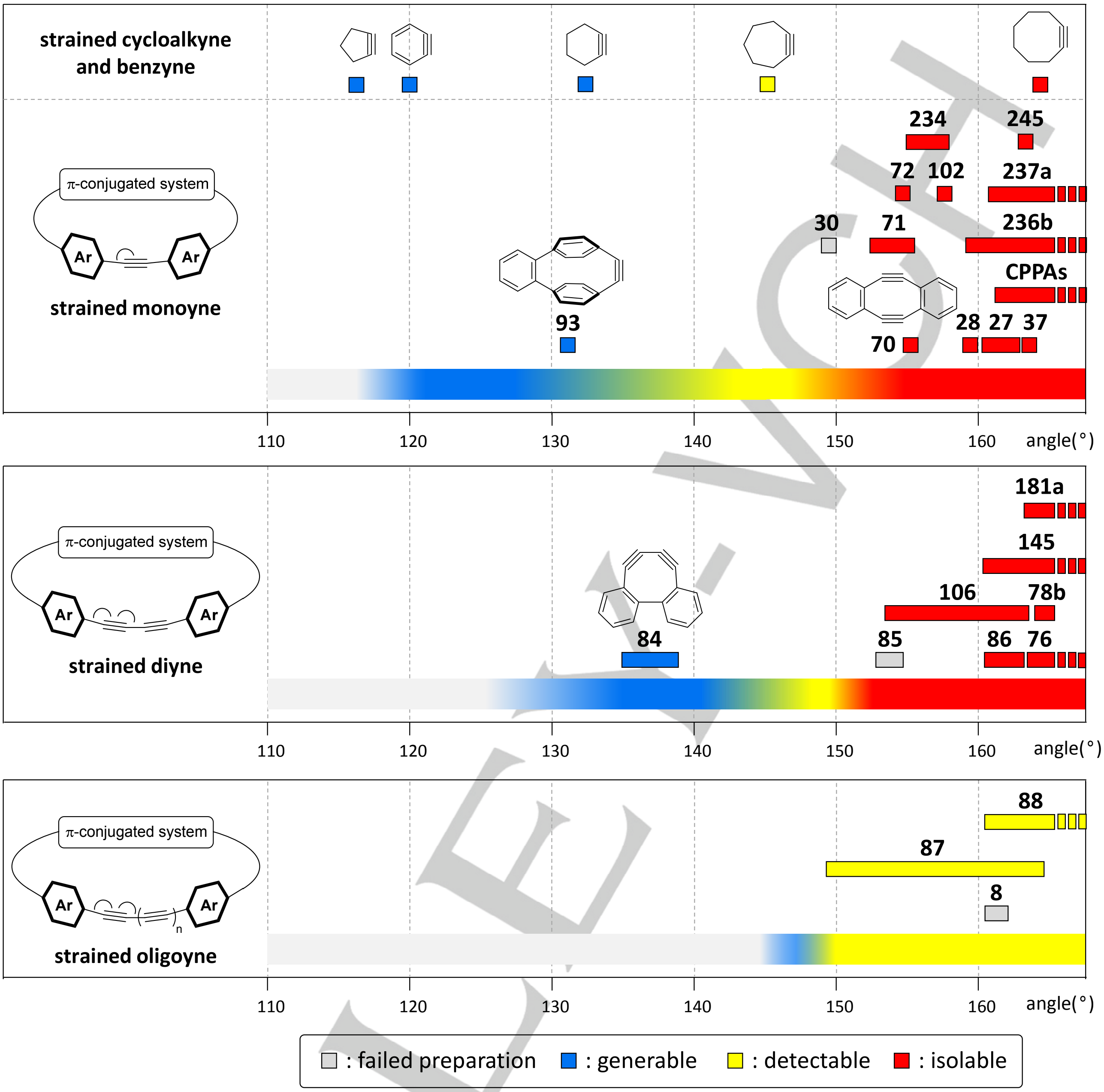

Figure 74. Bond angles ($\angle_{sp} < 165°$) of strained alkynes in π-conjugated macrocycles.

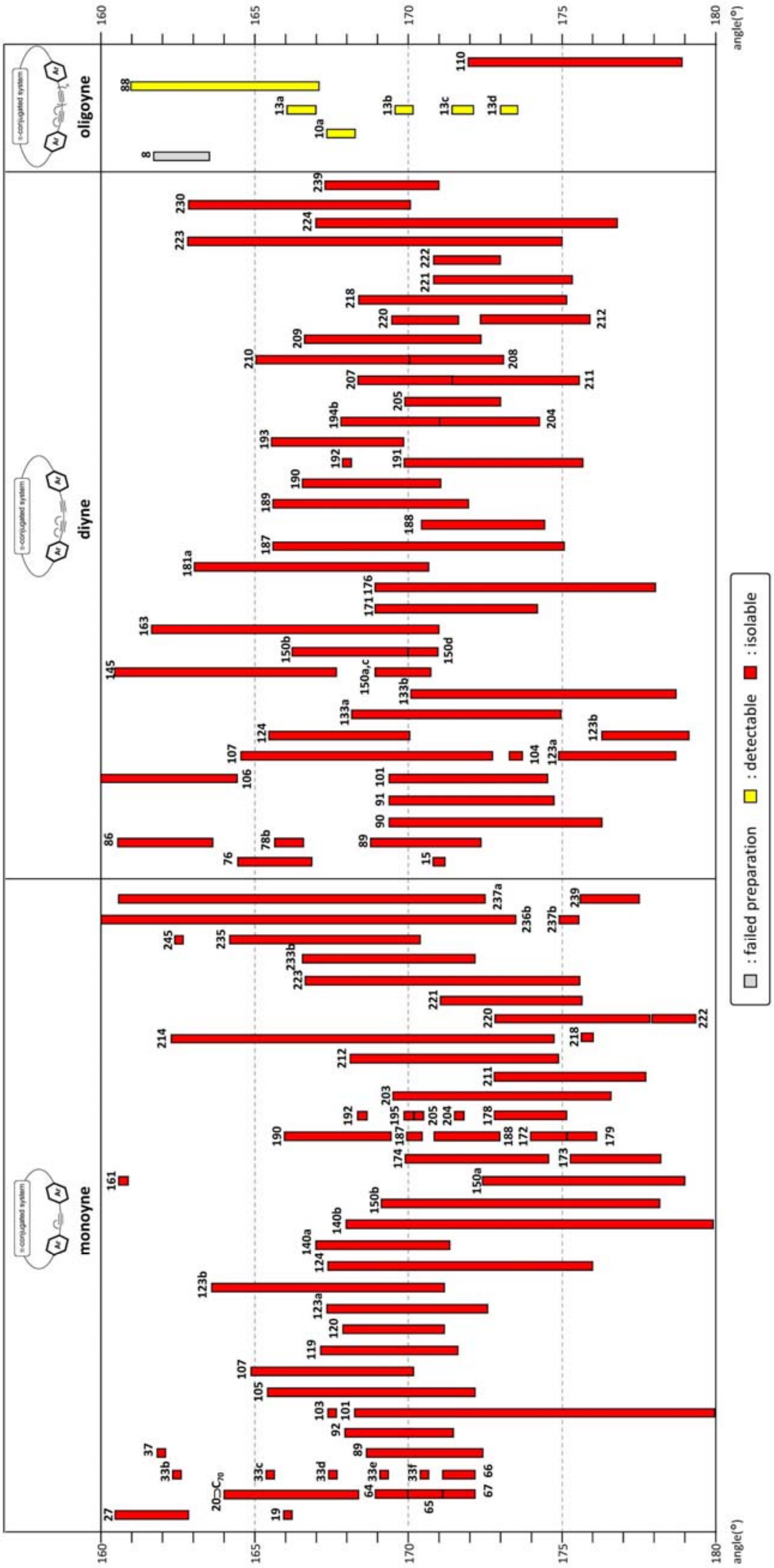

Figure 75. Bond angles (∠$_{sp}$ > 160°) of strained alkynes in π-conjugated macrocycles.

4. References

[1] H. Hopf, J. Grunenberg, in *Strained Hydrocarbons* (Ed.: H. Dodziuk), Wiley, Weinheim, **2009**, 375–397.

[2] E. M. Sletten, C. R. Bertozzi, *Acc. Chem. Res*. **2011**, *44*, 666–676.

[3] M. F. Debets, S. van Berkel, J. Dommerholt, A. J. Dirks, F. P. J. T. Rutjes, F. L. van Delft, *Acc. Chem. Res*. **2011**, *44*, 805–815.

[4] J. C. Jewett, C. R. Bertozzi, *Chem. Soc. Rev*. **2010**, *39*, 1272–1279.

[5] C. M. Gampe, E. M. Carreira, *Angew. Chem. Int. Ed*. **2012**, *51*, 3766–3778.

[6] P. M. Tadross, B. M. Stoltz, *Chem. Rev*. **2012**, *112*, 3550–3577.

[7] H. H. Wenk, M. Winkler, W. Sander, *Angew. Chem. Int. Ed*. **2003**, *42*, 502–528.

[8] G. Wittig, J. Meske-Schüller, *Justus Liebigs Ann. Chem*. **1968**, *711*, 65–75.

[9] C. Wentrup, R. Blanch, H. Briehl, G. Gross, *J. Am. Chem. Soc*. **1988**, *110*, 1874–1880.

[10] J. C. Gilbert, E. G. McKinley, D.-R. Hou, *Tetrahedron* **1997**, *53*, 9891–9902.

[11] J. M. Medina, T. C. McMahon, G. Jiménez-Osés, K. N. Houk, N. K. Garg, *J. Am. Chem. Soc*. **2014**, *136*, 14706–14709.

[12] D. P. Maurer, R. Fan, D. M. Thamattoor, *Angew. Chem. Int. Ed*. **2017**, *56*, 4499–4501.

[13] A. T. Blomquist, L. H. Liu, *J. Am. Chem. Soc*. **1953**, *75*, 2153–2154.

[14] R. A. G. de Graaff, S. Gorter, C. Romers, H. N. C. Wong, F. Sondheimer, *J. Chem. Soc., Perkin Trans. 2* **1981**, 478–480.

[15] F. Diederich, Y. Rubin, C. B. Knobler, R. L. Whetten, K. E. Schriver, K. N. Houk, Y. Li, *Science*, **1989**, *245*, 1088–1090.

[16] Y. Rubin, C. B. Knobler, F. Diederich, *J. Am. Chem. Soc*. **1990**, *112*, 4966–4968.

[17] Y. Rubin, M. Kahr, C. B. Knobler, F. Diederich, C. L. Wilkins, *J. Am. Chem. Soc*. **1991**, *113*, 495–500.

[18] Y. Tobe, T. Fujii, H. Matsumoto, K. Naemura, Y. Achiba, T. Wakabayashi, *J. Am. Chem. Soc*. **1996**, *118*, 2758–2759.

[19] Y. Tobe, T. Fujii, H. Matsumoto, K. Tsumuraya, D. Noguchi, N. Nakagawa, M. Sonoda, K. Naemura, Y. Achiba, T. Wakabayashi, *J. Am. Chem. Soc*. **2000**, *122*, 1762–1775.

[20] K. Kaiser, L. M. Scriven, F. Schulz, P. Gawel, L. Gross, H. L. Anderson, *Science* **2019** *365*, 1299–1301.

[21] S. E. Lewis, *Chem. Soc. Rev*. **2015**, *44*, 2221–2304.

[22] E. R. Darzi, R. Jasti, *Chem. Soc. Rev*. **2015**, *44*, 6401–6410.

[23] H. Omachi, Y. Segawa, K. Itami, *Acc. Chem. Soc*. **2012**, *45*, 1378–1389.

[24] R. Jasti, J. Bhattacharjee, J. B. Neaton, C. R. Bertozzi, *J. Am. Chem. Soc*. **2008**, *130*, 17646–17647.

[25] H. Takaba, H. Omachi, Y. Yamamoto, J. Bouffard, K. Itami, *Angew. Chem. Int. Ed*. **2009**, *48*, 6112–6116.

[26] S. Yamago, Y. Watanabe, T. Iwamoto, *Angew. Chem. Int. Ed*. **2010**, *49*, 757–759.

[27] T. Kawase, H. R. Darabi, M. Oda, *Angew. Chem. Int. Ed*. **1996**, *35*, 2664–2666.

[28] T. Kawase, K. Tanaka, N. Fujiwara, H. R. Darabi, M. Oda, *Angew. Chem. Int. Ed*. **2003**, *42*, 1624–1628.

[29] M. A. Majewski, M. Stępień, *Angew. Chem. Int. Ed*. **2019**, *58*, 86–116.

[30] A. Krebs, J. Wilke, *Top. Curr. Chem*. **1983**, *109*, 189–233.

[31] U. H. F. Bunz, Y. Rubin, Y. Tobe, *Chem. Soc. Rev*. **1999**, *28*, 107–119.

[32] T. Kawase, H. Kurata, *Chem. Rev*. **2006**, *106*, 5250–5273.

[33] M. Cholami, R. R. Tykwinski, *Chem. Rev*. **2006**, *106*, 4997–5027.

[34] K. Tahara, Y. Tobe, *Chem. Rev*. **2006**, *106*, 5274–5290.

[35] V. Maraval, R. Chauvin, *Chem. Rev*. **2006**, *106*, 5317–5343.

[36] E. L. Spitler, C. A. Johnson II, M. M. Haley, *Chem. Rev*. **2006**, *106*, 5344–5386.

[37] I. Hisaki, M. Sonoda, Y. Tobe, *Eur. J. Org. Chem*. **2006**, 833–847.

[38] S. Toyota, *Chem. Rev*. **2010**, *110*, 5398–5424.

[39] M. Iyoda, J. Yamakawa, M. J. Rahman, *Angew. Chem. Int. Ed*. **2011**, *50*, 10522–10553.

[40] M. K. Smith, O. Š. Miljanić, *Org. Biomol. Chem*. **2015**, *13*, 7841–7845.

[41] W. Zhang, J. S. Moore, *Angew. Chem. Int. Ed*. **2006**, *45*, 4416–4439.

[42] A. L. Sadowy, R. R. Tykwinski in *Modern Supramolecular Chemistry* (Ed.: F. diederich, P. J. Stang, R. R. Tykwinski), Wiley, Weinheim, **2008**, 185–231.

[43] S. Höger, *Pure Appl. Chem*. **2010**, *82*, 821–830.

[44] D. E. Gross, L. Zang, J. S. Moore, *Pure Appl. Chem*. **2012**, *84*, 869–878.

[45] C. Yu, Y. Jin, W. Zhang, *Chem. Rec*. **2015**, *15*, 97–106.

[46] K. Tahara, S. Lei, J. Adisoejoso, S. De Feyter, Y. Tobe, *Chem. Commun*. **2010**, *46*, 8507–8525.

[47] Y. Tobe, K. Tahara, S. De Feyter, *Bull. Chem. Soc. Jpn*., **2016**, *9*, 1277-1306.

[48] Y. Tobe, T. Wakabayashi, in *Acetylene Chemistry* (Ed.: F. Diederich, P. J. Stang, R. R. Tykwinski), Wiley, Weinheim, **2005**, 387–426.

[49] S.-L. Huang, T. S. A. Hor, G.-X. Jin, *Coord. Chem. Rev*. **2017**, *333*, 1–26.

[50] For ethynylplatinum macrocycles, see: Y. Ai, M. Ng, E. Y.-H. Hong, A. K.-W. Chan, Z.-W. Wei, Y. li, V. W.-W. Yam, *Chem. Eur. J.* **2018**, *24*, 11611–11618 and references therein.

[51] P. Siemsen, R. C. Livingston, F. Diederich, *Angew. Chem. Int. Ed*. **2000**, *39*, 2632–2657.

[52] F. Alonso, M. Yus, *ACS Catal*. **2012**, *2*, 1441–1451.

[53] K. S. Sindhu, G. Anilkumar, *RSC Adv.* **2014**, *4*, 27867–27887.

[54] K. S. Sindhu, A. P. Thankachan, P. S. Sajitha, G. Anilkumar, *Org. Biomol. Chem*. **2015**, *13*, 6891–6905.

[55] G. Zhang, H. Yi, G. Zhang, Y. Deng, R. Bai, H. Zhang, J. T. Miller, A. J. Kropf, E. F. Bunel, A. Lei, *J. Am. Chem. Soc*. **2014**, *136*, 924–926.

[56] F. Bohlmann, H. Schönowsky, E. Inhoffen, G. Grau, *Chem. Ber*. **1964**, *97*, 794–800.

[57] L. Fomina, B. Vazquez, E. Tkatchouk, S. Fomine, *Tetrahedron* **2002**, *58*, 6741–6747.

[58] M. H. Vilhelmsen ,J. Jensen, C. G. Tortzen ,M. B. Nielsen, *Eur. J. Org. Chem*. **2013**, 701–711.

[59] X. Qi, R. Bai, L. Zhu, R. Jin, A. Lei, Y. Lan, *J. Org. Chem*. **2016**, *81*, 1654–1660.

[60] C. R. Travis, L. E. Mazur, E. M. Peairs, G. H. Gaunt, D. D. Young, *Org. Biomol. Chem*. **2019**, *17*, 3396–3402.

[61] J. A. Marsden, J. J. Miller, M. M. Haley, *Angew. Chem. Int. Ed*. **2004**, *43*, 1694–1697.

[62] J. A. Marsden, J. J. Miller, L. D. Shirtcliff, M. M. Haley, *J. Am. Chem. Soc*. **2005**, *127*, 2464–2476.

[63] E. L. Spitler, J. M. Monson, M. M. Haley, *J. Org. Chem*. **2008**, *73*, 2211–2223.

[64] P. S. Bols, H. L. Anderson, *Acc. Chem. Res*. **2018**, *51*, 2083–2092.

[65] Y. Tobe, H. Matsumoto, K. Naemura, Y. Achiba, T. Wakabayashi, *Angew. Chem. Int. Ed*. **1996**, *35*, 1799–1802.

[66] Y. Tobe, R. Umeda, N. Iwasa, M. Sonoda, *Chem. Eur. J*. **2003**, *9*, 5549–5559.

[67] T. Yamato, K. Fujita, T. Abe, H. Tsuzuki, *New J. Chem*. **2001**, *25*, 728–736.

[68] Y. Uchikawa, K. Tazoe, S. Tanaka, X. Feng, T. Matsumoto, J. Tanaka, T. Yamato, *Can. J. Chem*. **2012**, *90*, 441–449.

[69] T. Akther, M. M. islam, T. Matsumoto, J. Tanaka, X. Feng, C. Redshaw, T. Yamato, *J. Mol. Struc*. **2016**, *1122*, 247–255.

[70] R. Shukla, D. M. Brody, S. V. Lindeman, R. Rathore, *J. Org. Chem*. **2006**, *71*, 6124–6129.

[71] F. Diederich, L. Gobbi, *Top. Curr. Chem*. **1999**, *201*, 43–79.

[72] Y. Tobe, in *Advances in Strained and Interesting Organic Molecules* (Ed.: B. Halton), JAI Press, Greenwich, **1999**, *7*, 153–184.

[73] P. W. Fowler, N. Mizoguchi, D. E. Bean, R. W. A. Havenith, *Chem. Eur. J*. **2009**, *15*, 6964–6972.

[74] V. Parasuk, J. Almlöf, M. W. Feyereisen, *J. Am. Chem. Soc*. **1991**, *113*, 1049–1050.

[75] D. A. Plattner, K. N. Houk, *J. Am. Chem. Soc*. **1995**, *117*, 4405–4406.

[76] S. Arulmozhiraja, T. Ohno, *J. Chem. Phys*. **2008**, *128*, 114301.

[77] R. O. Jones, *J. Chem. Phys*. **1999**, *110*, 5189–5200.

[78] F. Jensen, H. Koch, *J. Chem. Phys*. **1998**, *108*, 3213–3217.

[79] Y. Rubin, C. B. Knobler, F. Diederich, *J. Am. Chem. Soc*. **1990**, *112*, 1607–1617.

[80] T. Wakabayashi, M. Kohno, Y. Achiba, H. Shiromaru, T. Momose, T. Shida, K. Naemura, Y. Tobe, *J. Chem. Phys*. **1997**, *107*, 4783–4787.

[81] D. R. Kohn, P. Gawal, Y. Xiong, K. E. Christensen, H. L. Anderson, *J. Org. Chem*. **2018**, *83*, 2077–2086.

[82] F. Diederich, Y. Rubin, O. L. Chapman, N. S. Goroff, *Helv. Chim. Acta* **1994**, *77*, 1441–1457.

[83] G. A. Adamson, C. W. Ress, *J. Chem. Soc., Perkin Trans. 1* **1996**, 1535–1543.

[84] M. Kalathingal, C. Owais, D. S. P. Roy, R. S. Swathi, *ACS Omega* **2018**, *3*, 7542–7554.

[85] R. H. Baughman, *Science* **2006**, *312*, 1009–1010.

[86] H. Masai, J. Terao, *Polym. J*. **2017**, *49*, 805–814.

[87] U. H. F. Bunz, *Angew. Chem. Int. Ed*. **1996**, *35*, 969–971.

[88] W.-Y. Wong, P. D. Harvey, *Macromol. Rapid Commun*. **2010**, *31*, 671–713.

[89] Y. Tanaka, Y. Kato, T. Tada, S. Fujii, M. Kiguchi, M. Akita, *J. Am. Chem. Soc*. **2018**, *140*, 10080–10084.

[90] E. Kayahara, V. K. Patel, S. Yamago, *J. Am. Chem. Soc*. **2014**, *136*, 2284–2287.

[91] P. J. Evans, E. R. Darzi, R. Jasti, *Nat. Chem*. **2014**, *6*, 404–408.

[92] M. M. Haley, B. L. Langsdorf, *Chem. Commun*. **1997**, *33*, 1121–1122.

[93] Y. Tobe, R. Furukawa, M. Sonoda, T. Wakabayashi, *Angew. Chem. Int. Ed*. **2001**, *40*, 4072–4074.

[94] R. Umeda, T. Morinaka, M. Sonoda, Y. Tobe, *J. Org. Chem*. **2005**, *70*, 6133–6136.

[95] M. Ohkita, K. Ando, T. Tsuji, *Chem. Commun*. **2001**, *37*, 2570–2571.

[96] M. Srinivasan, S. Sankararaman, H. Hopf, B. Varghese, *Eur. J. Org. Chem*. **2003**, 660–665.

[97] A. Bandyopadhyay, B. Varghese, S. Sasnkararaman, *J. Org. Chem*. **2006**, *71*, 4544–4548.

[98] S. Lee, E. Chénard, D. L. Gray, J. S. Moore, *J. Am. Chem. Soc*. **2016**, *138*, 13814–13817.

[99] X. Zhou, R. R. Thompson, F. R. Fronczek, S. Lee, *Org. Lett*. **2019**, *21*, 4680–4683.

[100] V. K. Patel, E. Kayahara, S. Yamago, *Chem. Eur. J*. **2015**, *21*, 5742–5749.

[101] T. A. Schaub, J. T. Margraf, L. Zakharov, K. Reuter, R. Jasti, *Angew. Chem. Int. Ed*. **2018**, *57*, 16348–16353.

[102] E. R. Darzi, B. M. White, L. K. Loventhal, L. N. Zakharov, R. Jasti, *J. Am. Chem. Soc*. **2017**, *139*, 3106–3114.

[103] Y. García-Rodeja, I. Fernández, *J. Org. Chem*. **2019**, *84*, 4330–4337.

[104] T. Kawase, *Synlett* **2007**, 2609–2626.

[105] J. E. McMurry, *Chem. Rev*. **1989**, *89*, 1513–1524.

[106] H. R. Darabi, T. Kawase, M. Oda, *Tetrahedron Lett*. **1995**, *36*, 9525–9526.

[107] T. Kawase, N. Ueda, K. Tanaka, Y. Seirai, M. Oda, *Tetrahedron Lett*. **2001**, *42*, 5509–5511.

[108] T. Kawase, Y. Nishiyama, T. Nakamura, T. Ebi, K. Matsumoto, H. Kurata, M. Oda, *Angew. Chem. Int. Ed*. **2007**, *46*, 1086–1088.

[109] T. Kawase, K. Tanaka, Y. Seirai, N. Shiono, M. Oda, *Angew. Chem. Int. Ed*. **2003**, *42*, 5597–5600.

[110] T. Kawase, M. Oda, *Pure Appl. Chem*. **2006**, *78*, 831–839.

[111] T. Kawase, Y. Seirai, H. R. Darabi, M. Oda, Y. Sarakai, K. Tashiro, *Angew. Chem. Int. Ed*. **2003**, *42*, 1621–1624.

[112] I. G. Cuesta, T. B. Pedersen, H. Koch, A. S. de Merás, *ChemPhysChem* **2006**, *7*, 2503–2507.

[113] J.-M. Fan, L. Liu, K.-S. Song, Q.-X. Guo, *J. Mol. Struc. Theochem* **2002**, *617*, 209–217.

[114] T. Kawase, N. Fujiwara, M. Tsutumi, M. Oda, Y. Maeda, T. Wakahara, T. Akasaka, *Angew. Chem. Int. Ed*. **2004**, *43*, 5060–5062.

[115] Y. Zhao, D. G. Truhlar, *J. Am. Chem. Soc*. **2007**, *129*, 8440–8442.

[116] K. Yuan, Y.-J. Guo, T. Yang, S.-S. Dang, P. Zhao, Q.-Z. Li, X. Zhao, *J. Phys. Org. Chem*. **2014**, *27*, 772–782.

[117] I. González-Veloso, J. Rodríguez-Otero, E. M. Cabaleiro-Lago, *Phys. Chem. Chem. Phys*. **2016**, *18*, 31670–31679.

[118] T. Kawase, K. Tanaka, N. Shiono, Y. Seirai, M. Oda, *Angew. Chem. Int. Ed*. **2004**, *43*, 1722–1724.

[119] K. Miki, T. Matsushita, Y. Inoue, Y. Senda, T. Kowada, K. Ohe, *Chem. Commun*. **2013**, *49*, 9092–9094.

[120] K. Miki, K. Saeki, T. Umeyama, J. Beak, T. Noda, H. Imahori, Y. Sato, K. Suenaga, K. Ohe, *Small* **2018**, *14*, 1800720.

[121] T. Iwamoto, Y. Watanabe, Y. Sakamoto, T. Suzuki, S. Yamago, *J. Am. Chem. Soc*. **2011**, *133*, 8354–8361.

[122] M. M. Haley, *Synlett* **1998**, 557–565.

[123] M. K. Kiesewetter, R. C. Reiter, C. D. Stevenson, *Org. Lett*. **2005**, *7*, 2623–2626.

[124] H. N. C. Wong, F. Sondheimer, *Angew. Chem. Int. Ed*. **1976**, *15*, 117–118.

[125] H. N. C. Wong, P. J. Garratt, F. Sondheimer, *J. Am. Chem. Soc*. **1974**, *96*, 5604–5605.

[126] R. Destro, T. Pilati, M. Simonetta, *J. Am. Chem. Soc*. **1975**, *97*, 658–659.

[127] F. Xu, L. Peng, K. Shinohara, T. Morita, S. Yoshida, T. Hosoya, A. Orita, J. Otera, *J. Org. Chem*. **2014**, *79*, 11592–11608.

[128] F. Xu, L. Peng, K. Shinohara, T. Nishida, K. Wakamatsu, M. Uejima, T. Sato, K. Tanaka, N. Machida, H. Akashi, A. Orita, J. Otera, *Org. Lett*. **2015**, *17*, 3014–3017.

[129] D. A. Sutton, S.-H. Yu, R. Steet, V. V. Popik, *Chem. Commun*. **2016**, *52*, 553–556.

[130] M. Tera, Z. H. Taji, N. W. Luedtke, *Angew. Chem. Int. Ed*. **2018**, *57*, 15405–15409.

[131] R. A. G. de Graaff, S. Gorter, C. Romers, H. N. C. Wong, F. Sondheimer, *J. Chem. Soc. Perkin Trans II* **1981**, 478.

[132] C.-Y. Leung, T. C. W. Mak, H. N. C. Wong, *J. Chem. Crystal*. **1997**, *26*, 227–230.

[133] H. Oshima, A. Fukazawa, S. Yamaguchi, *Angew. Chem. Int. Ed*. **2017**, *56*, 3270–3274.

[134] J. Anthony, A. M. Boldi, C. Boudon, J.-P. Gisselbrecht, M. Gross, P. Seiler, C. B. Knobler, F. Diederich, *Helv. Chim. Acta* **1995**, *78*, 797–817.

[135] J. Anthony, C. B. Knobler, F. Diederich, *Angew. Chem. Int. Ed*. **1993**, *52*, 406–409.

[136] M. Kivala, F. Mitzel, C. Boudon, J.-P. Gisselbrecht, P. Seiler, M. Gross, F. Diederich, *Chem. Asian J*. **2006**, *1*, 479–489.

[137] O. M. Behr, G. Eglinton, A. R. Galbraith, R. A. Raphael, *J. Chem. Soc*. **1960**, 3614–3625.

[138] O. M. Behr, G. Eglinton, I. A. Lardy, R. A. Raphael, *J. Chem. Soc*. **1964**, 1151–1154.

[139] Q. Zhou, P. J. Carroll, T. M. Swager, *J. Org. Chem.* **1994**, *59*, 1294–1301.

[140] I. Hisaki, H. Shigemitsu, Y. Sakamoto, Y. Hasegawa, Y. Okajima, K. Nakano, N. Tohnai, M. Miyata, *Angew. Chem. Int. Ed*. **2009**, *48*, 5465–5469.

[141] K. Tahara, K. Inukai, N. Hara, C. A. Johnson II, M. M. Haley, Y. Tobe, *Chem. Eur. J*. **2010**, *16*, 8319–8328.

[142] H. Shigemitsu, I. Hisaki, E. Kometani, D. Yasumiya, Y. Sakamoto, K. Osaka, T. S. Thakur, A. Saeki, S. Seki, F. Kimura, T. Kimura, N. Tohnai, M. Miyata, *Chem. Eur. J*. **2013**, *19*, 15366–15377.

[143] H. Shigemitsu, I. Hisaki, H. Senga, D. Yasumiya, T. S. Thakur, A. Saeki, S. Seki, N. Tohnai, M. Miyata, *Chem. Asian J*. **2013**, *8*, 1372–1376.

[144] Z. Guo, K. Tahara, K. Inukai, H. Takeda, M. Kouno, K. Iritani, Y. Tobe, *J. Phys. Chem. C* **2015**, *119*, 15977–15981.

[145] I. Hisaki, K. Osaka, N. Ikenaka, A. Saeki, N. Tohnai, S. Seki, M. Miyata, *Cryst. Growth Des*. **2016**, *16*, 714–721.

[146] S. Fukushima, M. Ashizawa, S. Kawwauchi, T. Michinobu, *Helv. Chim. Acta* **2019**, *102*, e1900016.

[147] T. Takeda, K. Inukai, K. Tahara, Y. Tobe, *J. Org. Chem*. **2011**, *76*, 9116–9121.

[148] S. Nobusue, A. Yoshizak, M. Miki, H. Miyoshi, A. Shimizu, Y. Tobe, *Tetrahedron* **2014**, *70*, 8474–8479.

[149] M. Morimoto, S. Akiyama, S. Misumi, M. Nakagawa, *Bull. Chem. Soc. Jpn*. **1962**, *35*, 857–859.

[150] S.-i. Kato, N. Takahashi, Y. Nakamura, *J. Org. Chem*. **2013**, *78*, 7658–7663.

[151] N. Takahashi, S.-i. Kato, M. Yamaji, M. Ueno, R. Iwabuchi, Y. Shimizu, M. Nitani, Y. Ie, Y. Aso, T. Yamanobe, H. Uehara, Y. Nakamura, *J. Org. Chem*. **2017**, *82*, 8882–8896.

[152] H. N. C. Wong, F. Sondheimer, *J. Org. Chem.* **1980**, *45*, 2438–2440.
[153] X.-P. Yang, D.-M. Du, Q. Li, T. C. W. Mak, H. N. C. Wong, *Chem. Commun*. **1999**, *35*, 1607–1608.
[154] I. Hisaki, T. Eda, M. Sonoda, H. Niino, T. Sato, T. Wakabayashi, Y. Tobe, *J. Org. Chem.* **2005**, *70*, 1853–1864.
[155] S. K. Collins, G. P. A. Yap, A. G. Fallis, *Angew. Chem. Int. Ed*. **2000**, *39*, 385–388
[156] Y. Tobe, I. Ohki, M. Sonoda, H. Niino, T. Sato, T. Wakabayashi, *J. Am. Chem. Soc*. **2003**, *125*, 5614–5615.
[157] I. Hisaki, T. Eda, M. Sonoda, Y. Tobe, *Chem. Lett.* **2004**, *33*, 620–621.
[158] K. P. Baldwin, A. J. Matzger, D. A. Scheiman, C. A. Tessier, K. P. C. Vollhardt, W. J. Youngs, *Synlett* **1995**, 1215–1218.
[159] A. J. Matzger, K. P. C. Vollhardt, *Tetrahedron Lett*. **1998**, *39*, 6791–6794.
[160] H. S. Blanchette, S. C. Brand, H. Naruse, T. J. R. Weakley, M. M. Haley, *Tetrahedron* **2000**, *56*, 9581–9588.
[161] A. J. Boydston, M. M. Haley, *Org. Lett*. **2001**, *3*, 3599–3601.
[162] A. J. Boydston, M. M. Haley, R. V. Williams, J. R. Armantrout, *J. Org. Chem*. **2002**, *67*, 8812–8819.
[163] J. A. Marsden ,M. J. O'Connor, M. M. Haley, *Org. Lett*. **2004**, *6*, 2385–2388.
[164] H. Hinrichs, A. K. Fischer, P. G. Jones, H. Hopf, M. M. Haley, *Org. Lett.* **2005**, *7*, 3793–3795.
[165] H. Hinrichs, A. J. Boydston, P. G. Jones, K. Hess, R. Herges, M. M. Haley, H. Hopf, *Chem. Eur. J*. **2006**, *12*, 7103–7115.
[166] T. Takeda, A. G. Fix, M. M. Haley, *Org. Lett*. **2010**, *12*, 3824–3827.
[167] T. Takeda, M. M. Haley, *Can. J. Chem.* **2017**, *95*, 298–302.
[168] S. Nobusue, Y. Mukai, Y. Fukumoto, R. Umeda, K. Tahara, M. Sonoda, Y. Tobe, *Chem. Eur. J*. **2012**, *18*, 12814–12824.
[169] S. Nobusue, A. Shimizu, K. Hori, I. Hisaki, M. Miyata, Y. Tobe, *Angew. Chem. Int. Ed*. **2013**, *52*, 4184–4188.
[170] S. Nobusue, Y. Tobe, *Chem. Lett*. **2014**, *43*, 1210–1212.
[171] I. Hisaki, E. Kometani, H. Shigemitsu, A. Saeki, S. Seki, N. Tohnai, M. Miyata, *Cryst. Growth Des.* **2011**, *11*, 5488–5497.
[172] H. Shigemitsu, I. Hisaki, E. Kometani, N. Tohnai, M. Miyata, *Chem. Lett*. **2012**, *41*, 1535–1537.
[173] H. Shigemitsu, I. Hisaki, E. Kometani, D. Yasumiya, Y. Sakamoto, K. Osaka, T. S. Thakur, A. Saeki, S. Seki, F. Kimura, T. Kimura, N. Tohnai, M. Miyata, *Chem. Eur. J.* **2013**, *19*, 15366–15377.
[174] I. Hisaki, E. Kometani, N. Tohnai, M. Miyata, *CrystEngComm*. **2015**, *17*, 8079–8084.
[175] M. M. Haley, M. L. Bell, J. J. English, C. A. Johnson, T. J. R. Weakley, *J. Am. Chem. Soc*. **1997**, *119*, 2956–2957.
[176] A. J. Matzger, K. P. C. Vollhardt, *Tetrahedron Lett*. **1998**, *39*, 6791–6794.
[177] M. L. Bell, R. C. Chiechi, C. A. Johnson, D. B. Kimball, A. J. Matzger, W. B. Wan, T. J. R. Weakley, M. M. Haley, Tetrahedron 2001, 57, 3507–3520.
[178] L. Peng, F. Xu, Y. Suzuma, A. Orita, J. Otera, *J. Org. Chem*. **2013**, *78*, 12802–12808.
[179] K. P. Baldwin, R. S. Simons, D. A. Scheiman, R. Lattimer, C. A. Tessier, W. J. Youngs, *J. Chem. Crystallogr.* **1998**, *28*, 353–360.
[180] M. Ohkita, K. Ando, T. Suzuki, T. Tsuji, *J. Org. Chem*. **2000**, *65*, 4385–4390.
[181] C. W. Chan, H. N. C. Wong, *J. Am. Chem. Soc*. **1988**, *110*, 462–469.
[182] K. Y. Cheung, C. K. Chan, Z. Liu, Q. Miao, *Angew. Chem. Int. Ed*. **2017**, *56*, 9003–9007.
[183] M. Ohkita, K. Ando, K.-i. Yamamoto, T. Suzuki, T. Tsuji, *Chem. Commun*. **2000**, *36*, 83–84.
[184] T. Kawase, N. Ueda, M. Oda, *Tetrahedron Lett.* **1997**, *38*, 6681–6684.
[185] T. Kawase, N. Ueda, H. R. Darabi, M. Oda, *Angew. Chem. Int. Ed*. **1996**, *35*, 1556–1558.
[186] Y. Tobe, N. Utsumi, K. Kawabata, K. Naemura, *Tetrahedron Lett*. **1996**, *37*, 9325–9328.
[187] K. Tahara, J. Gotoda, C. N. Carroll, K. Hirose, S. De Feyter, Y. Tobe, *Chem. Eur. J.* **2015**, *21*, 6806–6816.
[188] K. Tahara, S. Lei, W. Mamdouh, Y. Yamaguchi, T. Ichikawa, H. Uji-i, M. Sonoda, K. Hirose, F. C. De Schryver, S. De Feyter, Y. Tobe, *J. Am. Chem. Soc*. **2008**, *130*, 6666–6667.
[189] Y. Tobe, J.-y. Kishi, I. Ohki, M. Sonoda, *J. Org. Chem*. **2003**, *68*, 3330–3332.
[190] S. K. Collins, G. P. A. Yap, A. G. Fallis, *Org. Lett*. **2002**, *4*, 11–14.
[191] L. M. Bannwart, L. Jundt, T. Müntener, M. Neuburger, D. Häussinger, M. Mayor, *Eur. J. Org. Chem*. **2018**, 3391–3402.
[192] M. Desroches, J.-F. Morin, *RSC Adv*. **2017**, *7*, 17117–17121.
[193] Y. Tobe, N. Nakagawa, K. Naemura, T. Wakabayashi, T. Shida, Y. Achiba, *J. Am. Chem. Soc.* **1998**, *120*, 4544–4545.
[194] Y. Tobe, N. Nakagawa, J.-y. Kishi, M. Sonoda, K. Naemura, T. Wakabayashi, T. Shida, Y. Achiba, *Tetrahedron* **2001**, *57*, 3629–3636.
[195] R. Umeda, M. Sonoda, T. Wakabayashi, Y. Tobe, *Chem. Lett*. **2005**, *34*, 1574–1579.
[196] Y. Tobe, R. Umeda, M. Sonoda, T. Wakabayashi, *Chem. Eur. J.* **2005**, *11*, 1603–1609.
[197] Y. Rubin, T. C. Parker, S. J. Pastor, S. Jalisatgi, C. Boulle, C. L. Wilkins, *Angew. Chem. Int. Ed*. **1998**, *37*, 1226–1229.
[198] Y. Rubin, T. C. Parker, S. I. Khan, C. L. Holliman, S. W. McElvany, *J. Am. Chem. Soc*. **1996**, *118*, 5308–5309.
[199] Y. Yamaguchi, S. Kobayashi, S. Miyamura, Y. Okamoto, T. Wakamiya, Y. Matsubara, Z.-i. Yoshida, *Angew. Chem. Int. Ed*. **2004**, *43*, 366–369.
[200] K. Miki, M. Fujita, Y. Inoue, Y. Senda, T. Kowada, K. Ohe, *J. Org. Chem*. **2010**, *75*, 3537–3540.
[201] S. Kobayashi, Y. Yamaguchi, T. Wakamiya, Y. Matsubara, K. Sugimoto, Z.-i. Yoshida, *Tetrahedron Lett.* **2003**, *44*, 1469–1472.
[202] Y. Tobe, A. Nagano, K. Kawabata, M. Sonoda, K. Naemura, *Org. Lett*. **2000**, *2*, 3265–3268.
[203] M. Sonoda, Y. Yamaguchi, K. Tahara, K. Hirose, Y. Tobe, *Tetrahedron* **2008**, *64*, 11490–11494.
[204] Y. Tobe, H. Nakanishi, M. Sonoda, T. Wakabayashi, Y. Achiba, *Chem. Commun*. **1999**, *35*, 1625–1626.
[205] C. A. Johnson II, B. A. Baker, O. B. Berryman, L. N. Zakharov, M. J. O'Connor, M. M. Haley, *J. Organomet. Chem*. **2006**, *691*, 413.
[206] E. L. Spitler, S. P. McClintock, M. M. Haley, *J. Org. Chem*. **2007**, *72*, 6692–6699.
[207] P. N. W. Baxter, J.-P. Gisselbrecht, L. Karmazin-Brelot, A. Varnek, L. Alloche, *Chem. Eur. J.* **2013**, *19*, 12336–12349.
[208] M. A. Heuft, A. G. Fallis, *Angew. Chem. Int. Ed.* **2002**, *41*, 4520–4523.
[209] P. N. W. Baxter, *J. Org. Chem.* **2001**, *66*, 4170–4179.
[210] P. N. W. Baxter, *Chem. Eur. J.* **2002**, *8*, 5250–5264.
[211] O. Henze, D. Lents, A. D. Schlüter, *Chem. Eur. J*. **2000**, *6*, 2362–2367.
[212] O. Henze, D. Lents, A. Schäfer, P. Franke, A. D. Schlüter, *Chem. Eur. J*. **2002**, *8*, 357–365.
[213] C. Grave, D. Lents, A. Schäfer, P. Samori, J. P. Rabe, P. Franke, A. D. Schlüter, *J. Am. Chem. Soc.* **2003**, *125*, 6907–6918.
[214] D. M. Opris, P. Franke, A. D. Schlüter, *Eur. J. Org. Chem.* **2005**, 822–837.
[215] J. L. Alonso-Gómez, A. Navarro-Vázquez, M. M. Cid, *Chem. Eur. J*. **2009**, *15*, 6495–6503.
[216] H. Abe, Y. Chida, H. Kurokawa, M. Inouye, *J. Org. Chem*. **2011**, *76*, 3366−3371.
[217] H. Abe, H. Kurokawa, Y. Chida, M. Inouye, *J. Org. Chem*. **2011**, *76*, 309−311.
[218] H. Abe, K. Ohtani, D. Suzuki, Y. Chida, Y. Shimada, S. Matsumoto, M. Inouye, *Org. Lett.* **2014**, *16*, 828−831.
[219] H. Abe, T. Yoneda, Y. Ohishi, M. Inouye, *Chem. Eur. J.* **2016**, *22*, 18944–18952.
[220] D. Suzuki, H. Abe, M. Inouye, *Org. Lett*. **2016**, *18*, 320−323.
[221] Y. Ohishi, N. Yamamoto, H. Abe, M. Inouye, *J. Org. Chem*. **2018**, *83*, 5766–5770.
[222] C. Werner, H. Hopf, I. Dix, P. Bubenitschek, P. G. Jones, *Chem. Eur. J.* **2007**, *13*, 9462–9477.
[223] A. G. Myers, P. S. Dragovich, *J. Am. Chem. Soc*. **1992**, *114*, 5859–5860.
[224] C. J. Kuehl, S. D. Huang, P. J. Stang, *J. Am. Chem. Soc*. **2001**, *123*, 9634–9641.
[225] A. Dubey, Y. J. Jeong, J. H. Jo, S. Woo, D. H. Kim, H. Kim, S. C. Kang, P. J. Stang, K.-W. Chi, *Organometallics* **2015**, *34*, 4507–4514.

[226] S. Maruyama, H. Hokari, T. Wada, H. Sasabe, *Synthesis* **2001**, 1794–1799.

[227] W. Zhang, J. S. Moore, *J .Am. Chem. Soc.* **2004**, *126*, 12796.

[228] W. Zhang, M. Hyeon, J. S. Moore, *Org. Synth*. **2007**, *84*, 177–191.

[229] A. D. Finke, D. E. Gross, A. Han, J. S. Moore, *J .Am. Chem. Soc.* **2011**, *133*, 14063–14070.

[230] Y. Che, D. E. Gross, H. Huang, D. Yang, X. Yang, E. Discekici, Z. Xue, H. Zhao, J. S. Moore, L. Zang, *J .Am. Chem. Soc.* **2012**, *134*, 4078–4082.

[231] T. Zhao, Z. Liu, Y. Song, W. Xu, D. Zhang, D. Zhu, *J. Org. Chem*. **2006**, *71*, 7422–7432.

[232] W. Huang, T.-Y. Zhao, M.-W. Wen, Z.-Y. Yang, E. Xu, Y.-P. Yi, L.-P. Xu, Z.-X. Wang, Z.-J. Gu, *J. Phys. Chem. C* **2014**, *118*, 6767–6772.

[233] C. Maeda, T. Yoneda, N. Aratani, M.-C. Yoon, J. M. Lim, D. Kim, N. Yoshioka, A. Osuka, *Angew. Chem. Int. Ed.* **2011**, *50*, 5691–5694.

[234] C. Maeda, N. Yoshioka, *Org. Biomol. Chem*. **2012**, *10*, 5182–5185.

[235] M. Masuda, C. Maeda, N. Yoshioka, *Org. Lett.* **2013**, *15*, 578–581.

[236] A. V. Aggarwal, A. Thiessen, A. Idelson, D. Kalle, D. Würsch, T. Stangl, F. Steiner, S.-S. Jester, J. Vogelsang, S. Höger, J. M. Lupton, *Nat. Chem*. **2013**, *5*, 964–970.

[237] A. Thiessen, D. Würsch, S.-S. Jester, A. V. Aggarwal, A. Idelson, S. Bange, J. Vogelsang, S. Höger, J. M. Lupton, *J. Phys. Chem. B* **2015**, *119*, 9949–9958.

[238] B. Schmaltz, A. Rouhanipour, H. J. Räder, W. Pisula, K. Müllen, *Angew. Chem. Int. Ed.* **2009**, *48*, 720–724.

[239] M. Iyoda, H. Shimizu, *Chem. Soc. Rev*. **2015**, *44*, 6411–6424.

[240] T. Kawase, H. R. Darabi, R. Uchimiya, M. Oda, *Chem. Lett.* **1995**, *24*, 499–500.

[241] K. Nakao, M. Nishimura, T. Tamachi, Y. Kuwatani, H. Miyasaka, T. Nishinaga, M. Iyoda, *J. Am. Chem. Soc*. **2006**, *128*, 16740–16747.

[242] M. Williams-Harry, A. Bhaskar, G. Ramakrishna, T. Goodson III, M. Imamura, A. Mawatari, K. Nakao, H. Enozawa, T. Nishinaga, M. Iyoda, *J. Am. Chem. Soc*. **2008**, *130*, 3252–3253.

[243] M. Iyoda, P. Huang, T. Nishiuchi, M. Takase, T. Nishinaga, *Heterocycles* **2010**, *82*, 1143–1149.

[244] M. Iyoda, *Pure Appl. Chem*. **2010**, *82*, 831–841.

[245] M. Iyoda, K. Tanaka, H. Shimizu, M. Hasegawa, T. Nishinaga, T. Nishiuchi, Y. Kunugi, T. Ishida, H. Otani, H. Sato, K. Inukai, K. Tahara, Y. Tobe, *J. Am. Chem. Soc*. **2014**, *136*, 2389–2396.

[246] H. Shimizu, J. D. Cojal González, M. Hasegawa, T. Nishinaga, T. Haque, M. Takase, H. Otani, J. P. Rabe, M. Iyoda, *J. Am. Chem. Soc*. **2015**, *137*, 3877–3885.

[247] M. Iyoda, H. Shimizu, S. Aoyagi, H. Okada, B. Zhou, Y. Matsuo, *Can. J. Chem*. **2017**, *95*, 315–319.

[248] J. D. Cojal González, M. Iyoda, J. P. Rabe, *Angew. Chem. Int. Ed*. **2018**, *57*, 17038–17042.

[249] J. E. Donehue, O. P. Varnavski, R. Cemborski, M. Iyoda, T. Goodson III, *J. Am. Chem. Soc*. **2011**, *133*, 4819–4828.

[250] A. Orita, J. Otera, *Chem. Rev*. **2006**, *106*, 5387–5412.

[251] S.-Q. Zhang, Z.-Y. Liu, W.-F. Fu, F. Liu, C.-M. Wang, C.-Q. Sheng, Y.-F. Wang, K. Deng, Q.-D. Zeng, L.-J. Shu, J.-H. Wan, H.-Z. Chen, T. P. Russel, *ACS Nano*, **2017**, *11*, 11701–11713.

[252] M. Mayor, C. Didschies, *Angew. Chem. Int. Ed*. **2003**, *42*, 3176–3179.

[253] G. Fuhrmann, T. Debaerdemaeker, P. Bäuerle, *Chem. Commun*. **2003**, *39*, 948–949.

[254] D. Solooki, V. O. Kennedy, C. A. Tessier, W. J. Youngs, *Synlett* **1990**, 427–428

[255] D. Solooki, J. D. Bradshaw, C. A. Tessier, W. J. Youngs, *Organometallics* **1994**, *13*, 451–455.

[256] M. Iyoda, A. Vorasingha, Y. Kuwatani, M. Yoshida, *Tetrahedron Lett.* **1998**, *39*, 4701–4704.

[257] D. Zhang, C. A. Tessier, W. J. Youngs, *Chem. Meter.* **1999**, *11*, 3050–3057.

[258] A. Sarkar, M. M. Haley, *Chem. Commun*. **2000**, *36*, 1733–1734.

[259] M. J. O'Connor, R. B. Yelle, L. N. Zakharov, M. M. Haley, *J. Org. Chem*. **2008**, *73*, 4424–4432.

[260] M. J. O'Connor, M. M. Haley, *Org. Lett*. **2008**, *10*, 3973–3976.

[261] M. J. O'Connor, R. B. Yelle, T. M. Linz, M. M. Haley, *C. R. Chimie* **2009**, *12*, 385–394.

[262] M. J. Marsella, I. T. Kim, F. Tham, *J. Am. Chem. Soc*. **2000**, *122*, 974–975.

[263] M. J. Marsella, G. Piao, F. S. Tham, *Synthesis* **2002**, 1113–1135.

[264] A. Fukazawa, H. Oshima, Y. Shiota, S. Takahashi, K. Yoshizawa, S. Yamaguchi, *J. Am. Chem. Soc*. **2013**, *135*, 1731–1734.

[265] A. Fukazawa, H. Oshima,S. Shimizu, N. Kobayashi, S. Yamaguchi, *J. Am. Chem. Soc*. **2014**, *136*, 8738–8745.

[266] H. Oshima, A. Fukazawa, T. Sasamori, S. Yamaguchi, *Angew. Chem. Int. Ed*. **2015**, *54*, 7636–7639.

[267] T. Nishinaga, S. Shiroma, M. Hasegawa, *Org. Lett.* **2018**, *20*, 3476–3429.

[268] T. Nishinaga, H. Hamaoka, *Chem. Commun*. **2019**, *55*, 1514–1517.

[269] H. A. Staab, E. Wehinger, W. Thorwart, *Chem. Ber*. **1972**, *105*, 2290–2309.

[270] H. Irngartinger, *Chem. Ber.* **1973**, *106*, 761–772.

[271] K. Utsumi, T. Kawase, M. Oda, *Chem. Lett*. **2003**, *32*, 412–413.

[272] R. Boese, A. J. Matzger, K. P. C. Vollhardt, *J. Am. Chem. Soc.* **1997**, *119*, 2052–2053.

[273] K. P. Baldwin, R. S. Simons, J. Rose, P. Zimmermanm, D. M. Hercules, C. A. Tessier, W. J. Youngs, *J. Chem. Soc., Chem. Commun*. **1994**, *30*, 1257–1258.

[274] D. Solooki, J. D. Bradshaw, C. A. Tessier, W. J. Youngs, *J. Organomet. Chem*. **1994**, *470*, 231–236.

[275] S. K. Collins, G. C. A. Yap, A. G. Fallis, *Org. Lett*. **2000**, *2*, 3189–3192.

[276] M. A. Heuft, S. K. Collins, A. G. Fallis, *Org. Lett.* **2003**, *5*, 1911–1914.

[277] S. Nobusue, H. Yamane, H. Miyoshi, Y. Tobe, *Org. Lett*. **2014**, *16*, 1940–1943.

[278] Y. Kim, S. Shin, T. Kim, D. Lee, C. Seok, M. Lee, *Angew. Chem. Int. Ed*. **2013**, *52*, 6426–6429.

[279] Y. Kim, M. Lee, *Chem. Eur. J*. **2015**, *21*, 5736–5740.

[280] T. Hayama, Y.-T. Wu, A. Linden, K. K. Baldridge, J. S. Siegel, *J. Am. Chem. Soc*. **2007**, *129*, 12612–12613.

[281] A. Bähr, A. S. Droz, M. Püntener, U. Neidlein, S. Anderson, P. Seiler, F. Diederich, *Helv. Chim. Acta* **1998**, *81*, 1931–1963.

[282] A. S. Droz, U. Neidlein, S. Anderson, P. Seiler, F. Diederich, *Helv. Chim. Acta* **2001**, *84*, 2243–2289.

[283] A. S. Droz, F. Diederich, *J. Chem. Soc., Perkin 1* **2000**, 4224–4226.

[284] T. Harada, S.-i. Matsui, T. M. T. Tuyet, M. Hatsuda, S. Ueda, A. Oku, M. Shiro, *Tetrahedron: Asymmetry* **2003**, *14*, 3879–3884.

[285] D. L. An, Q. Chen, J. Fang, H. Yan, A. Orita, N. Miura, A. Nakahashi, K. Monde, J. Otera, *Tetrahedron Lett*. **2009**, *50*, 1689–1692.

[286] D. L. An, T. Nakano, A. Orita, J. Otera, *Angew. Chem. Int. Ed*. **2002**, *41*, 171–173.

[287] A. Orita, D. L. An, T. Nakano, J. Yaruva, N. Ma, J. Otera, *Chem. Eur. J.* **2002**, *8*, 2005–2010.

[288] D.-L. An, Y.-J. Zhang, Q. Chen, W.-Y. Zhao, H. Yan, A. Orita, J. Otera, *Chem. Asian J*. **2007**, *2*, 1299–1304.

[289] C. Mang, C. Liu, K. Wu, *Mol. Phys.* **2012**, *110*, 1453–1460.

[290] G. R. Schaller, F. Topić, K. Rissanen, Y. Okamoto, J. Shen, R. Herges, *Nat. Chem*. **2014**, *6*, 608–613.

[291] L. P. Olson, *J. Mol. Struc. Theochem* **2004**, *680*, 65–71.

[292] C. Mang, C. Liu, K. Wu, *Spectrochim. Acta A Mol. Biomol. Spectrosc*. **2012**, *98*, 444–452.

[293] V. Kundl, M. M. Alam, P. P. Thankachan, *Phys. Chem. Chem. Phys*. **2015**, *17*, 6827–6833.

[294] M. M. Alam, V. Kundl, P. P. Thankachan, *Phys. Chem. Chem. Phys*. **2016**, *18*, 21833–21842.

[295] K. Miki, T. Noda, M. Gon, K. Tanaka, Y. Chujo, Y. Mizuhata, N. Tokitoh, K. Ohe, *Chem. Eur. J.* **2019**, 21, 9211–9216.

[296] X. Lu, S. Lee, Y. hong, H. Phan, T. Y. Gopalakrishna, T. S. Herng, T. Tanaka, M. E. Sandoval-Salinas, W. Zeng, J. Ding, D. Casanova, A. Osuka, D. Kim, J. Wu, *J. Am. Chem. Soc.* **2017**, *139*, 13173–13183.

[297] L. Zhang, H. Gopee, D. L. Hughes, A. N. Cammidge, *Chem. Commun*. **2010**, *46*, 4255–4257.

[298] L. Zhang, D. L. Hughes, A. N. Cammidge, *J. Org. Chem*. **2012**, *77*, 4288–4297.

[299] H. Wettach, S. Höger, D. Chaudhuri, J. M. Lupton, F. Liu, E. M. Lupton, S. Tretiak, G. Wang, M. Li, S. De Feyter, S. Fischer, S. Förster, *J. Mater. Chem*. **2011**, *21*, 1404–1415.

[300] K. Miyamoto, T. Iwanaga, S. Toyota, *Chem. Lett*. **2010**, *39*, 288–290

[301] S. Toyota, H. Miyahara, M. Goichi, S. Yamasaki, T. Iwanaga, *Bull. Chem. Soc. Jpn*. **2009**, *82*, 931–945.

[302] T. Ishikawa, T. Shimasaki, H. Akashi, S. Toyota, *Org. Lett*. **2008**, *10*, 417–420.

[303] T. Ishikawa, T. Shimasaki, H. Akashi, T. Iwanaga, S. Toyota, M. Yamasaki, *Bull. Chem. Soc. Jpn*. **2010**, *83*, 220–232.

[304] S. Toyota, H. Harada, H. Miyahara, T. Kawakami, K. Wakamatsu, T. Iwanaga, *Bull. Chem. Soc. Jpn*. **2011**, *84*, 829–838.

[305] S. Toyota, *Pure Appl. Chem*. **2012**, *84*, 917–929.

[306] S. Toyota, M. Yoshikawa, T. Saibara, Y. Yokoyama, T. Komori, T. Iwanaga, *ChemPlusChem* **2019**, *84*, 643–654.

[307] S. Toyota, M. Goichi, M. Kotani, *Angew. Chem. Int. Ed*. **2004**, *43*, 2248–2251.

[308] S. Toyota, M. Goichi, M. Kotani, M. Takezaki, *Bull. Chem. Soc. Jpn*. **2005**, *78*, 2214–2227.

[309] S. Toyota, H. Ikeda, T. Iwanaga, *ChemPlusChem* **2017**, *82*, 957–966.

[310] S. Toyota, H. Onishi, K. Wakamatsu, T. Iwanaga, *Chem. Lett.* **2009**, *38*, 350–351.

[311] T. Tsuya, T. Iwanaga, S. Toyota, *Bull. Chem. Soc. Jpn*. **2013**, *86*, 138–145.

[312] T. Tsuya, K. Iritani, K. Tahara, Y. Tobe, T. Iwanaga, S. Toyota, *Chem. Eur. J.* **2015**, *21*, 5520–5527.

[313] S. Toyota, H. Miyahara, M. Goichi, K. Wakamatsu, T. Iwanaga, *Bull. Chem. Soc. Jpn.* **2008**, *81*, 1147–1157.

[314] S. Toyota, T. Kawakami, R. Shinnishi, R. Sugiki, S. Suzuki, T. Iwanaga, *Org. Biomol. Chem*. **2010**, *8*, 4997–5006.

[315] M. Yoshikawa, S. Imigi, K. Wakamatsu, T. Iwanaga, S. Toyota, *Chem. Lett.* **2013**, *42*, 559–561

[316] M. Hoddmann, C. J. Wilson, B. Odell, H. L. Anderson, *Angew. Chem. Int. Ed*. **2007**, *46*, 3122–3125.

[317] P. Liu, Y. Hisamune, M. D. Peeks, B. Odell, J. Q. Gong, L. M. Herz, H. L. Anderson, *Angew. Chem. Int. Ed*. **2016**, *55*, 8358–8362.

[318] M. Hoffmann, J. KĜrnbratt, M.-H. Chang, L. M. Herz, B. Albinsson, H. L. Anderson, *Angew. Chem. Int. Ed*. **2008**, *47*, 4993–4996.

[319] P. Liu, P. Neuhaus, D. V. Kondratuk, T. S. Balaban, H. L. Anderson, *Angew. Chem. Int. Ed*. **2014**, *53*, 7770–7773.

[320] M. C. O'Sullivan, J. K. Sprafke, D. V. Kondratuk, C. Rinfray, T. D. W. Claridge, A. Saywell, M. O. Blunt, J. N. O'Shea, P. H. Beton, M. Malfois, H. L. Anderson, *Nature* **2011**, *469*, 72–75.

[321] J. K. Sprafke, D. V. Kondratuk, M. Wykes, A. L. Thompson, M. Hoffmann, R. Drevinskas, W.-H. Chen, C. K. Yong, J. Kärnbratt, J. E. Bullock, M. Maldois, M. R. Wasielewski, B. Albinsson, L. M. Herz, D. Zigmantas, D. Beljonne, H. L. Anderson, *J. Am. Chem. Soc.* **2011**, *133*, 17262–17273

[322] R. Haver, L. Tejerina, H.-W. Jiang, M. Rickjaus, M. Jirasek, I. Grübner, H. J. Eggimann, L. M. Herz, H. L. Anderson, *J. Am. Chem. Soc*. **2019**, *141*, 7965–7971.

[323] D. V. Kondratuk, J. K. Sprafke, M. C. O'Sullivan, L. M. A. Perdigao, A. Saywell, M. Malfois, J. N. O'Shea, P. H. Beton, A. L. Thompson, H. L. Anderson, *Chem. Eur. J.* **2014**, *20*, 12826–12834.

[324] D. V. Kondratuk, L. M. A. Perdigao, M. C. O'Sullivan, S. Svatek, G. Smith, J. N. O'Shea, P. H. Beton, H. L. Anderson, *Angew. Chem. Int. Ed*. **2012**, *51*, 6696–6699.

[325] D. V. Kondratuk, L. M. A. Perdigão, A. M. S. Esmail, J. N. O'Shea, P. H. Beton, H. L. Anderson, *Nat. Chem*. **2015**, *7*, 317–322.

[326] M. Rickhaus, A. Vargas Jentzsch, L. Tejerina, I. Grübner, M. Jirasek, T. D. W. Claridge, H. L. Anderson, *J. Am. Chem. Soc*. **2017**, *139*, 16502–16505.

[327] P. Neuhaus, A. Cnossen, J. Q. Gong, L. M. Herz, H. L. Anderson, *Angew. Chem. Int. Ed*. **2015**, *54*, 7344–7348.

[328] V. Posligua, A. Aziz, R. Haver, M. D. Peeks, H. L. Anderson, R. Grau-Crespo, *J. Phys. Chem. C* **2018**, *122*, 23790–23798.

[329] J. Cremers, R. Haver, M. Rickhaus, J. Q. Gong, L. Favereau, M. D. Peeks, T. D. W. Claridge, L. M. Herz, H. L. Anderson, *J. Am. Chem. Soc*. **2018**, *140*, 5352–5355.

[330] S. Liu, D. V. Kondratuk, S. A. L. Rousseaux, G. Gil-Ramírez, M. C. O'Sullivan, J. Cremers, T. D. W. Claridge, H. L. Anderson, *Angew. Chem. Int. Ed*. **2015**, *54*, 5355–5359.

[331] S. A. L. Rousseaux, J. Q. Gong, R. Haver, B. Odell, T. D. W. Claridge, L. M. Herz, H. L. Anderson, *J. Am. Chem. Soc*. **2015**, *137*, 12713–12718.

[332] M. D. Peeks, J. Q. Gong, K. McLoughlin, T. Kobatake, R. Haver, L. M. Herz, H. L. Anderson, *J. Phys. Chem. Lett*. **2019**, *10*, 2017–2022.

[333] M. D. Peeks, T. D. W. Claridge, H. L. Anderson, *Nature* **2017**, *541*, 200–203.

[334] P. S. Bols, H. L. Anderson, *Angew. Chem. Int. Ed*. **2018**, *57*, 7874–7877.

[335] A. J. Boydston, L. Bondarenko, I. Dix, T. J. R. Weakley, H. Hopf, M. M. Haley, *Angew. Chem. Int. Ed*. **2001**, *40*, 2986–2989.

[336] H. Hinrichs, A. K. Fischer, P. G. Jones, H. Hopf, M. M. Haley, *Org. Lett*. **2005**, *7*, 3793–3795.

[337] H. Hinrichs, A. J. Boydston, P. G. Jones, K. Hess, R. Herges, M. M. Haley, H. Hopf, *Chem. Eur. J.* **2006**, *12*, 7103–7115.

[338] I. Dix, L. Bondarenko, P. G. Jones, T. Oeser, H. Hopf, *Beilstein J. Org. Chem*. **2014**, *10*, 2013–2020.

[339] U. H. F. Bunz, *J. Organomet. Chem*. **2003**, *683*, 269–287.

[340] M. Altmann, J. Friedrich, F. Beer, R. Reuter, V. Enkelmann, U. H. F. Bunz, *J. Am. Chem. Soc*. **1997**, *119*, 1472–1473.

[341] U. H. F. Bunz, G. Roidl, M. Altmann, V. Enkelmann, K. D. Shimizu, *J. Am. Chem. Soc.* **1999**, *121*, 10719–10726.

[342] M. Laskoski, W. Steffen, M. D. Smith, U. H. F. Bunz, *Chem. Commun.* **2001**, *37*, 691–692.

[343] M. Laskoski, M. D. Smith, J. G. M. Morton, U. H. F. Bunz, *J. Org. Chem.* **2001**, *66*, 5174–5181.

[344] M. Laskoski, G. Roidl, M. D. Smith, U. H. F. Bunz, *Angew. Chem. Int. Ed.* **2001**, *40*, 1460–1463.

[345] M. Laskoski, G. Roidl, H. L. Ricks, J. G. M. Morton, M. D. Smith, U. H. F. Bunz, *J. Organomet. Chem.* **2002**, *673*, 13–24.

[346] M. Laskoski, W. Steffen, J. G. M. Morton, M. D. Smith, U. H. F. Bunz, *J. Organomet. Chem.* **2002**, *673*, 25–39.

[347] M. Laskoski, G. Roidl, M. D. Smith, U. H. F. Bunz, *Angew. Chem. Int. Ed.* **2002**, *41*, 2378–2382.

[348] H. Hopf, G. Maas, *Angew. Chem. Int. Ed*. **1992**, *31*, 931–954.

[349] F. Diederich, M. Kivala, *Adv. Mater*. **2010**, *22*, 803–812.

[350] R. R. Tykwinski, M. Gholami, S. Eisler, Y. Zhao, F. Melin, L. Echegoyen, *Pure Appl. Chem*. **2008**, *80*, 621–637.

[351] M. B. Nielsen, F. Diederich, *Chem. Rec.* **2002**, *2*, 189–198.

[352] F. Diederich, *Chem. Commun*. **2001**, *37*, 219–227.

[353] M. Schreiber, R. R. Tykwinski, F. Diederich, R. Spreiter, U. Gubler, C. Bosshard, I. Poberaj, P. Günter, C. Boudon, J.-P. Gisselbrecht, M. Gross, U. Jonas, H. Ringsdorf, *Adv. Mater*. **1997**, *9*, 339–343.

[354] C. Lepetit, M. B. Nielsen, F. Diederich, R. Chauvin, *Chem. Eur. J*. **2003**, *9*, 5056–5066.

[355] F. Mitzel, C. Boudon, J.-P. Gisselbrecht, P. Seiler, M. Gross, F. Diederich, *Chem. Commun.* **2003**, *39*, 1634–1635.

[356] F. Mitzel, C. Boudon, J.-P. Gisselbrecht, P. Seiler, M. Gross, F. Diederich, *Helv. Chim. Acta* **2004**, *87*, 1130–1157.

[357] S. Eisler, R. R. Tykwinski, *Angew. Chem. Int. Ed*. **1999**, *38*, 1940–1943.

[358] M. Gholami, F. Melin, R. McDonald, M. J. Ferguson, L. Echegoyen, R. R. Tykwinski, *Angew. Chem. Int. Ed*. **2007**, *46*, 9081–9085.

[359] M. Gholami, S. Ramsaywack, M. N. Chaur, A. H. Murray, R. McDonald, M. J. Ferguson, L. Echegoyen, R. R. Tykwinski, *Chem. Eur. J*. **2013**, *19*, 15120–15132.

[360] S. Ramsaywack, S. Karaca, M. Gholami, A. H. Murray, F. Hampel, R. McDonald, N. Elmaci, H. P. Lüthi, R. R. Tykwinski, *J. Org. Chem*. **2014**, *79*, 10013–10029.

[361] A. Bandyopadhyay, B. Varghese, H. Hopf, S. Sankararaman, *Chem. Eur. J*. **2007**, *13*, 3813–3821.

[362] A. Rives, V. Maraval, N. Saffon-Merceron, R. Chauvin, *Chem. Eur. J*. **2014**, *20*, 483–492.

Entry for the Table of Contents (Please choose one layout)

Layout 1:

REVIEW

Alkyne in ring system: Angle-strained alkynes show specific reactivity and properties. An overview of angle-strained alkynes in π-conjugated macrocycles is presented. Their synthetic methods and transformation, photophysical and supramolecular properties, and bond angles are summarized.

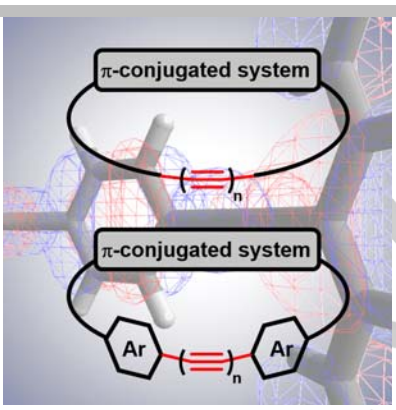

Prof. Koji Miki and Prof. Kouichi Ohe**

Page No. – Page No.

π-Conjugated Macrocycles Bearing Angle-Strained Alkynes